IOWA STATE UNIVERSITY
Digital Repository

Retrospective Theses and Dissertations

Iowa State University Capstones, Theses and Dissertations

1986

Optimization of the analytical performance of an inductively coupled plasma mass spectrometer

Joseph John Thompson
Iowa State University

Follow this and additional works at: https://lib.dr.iastate.edu/rtd

 Part of the Analytical Chemistry Commons

Recommended Citation
Thompson, Joseph John, "Optimization of the analytical performance of an inductively coupled plasma mass spectrometer " (1986). *Retrospective Theses and Dissertations*. 8315.
https://lib.dr.iastate.edu/rtd/8315

This Dissertation is brought to you for free and open access by the Iowa State University Capstones, Theses and Dissertations at Iowa State University Digital Repository. It has been accepted for inclusion in Retrospective Theses and Dissertations by an authorized administrator of Iowa State University Digital Repository. For more information, please contact digirep@iastate.edu.

www.manaraa.com

INFORMATION TO USERS

While the most advanced technology has been used to photograph and reproduce this manuscript, the quality of the reproduction is heavily dependent upon the quality of the material submitted. For example:

- Manuscript pages may have indistinct print. In such cases, the best available copy has been filmed.
- Manuscripts may not always be complete. In such cases, a note will indicate that it is not possible to obtain missing pages.
- Copyrighted material may have been removed from the manuscript. In such cases, a note will indicate the deletion.

Oversize materials (e.g., maps, drawings, and charts) are photographed by sectioning the original, beginning at the upper left-hand corner and continuing from left to right in equal sections with small overlaps. Each oversize page is also filmed as one exposure and is available, for an additional charge, as a standard 35mm slide or as a 17"x 23" black and white photographic print.

Most photographs reproduce acceptably on positive microfilm or microfiche but lack the clarity on xerographic copies made from the microfilm. For an additional charge, 35mm slides of 6"x 9" black and white photographic prints are available for any photographs or illustrations that cannot be reproduced satisfactorily by xerography.

8703774

Thompson, Joseph John

OPTIMIZATION OF THE ANALYTICAL PERFORMANCE OF AN INDUCTIVELY COUPLED PLASMA MASS SPECTROMETER

Iowa State University PH.D. 1986

University Microfilms International 300 N. Zeeb Road, Ann Arbor, MI 48106

PLEASE NOTE:

In all cases this material has been filmed in the best possible way from the available copy. Problems encountered with this document have been identified here with a check mark __✓__.

1. Glossy photographs or pages _____
2. Colored illustrations, paper or print _____
3. Photographs with dark background _____
4. Illustrations are poor copy _____
5. Pages with black marks, not original copy _____
6. Print shows through as there is text on both sides of page _____
7. Indistinct, broken or small print on several pages ✓
8. Print exceeds margin requirements _____
9. Tightly bound copy with print lost in spine _____
10. Computer printout pages with indistinct print _____
11. Page(s) _____ lacking when material received, and not available from school or author.
12. Page(s) _____ seem to be missing in numbering only as text follows.
13. Two pages numbered _____. Text follows.
14. Curling and wrinkled pages _____
15. Dissertation contains pages with print at a slant, filmed as received ✓
16. Other _____

_____

_____

University
Microfilms
International

Optimization of the analytical performance of an inductively coupled plasma mass spectrometer

by

Joseph John Thompson

A Dissertation Submitted to the
Graduate Faculty in Partial Fulfillment of the
Requirements for the Degree of
DOCTOR OF PHILOSOPHY

Department: Chemistry
Major: Analytical Chemistry

Approved:

Signature was redacted for privacy.

In Charge of Major Work

Signature was redacted for privacy.

For the Major Department

Signature was redacted for privacy.

For the Graduate College

Iowa State University
Ames, Iowa

1986

TABLE OF CONTENTS

DEDICATION

To my father,

a scientist at heart

CHAPTER I. INTRODUCTION

Since the introduction of inductively coupled plasma mass spectrometry (ICP-MS) by R. S. Houk et al. in 1980 [1], the state of the art in this field has progressed rapidly. In the development of any new analytical instrumentation, there are always periods when new complications arise which cloud the original expectations of the instrument's performance. The case of ICP-MS is no different, but it seems that, already, most of the serious problems of the technique have been ironed out. Perhaps this is because the manufacturers have foreseen the value of ICP-MS to the scientific community and, therefore, the profitability of providing a working instrument. It may be of use here to review important developments in the field of ICP-MS. A recent review by Gray does this in more detail [2].

The original "vision" of researchers in this field was that ICP-MS would determine trace elements in solution with detection limits equal to or better than contemporary multielement techniques such as inductively coupled plasma-atomic emission spectroscopy (ICP-AES). Perhaps as importantly, isotope ratio information could be obtained from solutions in a matter of minutes and with reasonable precision (relative standard deviations (RSDs) of 1% or less). The mass spectrometer is not subject to the extensive spectral overlap interferences experienced with atomic emission instruments

analyzing such richly emitting matrices as uranium or iron. This is because the mass spectrometer produces only one peak for every isotope of an element, and the most stable isotopes an element can have is ten (Sn); in fact, the average is only 3.4 isotopes for the ninety natural elements. Moreover, temperatures in the ICP are high enough to atomize and ionize most molecular species, including metal oxides, but not so high as to produce doubly charged ions which would clutter the mass spectrum [3]. The first background spectra taken confirmed that the region above m/z = 41 was largely devoid of any interfering peaks.

Although detection limits were quite good with the early design of the instrument, ions were being sampled through a "boundary layer" which formed in front of the small orifices used [1] (for a schematic diagram of the instrument see Fig. 1). This layer was cooler than the bulk plasma which aided oxide formation and produced other matrix effects [1]. Also, the small (50-60 μm) orifice would soon clog if concentrated salt solutions were analyzed for any length of time. These disadvantages were deemed intolerable and so "continuum flow" sampling [4] was adopted by ICP-MS researchers. This was the second important breakthrough in ICP-MS technology. The sampling orifices used were now large enough (1 mm) that the plasma could break through the boundary layer and thus be sampled directly by the mass spectrometer. An additional pumping stage was incorporated to handle the

higher gas load by means of a "skimmer" cone mounted directly behind the outer orifice.

Detection limits were initially much worse in the continuum sampling mode, but it was soon learned how to efficiently extract ions through the second orifice (skimmer) and into the quadrupole chamber. This work drew on experience in focusing molecular beams and the results are documented elsewhere [5]. As it turned out, the sampler - skimmer distance was critical for high ion transmission, as were the voltages placed on the skimmer (ground) and on the lenses immediately behind the skimmer.

Another problem associated with the larger orifice was that the plasma would "pinch" [1] or discharge as it passed through this constriction. This caused unacceptably high background at all masses, a spread of kinetic energies in the extracted ion beam which broadened mass spectral peaks, additional doubly charged ions from some elements, and a reduction in the lifetime of the sampling orifices.

Once again, research soon provided answers to these difficulties. Don Douglas' group at Sciex patented a method of grounding the ICP load coil which almost completely eliminated the "pinch" and its effects [6]. Shortly thereafter, in 1983, the first commercial ICP-MS was introduced by Sciex (VG Isotopes later entered this market). The background of these instruments was further reduced by addition of a photon baffle placed in the ion lens

and by placing the electron multiplier off the quadrupole axis.

Presently, ICP-MS is being refined and its performance evaluated. Interest in the technique is high, with over 70 units having been sold worldwide. Unfortunately, new operators with little experience in this field may be disappointed by the initial performance of their instrument on the type of samples they invariably want to run: small volumes of solutions (or solids) with trace elements present in a large matrix of some metal salt(s). Industry places additional demands of long term reproducibility, ease of operation (perhaps automation), hardware durability, and cost effectiveness on their equipment. If the "vision" of the original researchers is to become reality, ICP-MS must pass these tests.

Numerous reports already exist in the literature describing elemental and isotopic determinations with ICP-MS [7-12]. Houk and Thompson investigated the precision of isotope ratio determinations in both a continuous [7] and flow injection [8] mode of sample introduction. Applications to determining minor elements in steel [9], Cd in human blood [10], and to water analysis [11] have been reported. Date and Gray have analyzed several of the NBS standard geological materials for rare earth elements and found good agreement between their results and the accepted values [12]. Indeed, ICP-MS is even now the method of choice for trace rare earth

determinations. However, all of these analyses were done either on outmoded equipment or on samples which are not really difficult to the ICP-MS user. There is a need to delineate just how ICP-MS performs on solutions of moderate salt concentration (up to 1% w/w).

Two important problems currently facing ICP-MS practitioners are the instrument's susceptibility to ionization suppression and long term drifting of the analyte signal [13]. The extent to which these occur depends somewhat on the design of the instrument, but with all instruments they are problems which must be reckoned with before ICP-MS gains the full acceptance of scientists. Ironically, the ICP has traditionally been seen as the ideal emission source for the very reason that it has proven to be relatively free from ionization suppression as well as other matrix effects [14-15]. Perhaps, for that reason, potential clients have shied away from ICP-MS because they feel that there is something "wrong" with the instrument in its present configuration which will be remedied sometime in the future. Finding the causes of ionization suppression in ICP-MS is a topic of current interest and is not addressed here, but it is the author's opinion that suppression will never be minimized to the extent it is in ICP-AES. The second problem, signal drift, may well be due to hardware faults, and these are currently being remedied by the manufacturer.

The purpose of this dissertation then, is to show that the commercial ICP-MS instrument "works," regardless of whether future modifications will make it "work better." Analysis optimization procedures are discussed in Chapter II, after a brief experimental section. There, we develop an optimization strategy specifically to deal with ionization suppression. It must be noted that this suppression is detrimental for only two reasons:

1) Analyte signal is suppressed in the presence of a much larger amount of an easily ionized element; therefore, detection limits become poorer.
2) Differing amounts of the matrix element will cause variations in the analyte sensitivity from sample to sample resulting in loss of accuracy.

By the use of ultrasonic nebulization we can preserve detection limits and still optimize conditions so that an internal standard will effectively compensate for changes in the background matrix. Using ionization suppression curves and detection limits as criteria, Chapter II compares ultrasonic nebulization with the more conventional pneumatic nebulization under a wide range of operating conditions. The choice of measurement parameters (measurement time, scanning mode etc.) is also important in this process. Chapters III and IV show ways in which an optimized ICP-MS can improve on present methods (uranium analysis or liquid chromatographic detection) or open up whole new areas of research, as in

stable isotope tracing of various elemental species. Finally, a wide variety of analyses which were performed both for outside clients or as part of this dissertation are summarized at the end of Chapter III, along with some "pointers" that the author has gained from experience.

Although all data in this dissertation were taken solely on the Sciex instrument, we do not wish to come across as "selling" this particular instrument. Over the last five years, work has proceeded openly amongst the various ICP-MS groups. Many ideas have been shared, which is the main reason why ICP-MS has progressed so rapidly. Rather, it is pride in our work which is our motivation in seeking the acceptance of ICP-MS as a valid and highly useful analytical technique.

CHAPTER II. ANALYSIS OPTIMIZATION

Experimental

All work was performed on the Sciex ELAN Model 250 ICP-MS. A schematic diagram of the instrument is shown in Fig. 1. The solutions to be analyzed are either aspirated into a pneumatic nebulizer or pumped by a peristaltic pump into an ultrasonic nebulizer. The pneumatic nebulizer was a concentric, Meinhard type, which was supplied as standard with the Sciex instrument. It was used in conjunction with the standard Sciex ICP torch (see Fig. 2).

The ultrasonic nebulizer [16,17] employed (similar to Fig. 3) was constructed at the Ames Laboratory. Transducers (Model CPMT-5802-1.4 MHz) were obtained from Channel Products, Inc. (Chesterland, Ohio). The quartz plate disks, 0.0776" thick, were purchased from Swift Glass Co. (Elmira, NY). A better mist was obtained by gluing the ground quartz side to the transducer, leaving the smooth side of the disks facing the solution to be nebulized. The transducer was connected to a RF power supply (Model UNPS-1, Plasma-Therm Inc., Kresson, NJ) which supplied about 45 W of power at 1.37 - 1.40 MHz. The amount of mist produced by the ultrasonic nebulizer could be optimized by turning to full power and adjusting the frequency. Ice water recirculated past the transducer in order to cool it. The resistance presented to the RF circuit

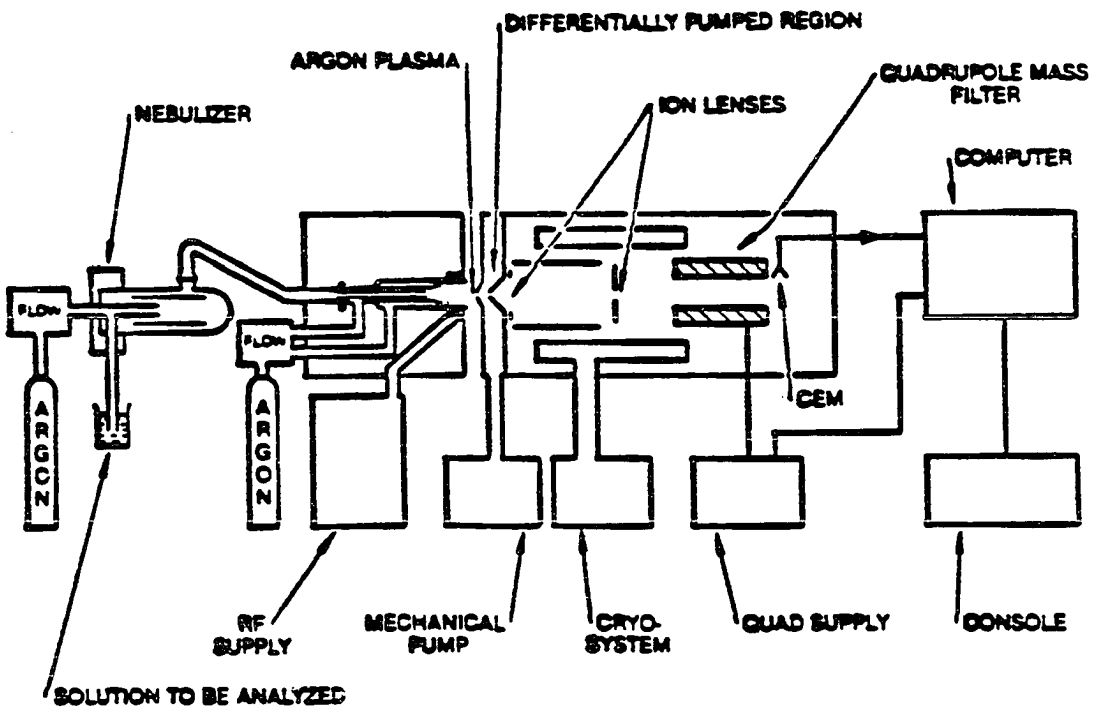

Figure 1. Schematic diagram of the Sciex ICP-MS instrument. This and subsequent Sciex figures have been reproduced from operator's manual with permission

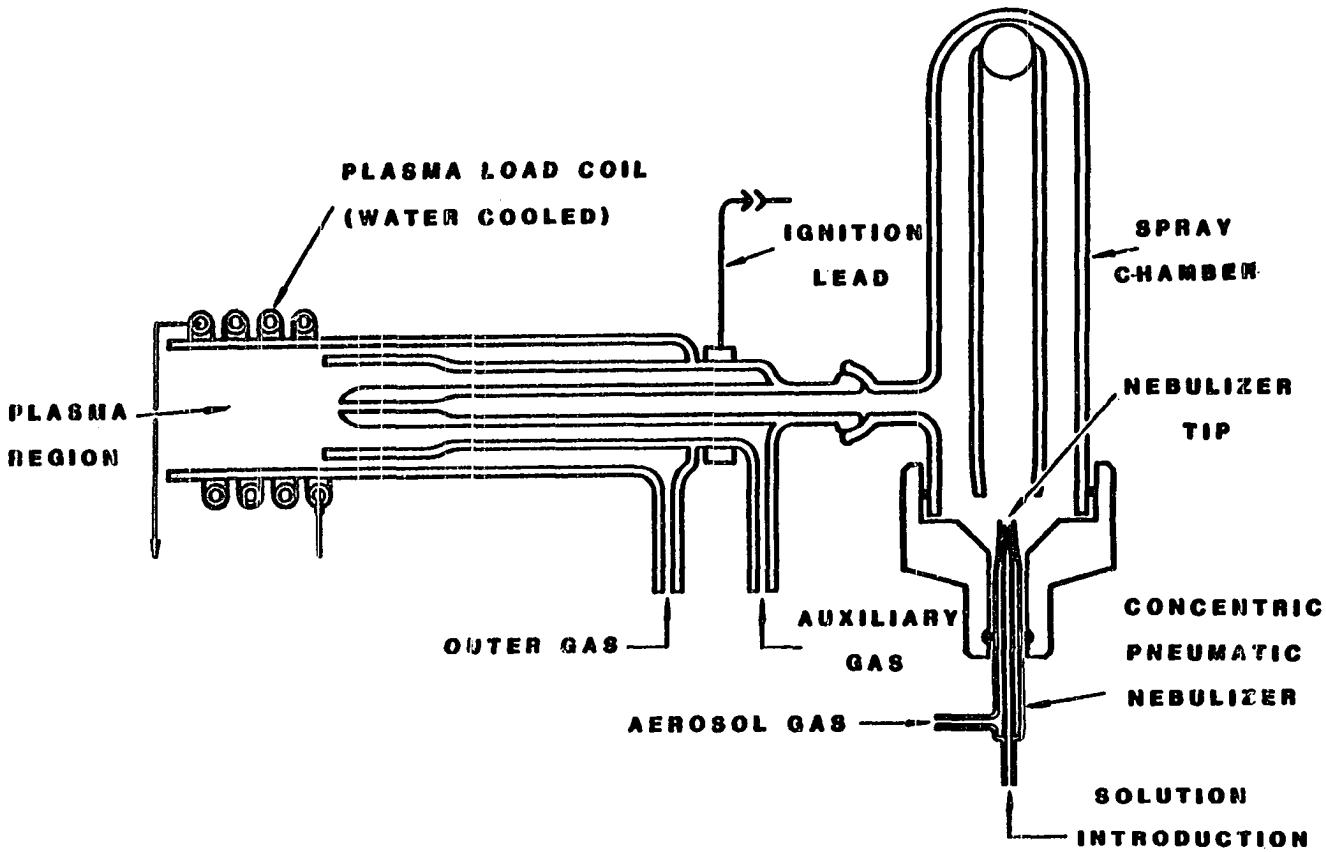

Figure 2. Schematic diagram of the Sciex pneumatic nebulizer connected to standard Sciex ICP torch

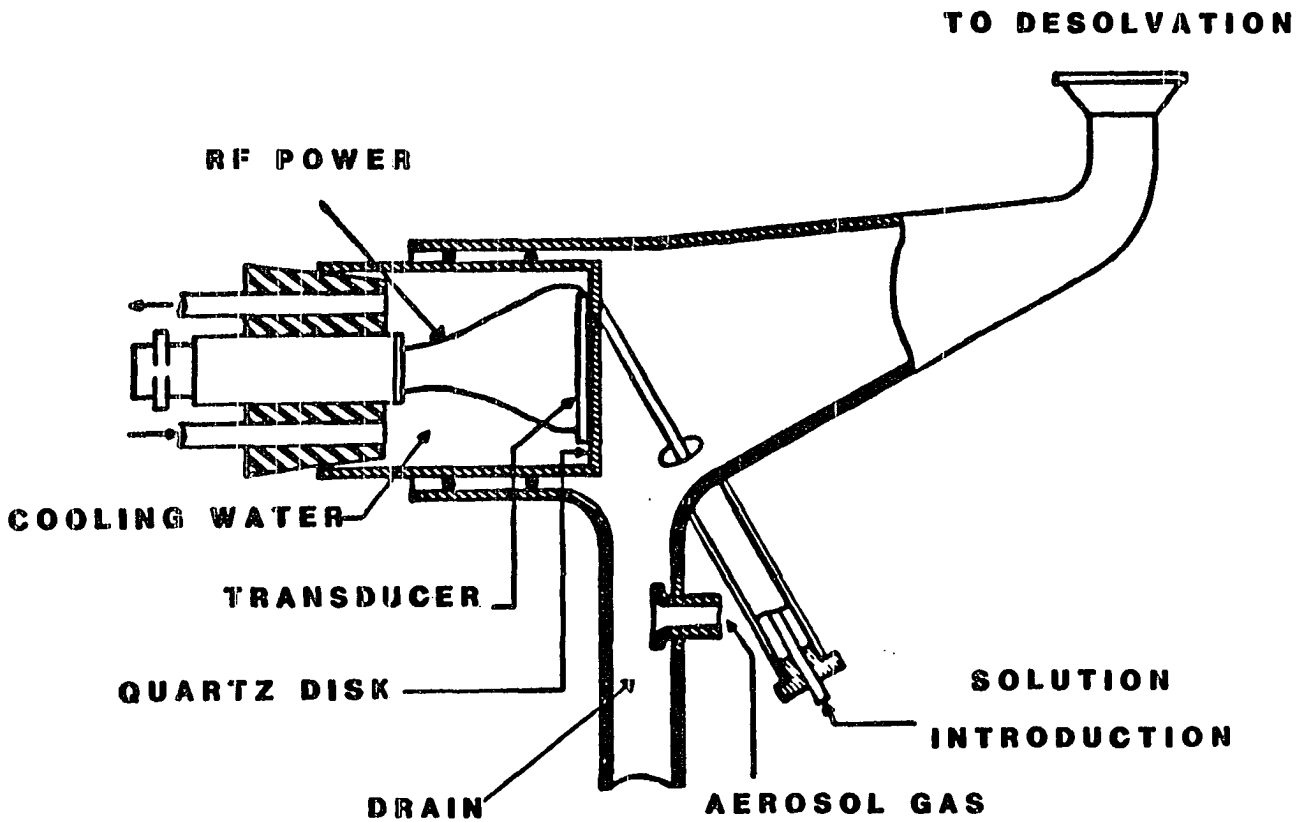

Figure 3. Schematic diagram of an ultrasonic nebulizer (adapted from Ref. [17] with permission)

by this water, which was in contact with the wires soldered to the transducer, was kept above 1 M ohm.

The efficiency of this ultrasonic nebulizer was measured to be 35% with a fresh transducer and under normal operating conditions (i.e., at 1.2 L min^{-1} aerosol gas flow rate, desolvation apparatus connected and heated, and with water blocking the drain tubes). This result was obtained by pumping 100 mL of deionized water onto the transducer at 1.5 mL min^{-1} and collecting the unnebulized solution at the drain with a graduated cylinder. After a few weeks, the efficiency dropped to about 10% and remained constant for the remaining life of the transducer (about 6 months). No mixing baffles [17] were placed in the spray chamber in the present system.

A stream of argon, called the aerosol gas flow, was introduced into the drain tube of the ultrasonic spray chamber (Fig. 3) and, providing water was present in the drain, pushed the mist out through a desolvation tube. This glass tube was about 40 cm in length and wrapped with a resistance heater, which created an aerosol exit temperature of about 100°C. At this temperature, much of the water was removed by passing it through a condenser, which was chilled by the same ice water as the transducer. The liquified water fell to a waste container. This container was also kept blocked with liquid, so that the stream of argon carrying small solid particles of the analyte, was carried into the plasma. An Ames Laboratory torch [18] with an extended outer tube (38 mm from the aerosol injector tip) was usually used with the ultrasonic nebulizer.

The design and function of an ICP torch are described in detail elsewhere [18]. Basically, the outer and auxiliary flows keep the hot plasma off the walls of the quartz tubes and aerosol injector tip, while the aerosol flow "punches" the analyte particles up through the central axis of the plasma (Fig. 2). Energy from the load coil, supplied by a RF generator (27.12 MHz, up to 2.0 kW) is coupled into the plasma, which, in turn, heats the axial channel. At the position at which we normally sample ions, about 25 mm above the load coil, the temperatures are about 5000-7000K [19]. The exact mechanisms of energy transfer processes in the ICP are still under investigation [20]. For optimal sensitivity, the ICP is simply centered on the sampling cone.

The Sciex ICP employs a metal strap soldered to the middle of the four-turn load coil [21]. This has been found to reduce the energies of ions produced in the plasma, as well as control the "pinch" discharge that occurs when a large sampling orifice is used [1].

Solid particles in the aerosol are further desolvated in the ICP, and then atomized and ionized. These processes take place in a few ms as the analytes traverse the central channel of the ICP carried by the aerosol gas flow [14]. The ICP, considered as an ion source for a mass spectrometer, is very efficient - elements with first ionization potentials below about 8 eV are nearly 100% ionized [1]. Very few second ionization potentials are low enough (10-13 eV) to produce

appreciable amounts of doubly charged ions in the plasma [22]. Also, only very stable molecular species can survive the high temperatures of the plasma. For these reasons, the background spectrum, such as shown in Fig. 4, is relatively "clean" for a mass spectrum. Only the usual gas ions are seen in the background: O^+, N^+, OH^+, NO^+, O_2^+, Ar^+, etc. Only ArN^+, ArO^+, and Ar_2^+ (too small to be seen in Fig. 4) interfere with possible analyte ions (Cr, Fe and Se) above m/z = 41. Since there is no separate source of ionization inside the mass spectrometer, simple organic ions (e.g., from the pump oil) do not appear in the background. However, the presence of mineral acids in the blank does cause some spectral interferences [3,23,24].

The critical part of the ICP-MS instrument is the interface (Fig. 5), which must efficiently transfer the analyte ions from a region of high temperature and atmospheric pressure to a region of room temperature and high vacuum. A detailed description of ion sampling is given in Ref. [5]. Ions from the ICP stream through an outer 1.2 mm diameter orifice (the sampler) into a region of intermediate pressure (1 torr) pumped by a mechanical pump. This is sometimes called the expansion stage because here the ions form a supersonically expanding beam, which cools the ions and decreases the frequency of collisions. A second 0.90 mm orifice (the skimmer) collects the central portion of this beam. Immediately behind the skimmer, ions are collected

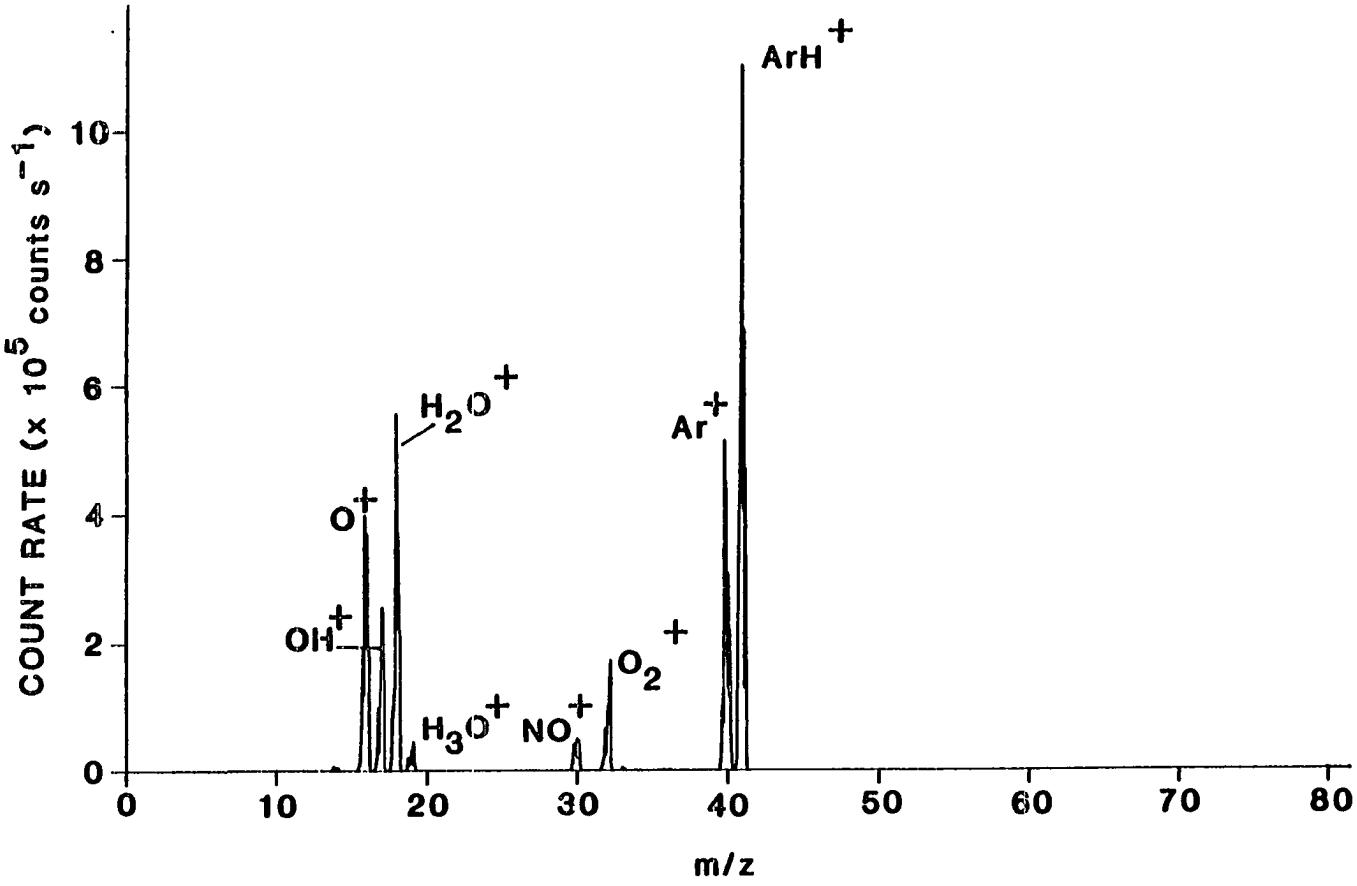

Figure 4. Typical background spectrum obtained from the Sciex device while introducing deionized water into the ICP. The splitting of the peaks at m/z = 40 and 41 indicates that counting losses occurred at these masses

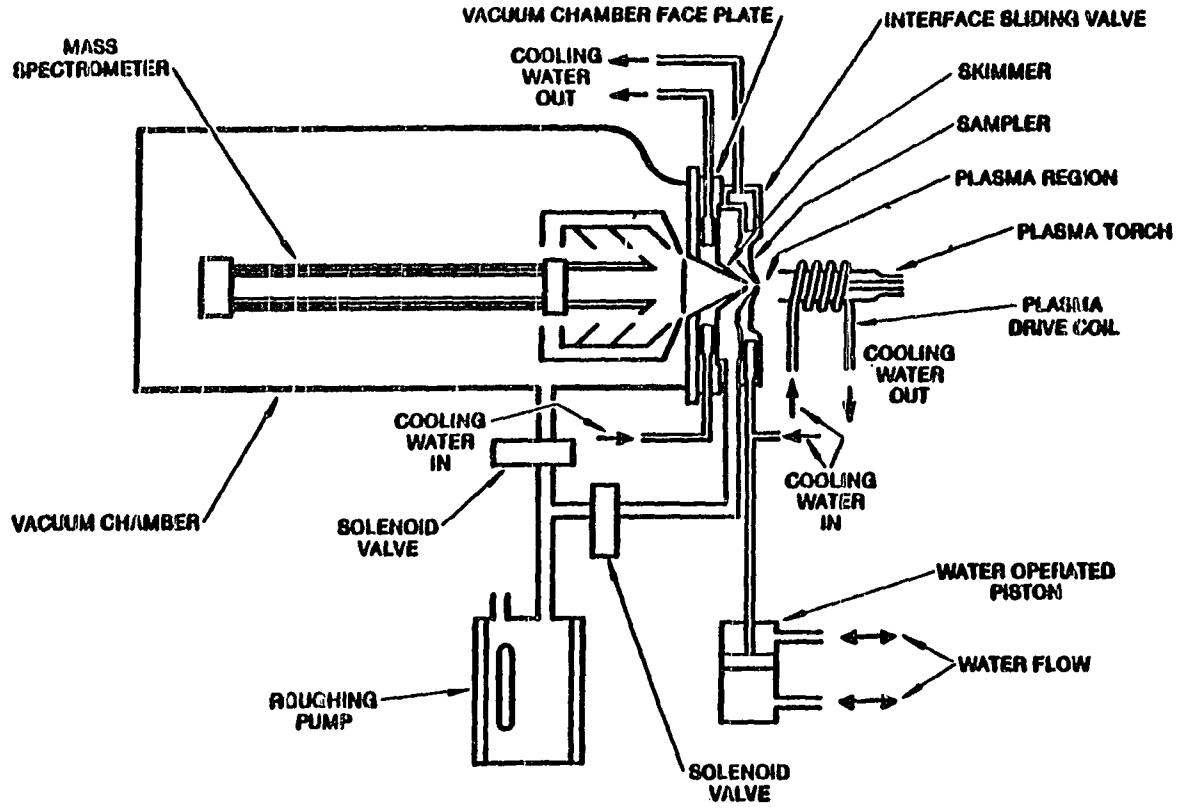

Figure 5. Sciex ICP-MS interface region

and focused by an ion lens system (Fig. 6) into the quadrupole mass filter. This ion lens configuration was used to collect all data in this thesis unless otherwise stated. An optical baffle in the center of the lens prevents high energy ICP photons from reaching the detector, reducing background count rates (normally <100 counts s^{-1}). In the quadrupole mass analyzer, the ions are separated according to their mass/charge ratio by varying the DC and AC voltages supplied to the rods [25]. Ions exiting the quadrupole are focused by more lenses, and repelled by a high positive voltage on a "deflector" lens into the mouth of a channel electron multiplier (CEM-Fig. 7). The CEM is mounted at right angles to the quadrupole axis to reduce the background due to stray photons. It is operated in a pulse counting mode [26], meaning that individual ions are counted instead of a total current. At high count rates (>10^6 Hz) the pulses begin to "pile up" (two ions counted as one) and the multiplier loses its linearity.

The entire ELAN instrument is under computer control except for the adjustments of ICP and nebulizer parameters, and the multiplier, deflector, and ion lens settings. Routine analytical procedures such as concentration calibration, mass calibration, spectral display, qualitative and quantitative analysis are performed by separate software programs. All programs, however, require a "parameter set" be made first, with appropriate measurement parameters inserted for the job at hand. This presents a problem for the novice ICP-MS user:

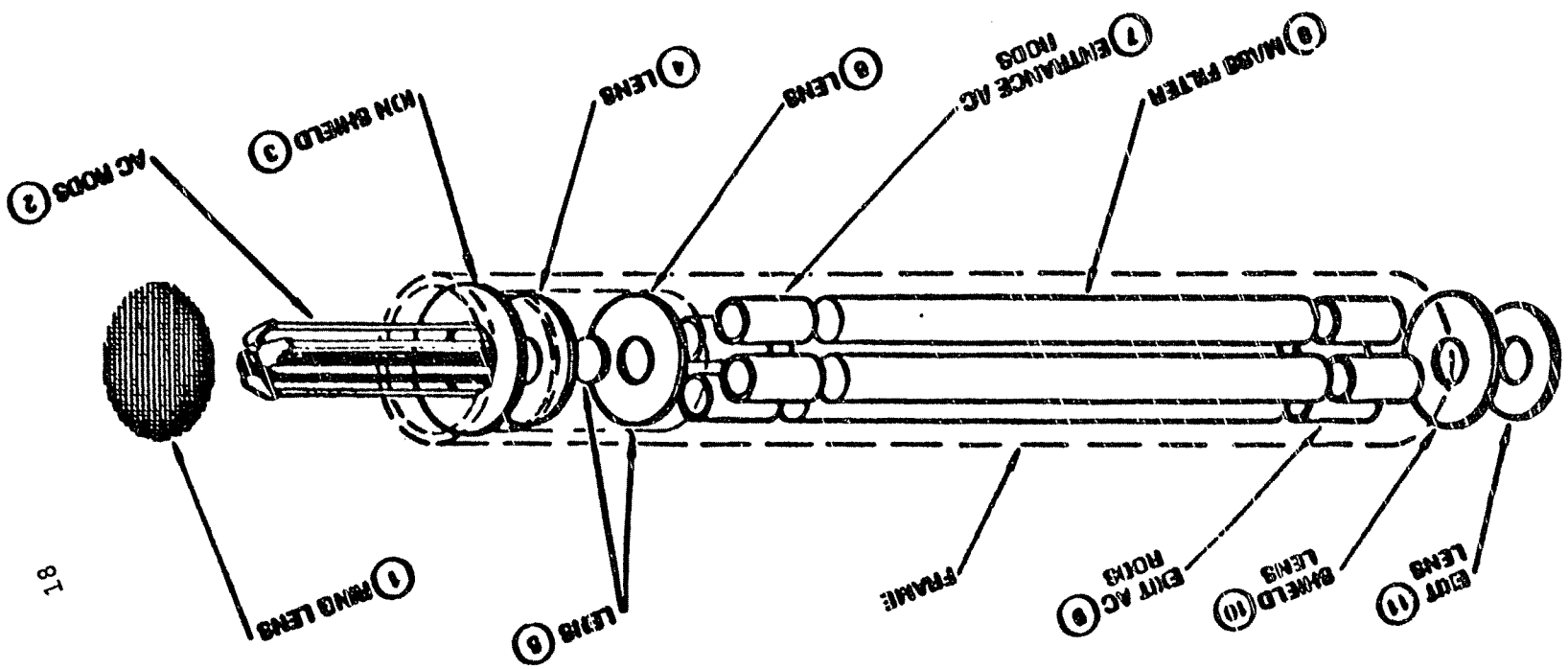

Figure 6. Sciex ion lens and mass analyzer

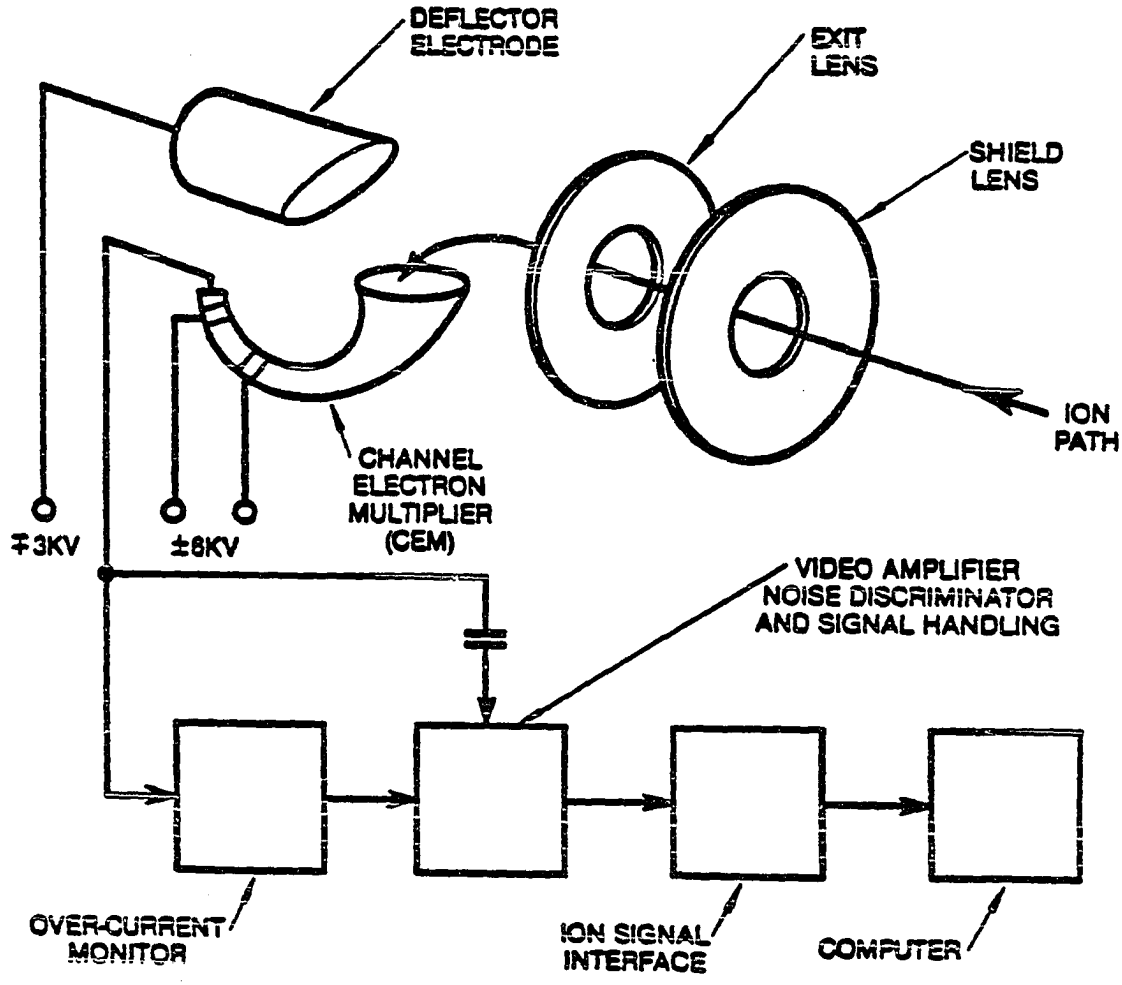

Figure 7. Sciex detection system

what parameters work best for each application? The following section attempts to answer this question based on the author's trial and error experience.

Effect of Measurement Parameters

Terminology

To begin this section, we describe the measurement options available with the ELAN instrument, and define some terms which will, hopefully, give a better understanding of the subject. A scan will be defined as one pass (sweep) of the mass spectrometer over a requested mass range. A determination or repeat is the result of one or more scans such that a number of significance (i.e., a ratio or intensity) is actually output from the computer. An integration is a set of one or more determinations that will be continuously run by the computer every time the operator initializes an analysis. Once the run of a sample has been started, the computer stops only when the integration period has expired, or if the operator exits from the program. However, the results of individual determinations are still available to the analyst. Scan results are not visible unless only one scan has been made (multiple scans are averaged and reported in the determination results).

There are two measurement modes available to the Sciex user at present, which affect the basic way in which the data

are collected. In sequential mode, as the name implies, each requested m/z value is scanned, one after the other, for a chosen measurement time. One scan, therefore, constitutes a determination in this case. In the multichannel mode, the total measurement time is broken up into smaller chunks called dwell times. The mass spectrometer makes an initial scan of the masses of interest, hopping from one peak to the next, spending only one dwell time at each measurement point. After the completion of one scan, additional scans are made until the sum of the accumulated dwell times equals or exceeds the requested total measurement time. Thus, several scans make up one determination in this case.

Note that although there is no fundamental difference in the two measurement modes, there is a practical difference. For example, one would think that using a very short measurement time (say 50 ms) and many repeats per integration (20) in the sequential mode would be equivalent to using multichannel mode with a 50 ms dwell time, 1.0 s total measurement time and a single repeat. The difference is that in the former case the computer would output 20 numbers, whereas in the latter case only a single datum would be produced.

Figures 8 and 9 illustrate some further options available to the ICP-MS analyst. These figures are actual parameter sets from the Sciex device using the sequential and multichannel modes, respectively (line 11). Common to both

sets are the entries in the top half of the form. Here, one can log experimental conditions such as multiplier high voltage, quadrupole offset potential, ICP power, and the three plasma flow rates. None of these items is under computer control. The very first item, resolution, is controlled from the console, however. In high resolution, each peak has a width of m/z = 0.6 at 10% of its maximum height, regardless of whether it is at high or low mass. Also, a mass spectrometer stepping size is implied: 20 steps across a peak in high or manual resolution, and 10 steps in low resolution. In manual, the user can turn a potentiometer to adjust the resolution. Also, common to both sets is the "measurements per peak" entry. In order to compensate for slight errors in mass calibration, it is possible to take multiple measurements along a peak's profile and average them. In high resolution, these measurements are centered on the calibrated mass and spaced m/z = 0.05 apart, in low resolution, m/z = 0.1. In some instances, if the number of measurements/peak is high, the computer will estimate peak area rather than peak height.

There are three scanning modes possible for either multichannel or sequential operation. If elemental scanning is chosen, the user must enter a list of elements in the parameter set (see Fig. 9). The computer will "peak hop" to each element automatically using the most abundant isotope unless alternate ones are specifically entered. This mode is best for quantitative analysis. Isotopic scanning is similar,

PARAMETER SET: WIDESCAN

SCAN WHOLE SPEC

Resolution	(High, Low, Man.)	[H]	H
Ion Multiplier HV	(2500 to 6000)	[4000]	4900
Rod Offset volts	(-50.0 to 50.0)	[5.0]	0.0
Plasma RF Pwr watts	(500 to 2500)	[1200]	1350
Auxiliary Flow L/min	(0 to 2.2)	[2.0]	2.0
Plasma Flow L/min	(0 to 22.0)	[12.0]	12.0
Nebulizer Pressure psi	(0 to 40.0)	[24.0]	40.0
Sample Flow	(0 to 2000)	[1000]	1000
Measurement Mode	(Seq., Multichan.)	[S]	S
Scanning Mode	(Elem., Iso., Range)	[E]	R
Meas. Time Sec	(0.001 to 8)	[1]	0.100
Measurements/Peak	(1 to 20)	[3]	1
Repeats/Integration	(1 to 32000)	[10]	10
Threshold Ions/sec	(1 to 50000)	[200]	300
Counting Precision %	(0.050 to 20)	[5]	5.000

RANGE SCAN:	START MASS	END MASS	P
	3	250	+

Figure 8. Example of a parameter set using sequential mode. Default parameters are shown in brackets

PARAMETER SET: PALMTRACE6

HIGH MASS HALF OF MARGOS OTHER 10 PPB ELEMENTS FROM URANIUM

CHANGE PARAMETERS

HIGH MASS HALF OF MARGOS OTHER 10 PPB ELEMENTS FROM URANIUM			
Resolution	(High, Low, Man.)	[H]	L
Ion Multiplier HV	(2500 to 6000)	[4000]	4000
Rod Offset volts	(-50.0 to 50.0)	[5.0]	0.0
Plasma RF Pwr watts	(500 to 2500)	[1200]	1300
Auxiliary Flow L/min	(0 to 2.2)	[2.0]	0.8
Plasma Flow L/min	(0 to 22.0)	[12.0]	12.0
Nebulizer Pressure psi	(0 to 40.0)	[24.0]	0.0
Sample Flow	(0 to 2000)	[1000]	250
Measurements/Peak	(1 to 20)	[3]	3
Scanning Mode	(Elem., Iso., Range)	[E]	E
Measurement Mode	(Seq, Multi, Trans)	[S]	M
Meas. Time sec	(0.001 to 8)	[1]	0.500
Repeats/Integration	(1 to 32000)	[10]	2
Dwell Time ms	(1 to 1000)	[1]	100
Cycle Time sec	(0.001 to 10)	[0.1]	0.100

ELEMENT	SYM	P	C	I	MEASUREMENT EQUATION
Barium	Ba	+	U		1.0000*Ba138
Cadmium	Cd	+	U		1.0000*Cd114
Cesium	Cs	+			1.0000*Cs133
Hafnium	Hf	+	U		1.0000*Hf180
Niobium	Nb	+			1.0000*Nb93
Lead	Pb	+			1.0000*Pb208
Thorium	Th	+			1.0000*Th232
Yttrium	Y	+			1.0000*Y89
Zirconium	Zr	+			1.0000*Zr90
Holmium	Ho	+		I	1.0000*Ho165

Figure 9. Example of a parameter set using multichannel mode. Default parameters are shown in brackets

except some additional options make this better suited to measuring several isotopes of the same element (for isotope dilution or isotope ratio experiments). Finally, range scanning works best for qualitative analysis or spectral display (see Fig. 8). Here, the mass spectrometer will sweep every m/z continuously over a specified range.

The bottom halves of Figures 8 and 9 take on different forms depending on whether the measurement mode is input as 'S' (sequential) or 'M' (multichannel). If it is 'S', a "threshold ions/sec" can be specified so that the mass spectrometer does not waste time counting background. If, for example, the parameter set contains Zn in its element list, and the sample does not contain Zn, the computer will skip this peak (m/z = 64) as soon as it realizes that the number of counts is below the threshold. In the same way, proper setting of the "counting precision" insures that the mass spectrometer will not waste time counting very large peaks if the desired counting precision has already been obtained. This value should be set to a value just below the precision level usually obtained from the operating parameters (ICP, nebulizer, etc.). Perhaps the fact that the default value is 5% indicates that the manufacturer realizes that there is a drifting problem associated with the ELAN!

For multichannel parameter sets, the different entries are the dwell time and cycle time. Dwell time has already been discussed. The cycle time, confusingly, is only operative in

one case, otherwise it is meaningless. When the scanning mode is isotopic, the cycle time represents the total measurement time, including an estimate of any software overhead time. The normal "measurement time" is then inoperative. Using isotopic scanning in the multichannel mode, it is possible to allocate more dwell times in each cycle to the less abundant isotopes so that they are counted with the same precision as larger ones. However, the software overhead time associated with this operation is formidable (see Chapter III, isotope ratio determinations).

By way of example, Fig. 8 is the parameter set we normally use for obtaining a full spectral display. High resolution is used for clarity. In this application, the speed with which the spectrum can be produced is of importance, not the accuracy. Hence, the sequential mode is used (which is faster than multichannel) with range scanning from m/z = 3-250. A short measurement time is used, and only one measurement per peak is necessary. The computer will skip over the large parts of a background spectrum where the threshold counts are below 300 counts s^{-1}. Also, the large background peaks at m/z = 16, 18, 40, and 41 would not be counted for very long, as the counting precision is set at 5%.

In contrast, Fig. 9 is the parameter set used for a very tricky analysis - the quantitation of 10 μg L^{-1} metals in a uranium matrix (Chapter III, uranium analysis). The multichannel mode is recommended for maximal precision (see

below) and low resolution was necessary to get the maximal count rates from the trace elements. Three measurements/peak were used for good precision. A compromise measurement time of 0.5 s was adopted due to the large number of metals being determined in the elemental scanning mode (ideally it should be longer). The cycle time was inoperative. Thus, using this parameter set, the computer would go to the lowest mass, m/z = 89 (Y), and take three measurements of 100 ms (dwell time) centered on the peak spaced m/z = 0.1 apart. It would then hop to m/z = 93 (Nb) and do the same thing. After the last peak (Th) was scanned, the mass spectrometer would return to Y and start over again. This would continue five times until the accumulated dwell time equalled the measurement time of 0.5 s. Then the total counts in each of the three channels atop each analyte peak would be averaged to produce an average peak intensity. At this point, the average intensities of each element were divided by the average intensity of holmium, the internal standard (marked with an 'I' in the element list), and these ratios were output from the computer. This whole process was repeated because the "repeats per integration" was set at two. The total analysis time for the ten elements was therefore 3 X 10 X 0.5 = 15 s per determination.

Optimization

From the above tutorial, it should be clear that control of the measurement processes, let alone other experimental parameters, is at best bewildering to the first time ICP-MS analyst. There are very few indications from the manufacturer as to what values to use in the parameter sets other than the default values. This is, after all, a brand new technique. Hence, we began a systematic investigation of the effects of these parameters on ICP-MS performance. This trial and error process will be recounted in a chronological manner.

To understand the effectiveness of the optimization procedures employed in the rest of this chapter, it is necessary to document initial conditions as set up by the installation engineer from Sciex. These are listed in Table 1. Under these conditions, the percentage of MO^+/M was at least 10% for several rare earth elements, intensities drifted (generally downward) by 10% or more per hour, and short term precision of elemental ratios was generally 5% RSD or worse using default measurement parameters (Figs. 8 and 9). Furthermore, ionization suppression was severe: 98% suppression of Co from 2000 mg L^{-1} Na.

The drifting problem was judged to be the most serious. Having an ICP-MS without stability of signal is like buying a large, well figured telescope, only to find that its tripod shakes in the slightest breeze - totally useless! It was thought that internal standardization might alleviate this

Table 1. Sciex ICP-MS instrument settings upon installation[a]

Nebulizer	Sciex pneumatic
ICP torch	Sciex standard torch
Outer argon flow rate	12 L min^{-1}
Auxiliary flow rate	2.0 L min^{-1}
ICP forward power	1.35 kW
Aerosol flow rate	0.5 L min^{-1} (40-45 psi)
Solution uptake rate	2 mL min^{-1}
Ring lens (#1 in Fig. 6)	Setting: 25 (-15.02 V at TP)
Lens #4	Setting: 50 (-9.93 V at TP)
Lens #5	Setting: 65 (+6.19 V at TP)
Lens #6	Setting: 60 (-11.92 V at TP)
Deflector	+4020 V (at TP)
Electron multiplier	-3270 V (-4.90 V at TP)

[a]TP = test point. Test point voltages are not necessarily equal to voltages supplied to the device.

problem. Thus, the criterion for optimizing the measurement parameters was the improvement of precision in analyte/internal standard ratios. If these ratios drifted, then the corresponding calibration curves would certainly drift.

Initial experiments were performed using the Sciex nebulizer and torch (Fig. 2). The RSD (relative standard deviation) of 10 consecutive determinations of a Co/Mn ratio (both 1 mg L^{-1}) was measured at various measurement times (MT) in sequential mode, using 7 measurements/peak (M/P). These data are shown in Fig. 10. Optimal precision seemed to be obtained around 0.1 s MT. Interestingly, this was also the ideal MT (or "acquisition time" as it was called) the author experienced while working with the custom built ICP-MS and data system described in Ref. [5]. This period also happens to be the ideal dwell time for a multichannel scan (see Table 18, Chapter III). This result can be rationalized as follows. At a very low MT, precision is limited by counting statistics. If, for example, a 0.01 s MT is used for a 1 mg L^{-1} solution of Co which yields 100,000 counts s^{-1}, then each measurement yields only 1000 counts. The RSD of each measurement should thus be at least $\sqrt{1000}/1000 = 3$ %. If the MT is increased to 0.1 s, the counting precision becomes 1 %. However, the precision does not keep getting better because if the MT is too long, plasma flicker and other sources of noise are more apt to affect one or more of the measurements. Apparently,

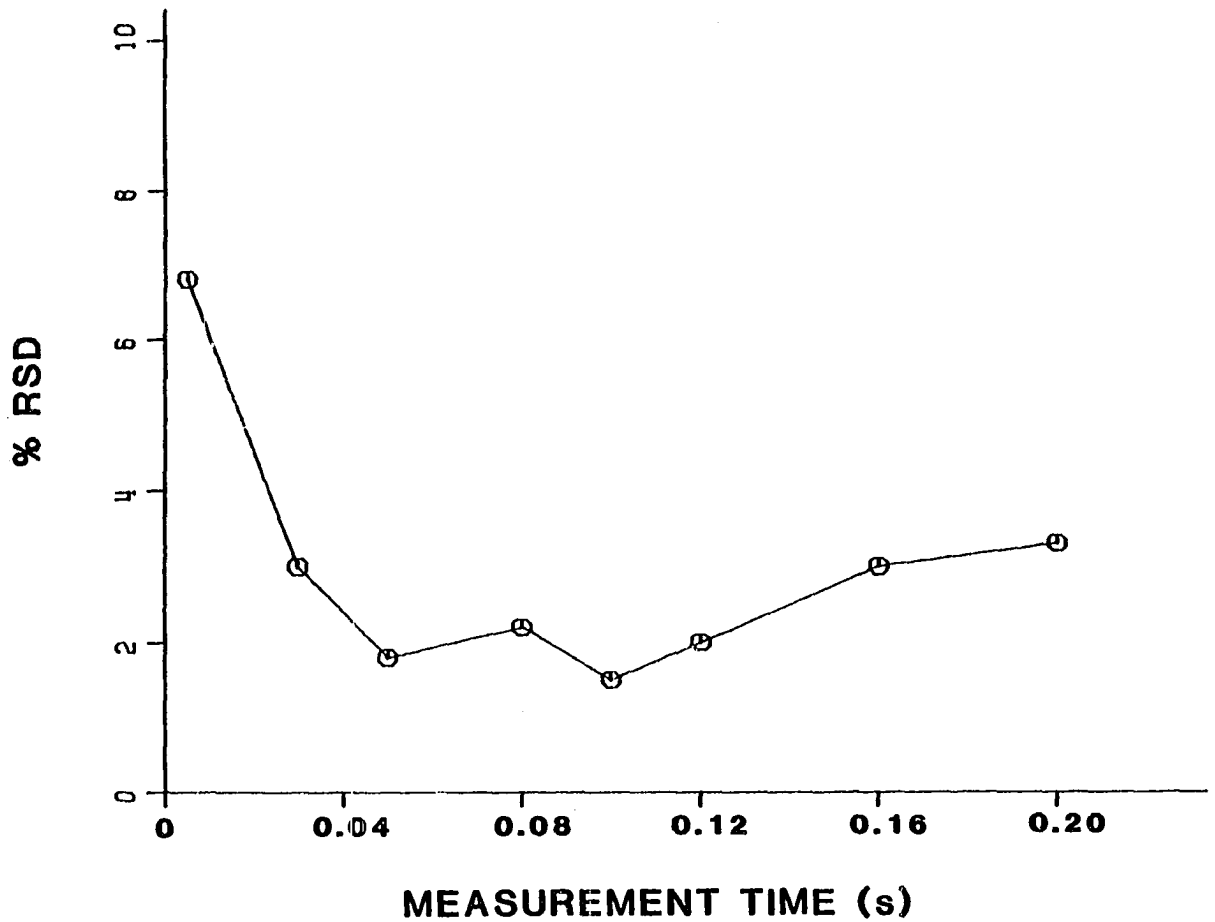

Figure 10. RSD of ten determinations as a function of measurement time in sequential mode

the frequency of the noise sources is similar in the two different ICP-MS instruments. This discussion of precision is extended to the multichannel mode in Chapter III in relation to the measurement of Zn isotope ratios.

Some other points were soon learned about sequential mode scanning. Three M/P invariably worked best. A larger number of M/P wasted time and also lowered the apparent intensity of the peak because some of the points near the side of the peak were averaged with measurements nearer the top. One M/P never gave good precision. After a certain point, increasing the number of repeats/integration did not improve precision, as shown in Table 2. A good indication that the right number of determinations were being taken was that the ratio of the averaged intensities for all determinations was very close to the average of the individual ratios (also see Table 18).

The multichannel mode was examined next with emphasis on determining ratios of trace elements in a uranium matrix with good precision. First, it was discovered that using low resolution significantly enhanced precisions for 10 μg L^{-1} rare earth determinations in 100 mg L^{-1} U (Table 3). Presumably, this was because of the increased count rates, but some ratios were more precise even though there was no increase in the count rate! Possibly, the use of low resolution, in addition to the use of 3 M/P, helped correct for any errors in mass calibration; the low resolution peak would be significantly broader than a high resolution peak,

Table 2. Precision of Co/Mn (each 1 mg L^{-1}) as a function of the number of determinations[a]

# determinations	5	10	20	30
RSD	9.2	4.7	5.0	4.5

[a]MT = 0.05 s, sequential mode, 5 M/P.

Table 3. Count rates and precision of 10 μg L^{-1} rare earth ratios (Lu internal standard) in 100 mg L^{-1} U in high and low resolution[a]

Element	Hi Res counts s^{-1}	Lo Res counts s^{-1}	Hi % RSD	Lo %RSD
Ce	68	158	14	2
Dy	44	64	17	12
Er	44	62	6	8
Eu	51	93	11	4
Gd	41	67	10	4
Ho	76	162	4	3
La	72	137	11	7
Lu	55	117	--	--
Nd	33	58	17	7
Pr	71	162	17	5
Sm	37	61	9	6
Tb	68	154	7	2
Hf	38	48	10	3
Th	89	80	7	5
Tl	60	60	16	7
Tm	67	141	8	1
Yb	43	56	11	5
Zr	36	36	12	3

[a]Multichannel mode, 0.8 s MT, 100 ms DT, 3 M/P; background was about 30 counts s^{-1}. Zr, Tl, Th, were not in the solution.

thus avoiding any measurements on a sharply sloping peak profile. No immediate connection could be found between precision and dwell time (DT) or MT, but this might have been because of the uranium matrix and the ICP operating parameters used. A DT of 100 ms was adopted, which later proved to be nearly optimal (see Chapter III).

At this point, short term precision (1-4%) had been improved somewhat but long term drifting of calibration curves was still a problem. Figure 11 shows four calibration curves taken over a one hour period using 2-15 $\mu g\ L^{-1}$ of a rare earth with a Lu internal standard. To give an idea of the magnitude of the drift, a 2 $\mu g\ L^{-1}$ standard read 0.4 $\mu g\ L^{-1}$ after one hour. It was suggested [27] that the location of the nebulizer inside the ICP shielding box might be the cause of thermally induced fluctuations in the nebulizer.

An ultrasonic nebulizer was therefore mounted outside the instrument. Initially, higher count rates were obtained, and ionization suppression was as bad, or worse, but absolute ratios did not change as much with a change in matrix (Table 4); however, this was later found to be dependent on ICP parameters and on the choice of internal standard. Also, ratios originally drifted by 10% over 15 minutes, but this was later reduced to 5% over a half hour. These data were obtained using the same Sciex torch, so it was concluded that the pneumatic nebulizer was a cause for at least some of the drifting.

The Sciex ICP torch did not perform consistently well, so

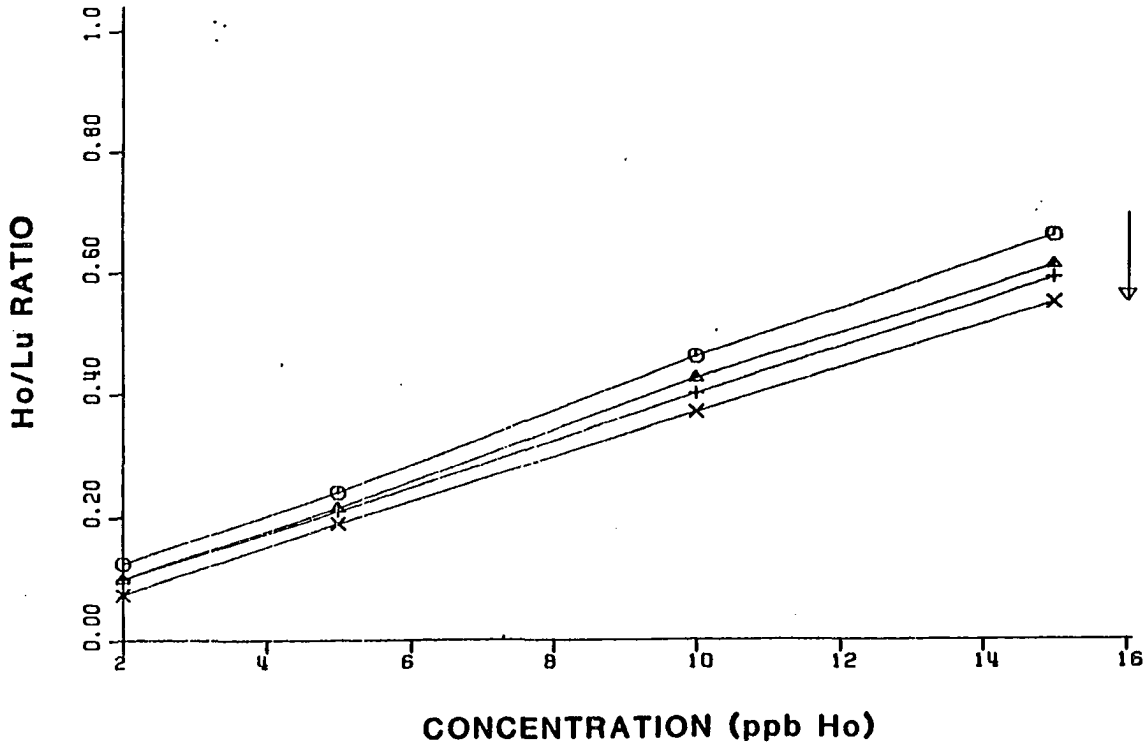

Figure 11. Demonstration of initial calibration drift over one hour with the Sciex nebulizer and torch. The initial curve drifted downward as shown by arrow

Table 4. Initial test of matrix effects with ultrasonic nebulizer and Sciex torch using 1 mg L^{-1} Ho, Lu[a]

[U] (mg L^{-1})	Ho(c/s)	Lu(c/s)	Ho/Lu
0	205000	174000	1.18
20	65500	59500	1.10
50	17500	17700	0.98
100	1000	1040	0.96
500	150	143	1.04

[a]Multichannel mode, 1.0 s MT, 100 ms DT, 3 M/P.

Table 5. Initial test of matrix effects and precision with ultrasonic nebulization and Ames Laboratory torch using 1 mg L^{-1} Mn, Co

[Na] (mg L^{-1})	Mn/Co	% RSD[a]
0	1.12	1.4
20	1.22	2.2
50	1.17	1.4
100	1.19	3.0
500	1.21	3.2
1000	1.24	0.8
2000	1.37	2.4
0 (repeat)	1.13	1.8

[a]Four determinations.

the Ames Laboratory torch was installed. This design had a wider aerosol jet (4 mm) which was tapered to 2 mm just before it reached the plasma, in contrast to the Sciex torch which had a 4 cm length of 2 mm i.d. tubing. Table 5 shows the behavior of Co/Mn ratios at the 1 mg L^{-1} level, in varying concentrations of Na with this combination of torch and nebulizer. Intensity data were not recorded. The RSDs for 4 determinations were excellent. Table 6 illustrates the long term precision that was initially obtained. Calibration curves were prepared using 2, 5, 10, and 30 μg L^{-1} standards and a Lu internal standard. Some of these standards were used to check the accuracy of the curves at various time intervals after the original calibration. Apparently, long and short term drifting were now under control. While at first, we did not obtain results like this every day, experience gained in the optimization of ICP-MS parameters, described in the next section, soon made this routine. More examples of the performance of this system are given in Chapter III.

In summary, the interrelatedness of the operational and measurement parameters made it hard to ascertain exactly which factors caused the greatest improvements in signal stability. Internal standardization certainly helped, because the precision of ratios was always better than precision of intensities. The multichannel mode was undoubtedly better for careful work because it enabled low frequency noise to be averaged out. Low resolution gained more sensitivity and the use of 3 M/P was strongly indicated. As far as hardware is

Table 6. Long term stability initially obtained with ultrasonic nebulization and Ames Laboratory torch as evidenced by drift in calibration curve standards. The determined concentrations of the indicated standards are listed at different times after the calibration curve was made[a]

Standard:	10 $\mu g\ L^{-1}$	5 $\mu g\ L^{-1}$	30 $\mu g\ L^{-1}$
Element	Fresh	20 min later	1 hour later
Ho	10.3	5.1	31.3
Eu	10.8	4.9	31.8
Yb	10.3	5.9	31.0
Tb	10.3	4.9	30.6
Tm	10.0	4.8	30.3
Dy	11.1	5.3	29.7
Nd	10.9	5.2	33.5
Ce	11.4	5.3	37.1
Er	10.5	5.5	31.2
Gd	11.1	5.6	32.6
La	11.4	5.5	38.7
Sm	12.7	6.1	31.6
Pr	10.2	4.8	35.0

[a]Matrix was 50 mg L^{-1} U; same measurement parameters as in Table 4. Lu internal standard.

concerned, it is possible that the Sciex torch and nebulizer could give good stability, but the ultrasonic nebulizer and Ames Laboratory torch have been found to work quite well (see also Table 8). Other advantageous aspects of ultrasonic nebulization will be seen in later parts of this dissertation.

Effect of Operating Parameters

In this section, several points will be addressed. Again, the emphasis will be on practical operation of the instrument as it relates to choosing operating parameters that will reduce matrix effects and improve stability. Ref. [28] has already documented the effects that these various parameters have on the analyte signal. The usefulness of internal standardization will also be evaluated.

Introduction

In this section, "interference effect" means any change in analyte count rate due to the presence of another element or elements in the same solution, but excluding "spectral interferences" such as occur in ICP-MS when a molecular oxide species is formed which has the same mass as the analyte ion. Others [3,23,24] have discussed the possibilities of spectral interference in ICP-MS in some detail.

Interference effects in ICP-AES have been investigated extensively by Boumans and de Boer [29,30] using ultrasonic

nebulization and by Larson et al. [15] using a pneumatic nebulizer. They have identified several different types of interelement interferences which are either associated with the sample introduction system (desolvation interferences, nebulizer interferences) or the ICP (stable-compound-formation interferences or ionization interference). The results of these studies show that, under most conditions, the total matrix effect (i.e., intensity in matrix/intensity in pure water) from all these sources is quite moderate in ICP-AES. Boumans and de Boer, for example, observed a ±10% change in analyte signal due to the addition of a 2000 mg L^{-1} KCl matrix [29]. Furthermore, under compromise conditions intended to reduce matrix effects, Ref. [29] reports that the same matrix caused an average matrix effect of only ±7% for over 30 elements in the same solution (using ultrasonic nebulization). Detection limits obtained under these compromise conditions were not degraded by more than a factor of 7 compared to the best attainable detection limits. Larson et al. report that little change in emission intensity was observed for Mo when it was measured in matrices of 2500 mg L^{-1} K, Na, Al, Cu, or Zn [15]. It should also be noted that many of these studies used ion lines for the elements measured, and that the measurements were collected under a variety of operating conditions (forward power, aerosol gas flow rate, and type of nebulizer). Results of this kind have been repeatedly demonstrated by users of ICP-AES [17], which

is a major reason why the technique has become industry's workhorse for multielemental analysis.

The reasons for the above observations can be simply explained as follows. The ICP operates at a higher temperature than other flames and plasmas that have been used for emission spectroscopy. A typical nitrous oxide-acetylene flame burns at a temperature of only 3200 K; a direct current plasma or microwave plasma operate at electron temperatures of about 5000-6000 K. Temperatures in the analytical region of an ICP are estimated to be about 6500 K [19]. Thus, problems with incomplete vaporization of the sample or stable compound formation in the ICP are avoided at these high temperatures. The one type of interference which would be expected to play a significant role in the ICP is an ionization interference. Consider the following equilibrium for some analyte species M in the plasma:

$$M = M^{+} + e^{-}$$

If a large amount of an easily ionized element (e.g., Na) is added to the ICP, the supply of electrons could increase and shift the above equilibrium to the left, suppressing analyte ion formation. However, if the "pool" of free electrons in the plasma is very large, the relative change in the electron population from the matrix element would be small, and little change in the analyte atom or ion population would be observed.

The extent of ionization of both the analyte and matrix element is a function of the temperature of the ICP. The fact that observed interference effects from an easily ionized matrix element are less than what would be expected from measured excitation temperatures in the ICP [19] is a manifestation of "suprathermal ionization" [20]: the electron density (or ion density - the plasma is neutral) is higher than would be expected from a measurement of the gas or excitation temperature alone ($T_{ion} > T_{gas}$ or T_{exc}). This is an advantage of the ICP over other plasma sources for analytical work. The causes of this phenomenon are still under investigation [20].

Considering the explanation above, it is logical that factors which decrease the temperature of the ICP will also render it more susceptible to interferences. This has been shown to be the case. Ultrasonic nebulization produces more interference effects than pneumatic nebulization, because it introduces more material into the ICP, which requires more energy to vaporize and atomize the material [17,30,31]. Parameters such as aerosol gas flow rate and forward power have a direct bearing on plasma temperature and thus have been shown to influence the extent of interelement effects [29].

Interference effects have also been examined in ICP-MS [31], but that study only employed a single set of operating parameters, a single type of nebulizer (ultrasonic), and it did not use a commercial instrument, and thus could not be

referenced to other laboratories' work. Thus, it is our purpose here to document the extent of ionization suppression over a wide range of operating conditions, analyte elements, and matrix elements, and then to compare our results with other interference studies done with ICP-MS and ICP-AES. The term "ionization suppression" is used below to mean "matrix effect", because in all cases observed, the analyte ion count rate has only decreased due to the concomitant matrix element; this is in contrast to elevations of analyte signal observed in some ICP-AES or ICP-MS studies.

Ionization suppression with the pneumatic nebulizer

Figures 12 and 13 illustrate the effect of nebulizer pressure and forward power on ionization suppression by monitoring the Co intensity and Ni/Co ratio as a function of Na^+ concentration (added as NaCl). All data were taken with the Sciex pneumatic nebulizer and torch. When using a nebulizer of this type, opening the needle valve upstream of the nebulizer will only slightly increase the gas flow rate (a few hundreths of a L min^{-1}) because the flow of argon is obstructed by the narrow constriction at the tip of the nebulizer (Fig. 2). Therefore, monitoring the gas line pressure (downstream of the needle valve) yields a more sensitive measure of aerosol gas flow rate [32]. As the nebulizer pressure increases, the gas flow rate increases slightly, and the amount of mist produced by the pneumatic

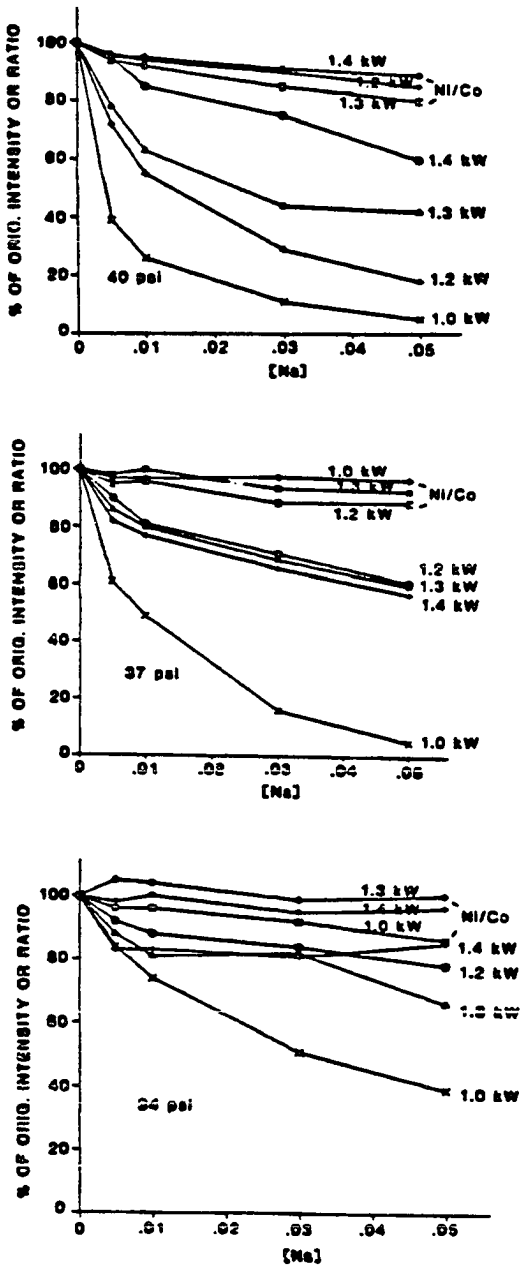

Figure 12. Effect of forward power on ionization suppression of Co by NaCl while operating the Sciex pneumatic nebulizer at three different aerosol pressures. In this and subsequent figures, default values for the auxiliary and outer gas flow rates are 1.4 and 12 L min^{-1}, and the sampler is located 21 mm from the load coil

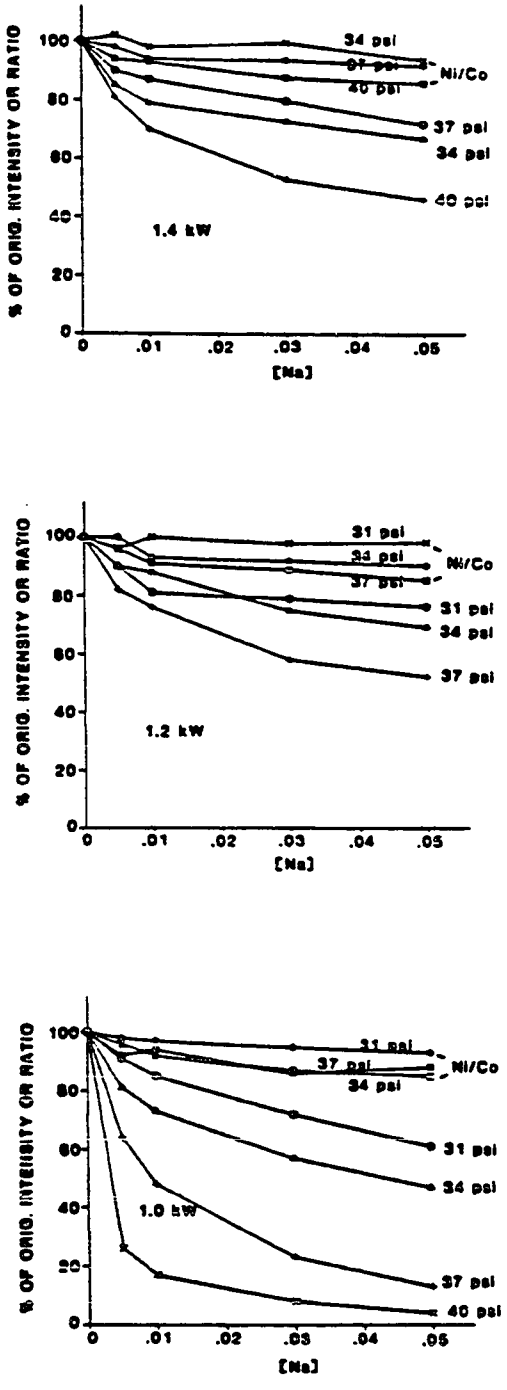

Figure 13. Effect of aerosol pressure on ionization suppression at three different forward powers

nebulizer increases, so that more material enters the plasma. In all of the following suppression curves the zero point reference solution (i.e., the one with no Na^+) was introduced before and after each solution containing Na^+, so that instrumental drift could be checked. The Co intensity and the Ni/Co ratio of the salt solutions were then normalized to the average intensity from the reference solution and plotted.

Figure 12 shows that, as expected, an increase in forward power caused the extent of suppression in the Co signal to decrease or remain the same at all three aerosol gas flow rates (pressures) chosen. Interference effects were particularly bad as the power was dropped from 1.2 to 1.0 kW. Even the Ni/Co ratio was affected, although in almost all cases the change in this ratio amounted to less than 10% at 0.05 M NaCl. Thus, internal standardization was effective in compensating for changes in the background matrix.

Figure 13 reveals similar information as Fig. 12; this time the nebulizer pressure was varied at constant forward power. These data were determined independently from those in Fig. 12, i.e., the data were not merely rearranged to be presented in this format. Again, it is obvious that high aerosol gas flow rates and low forward powers are major contributors to ionization suppression.

Figure 14 shows the effect of auxiliary flow rate on ionization suppression at various combinations of forward power and nebulizer pressure. The same procedures were used to collect these data as in Figs. 12 and 13, only this time

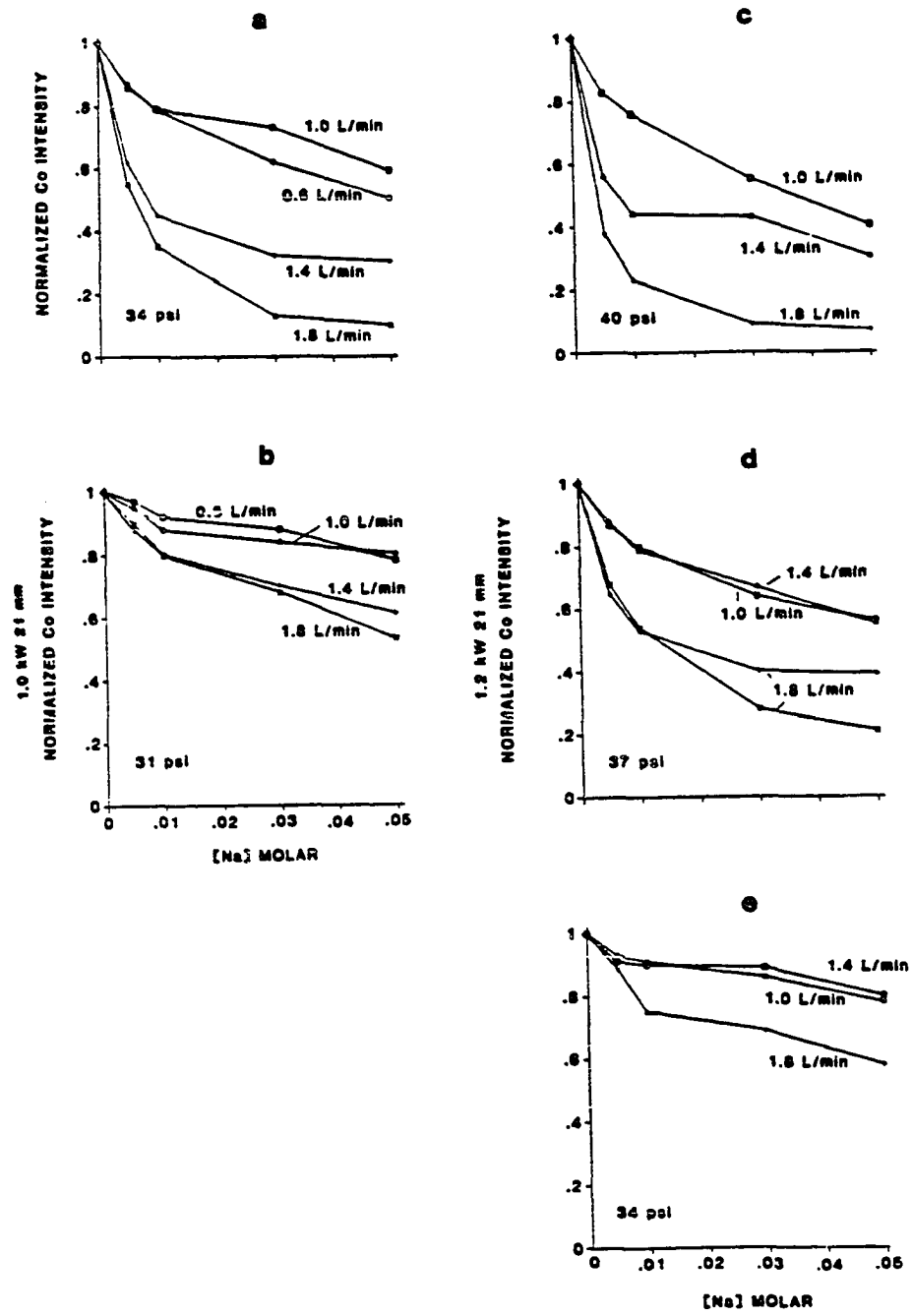

Figure 14. Effect of auxiliary flow rate on ionization suppression at different forward powers (columns) and aerosol pressures (rows)

the Ni/Co ratio was not plotted since it was found to remain constant within ± 10% in all cases. The data indicate that the extent of the interference does depend on auxiliary gas flow rate, with minimal interference at about 1.0 L min^{-1}. The Sciex recommended flow rate of 2.0 L min^{-1} (Table 1) clearly caused a greater extent of suppression. These data make sense intuitively, since the higher gas flows would "cool" the plasma, making it more susceptible to ionization interferences. However, at lower auxiliary flow rates, this cooling is probably negligible compared to that produced by the aerosol gas flow, since the auxiliary flow only indirectly cools the axial channel. Note that it was always easier to see the effects of each parameter when the ICP was running at low power and/or with a high aerosol gas flow rate (Fig. 14a,c). Under the opposite conditions, the suppression curves tended to bunch together (Fig. 14e).

In Fig. 15, the effects of various outer argon flow rates on suppression are illustrated at two different auxiliary flow rates and at several combinations of aerosol gas flow (pressure) and forward power. In Fig. 15a, for example, the three upper curves are for a 1.0 L min^{-1} auxiliary flow while the bottom three represent data collected at 1.4 L min^{-1}. As forward power increased and aerosol gas flow rate decreased, it was hard to distinguish between the six curves (Fig. 15f). An outer flow rate of about 15 L min^{-1} appeared optimal in those cases where a difference could be seen.

Next, the dependence of ionization suppression on the type

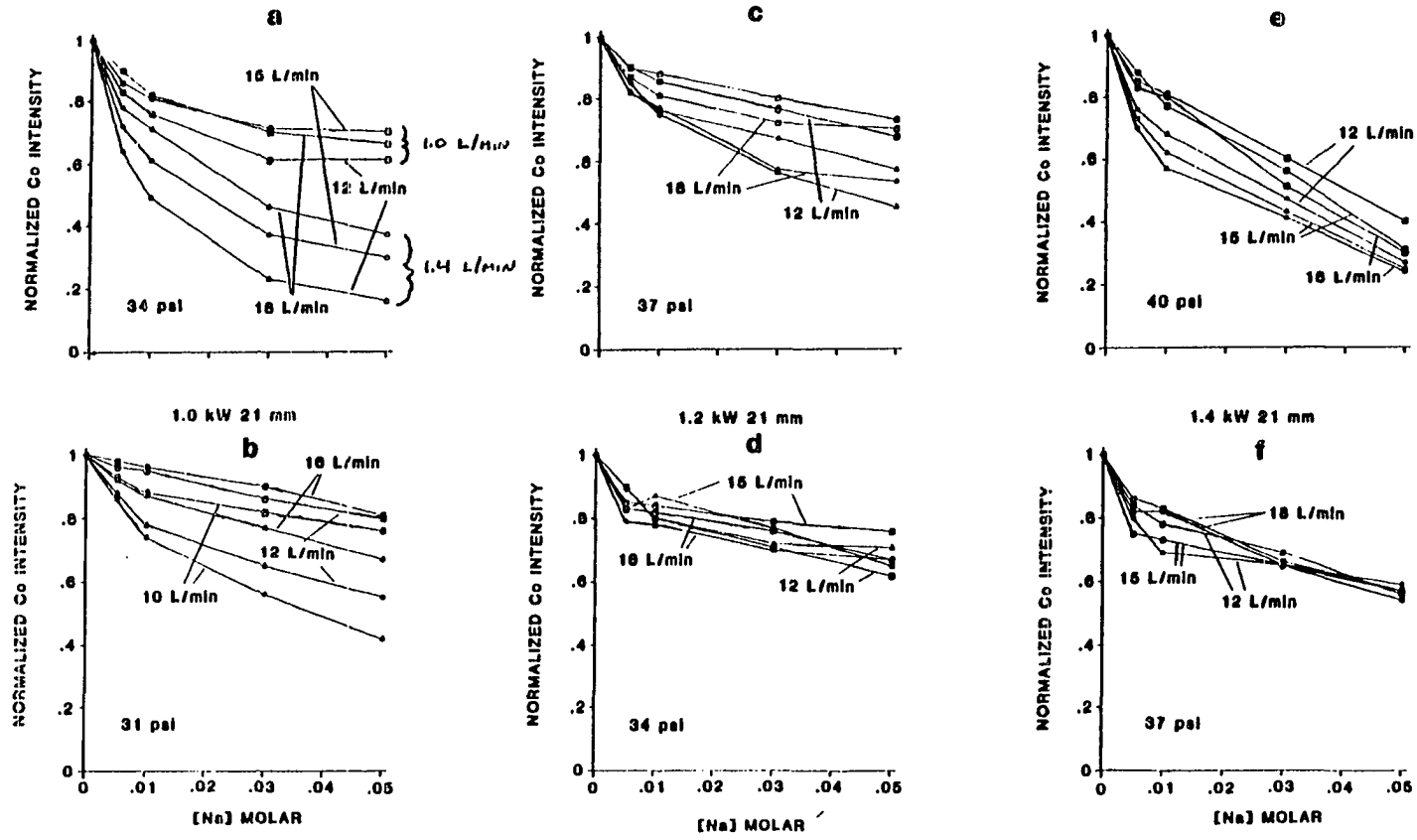

Figure 15. Effect of outer argon flow rate on ionization suppression at different forward power, aerosol pressure and auxiliary gas flow rate. In a,b,c, and e the upper set of three curves is easily identified as those taken at 1.0 L min^{-1} auxiliary flow rate, while the bottom three were taken at 1.4 L min^{-1}. In d and f, the curves merge

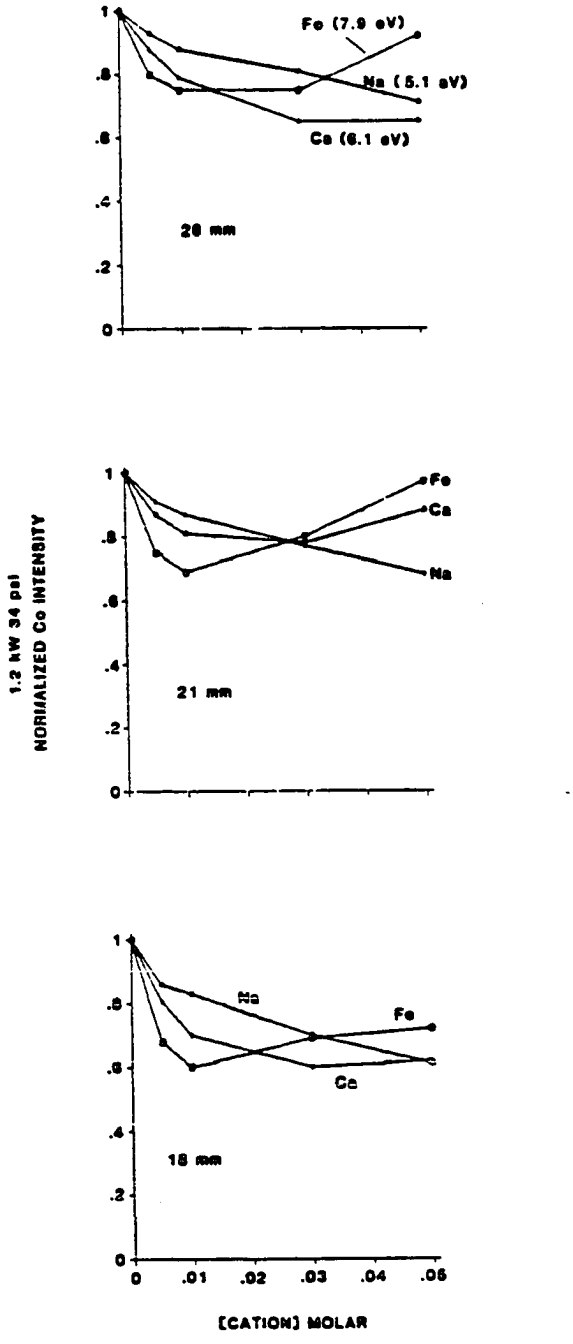

Figure 16. Effect of matrix ion on ionization suppression at 1.2 kW, 34 psi at three different ICP positions

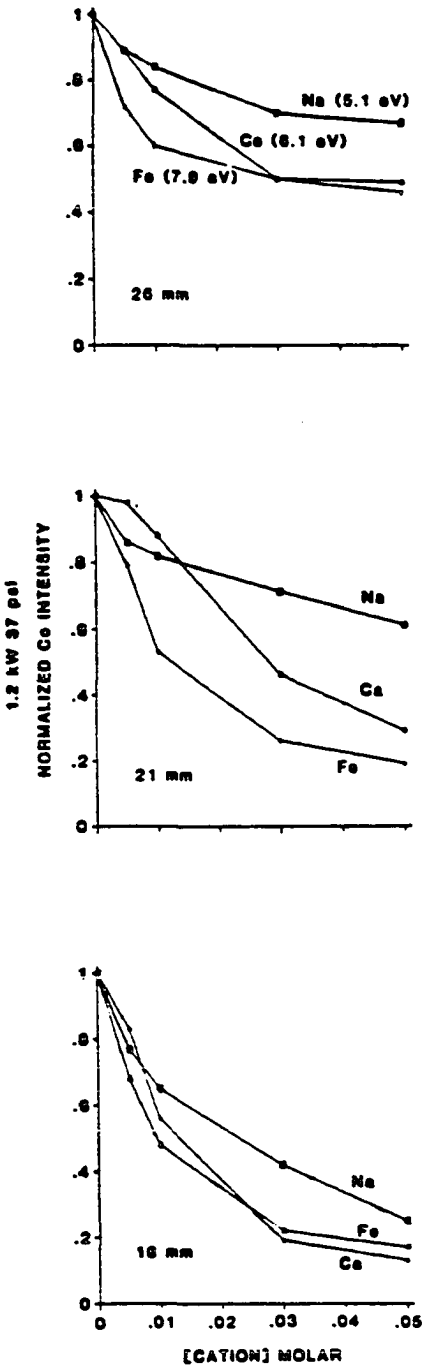

Figure 17. Effect of matrix ion on ionization suppression at 1.2 kW, 37 psi at three different ICP positions

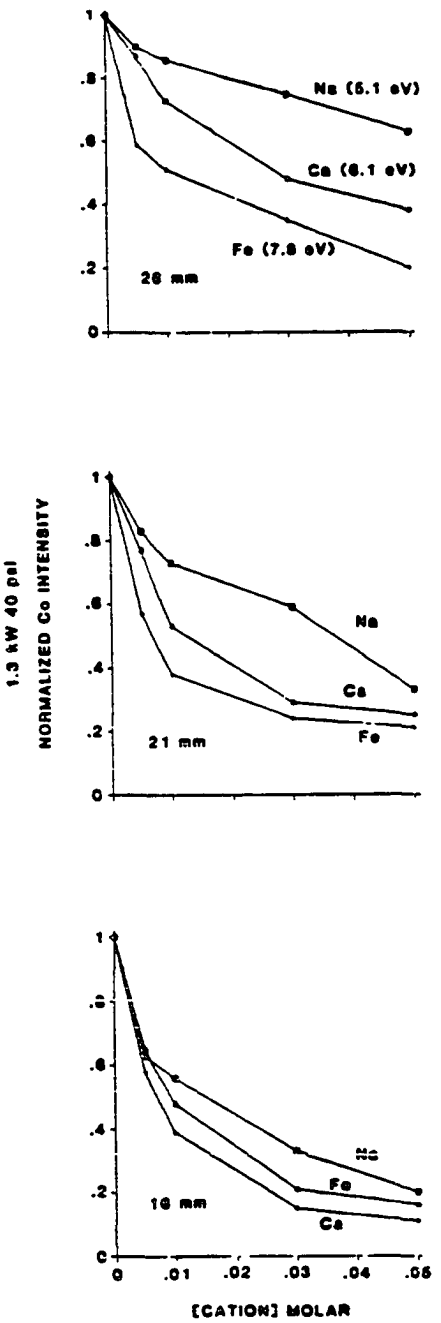

Figure 18. Effect of matrix ion on ionization suppression at 1.3 kW, 40 psi at three different ICP positions

of matrix ion was investigated. In Figs. 16-18 the position of the sampler relative to the outer turn of the load coil was varied under different conditions of forward power and aerosol flow rate. The matrix blanks were subtracted and the matrix concentrations were verified by a quantitative analysis. Suppression of Co was considerably different in the presence of equimolar amounts of Na^+, Ca^+, and Fe^+. For these matrix elements, with first ionization energies less than 8 eV, the extent of interference did not correlate with ionization energy. In fact, the order of suppression seemed to be Fe>Ca>Na, which corresponded to the heaviest element causing the most suppression. This agreed with the observations found in Chapter III, that in the analysis of uranium, the U matrix caused a great deal of suppression, even at 100 mg L^{-1}. Note that suppression was actually minimized as the sampler was moved <u>further away</u> from the load coil (Fig. 18 shows this clearly). This is contrary to the findings for ICP-AES in reference [30], which claims that, in general, matrix effects increase at higher observation heights. These observations, and the strange looking suppression curves obtained in Fig. 16 may be due to physical changes occurring in the ICP itself which are changing the position of the analyte ions in the plasma. Thus, the local concentration of Co^+ ions in a particular region of the plasma could change depending on how the "shape" (i.e., distribution of ions) of the plasma was modified by the salt solutions at a given forward power and

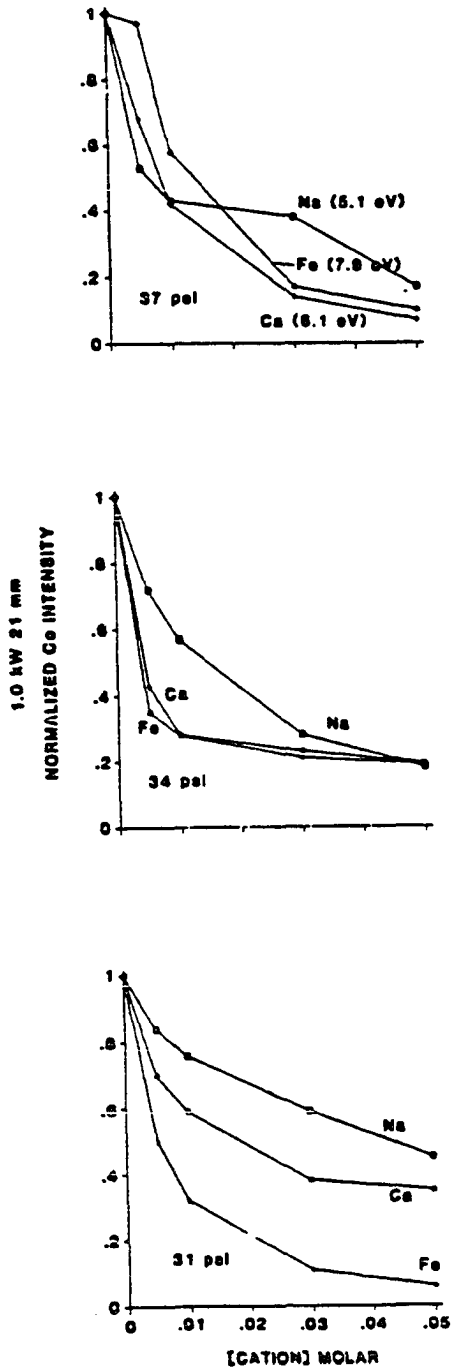

Figure 19. Effect of matrix ion on ionization suppression at 1.0 kW, 21 mm at three different aerosol pressures

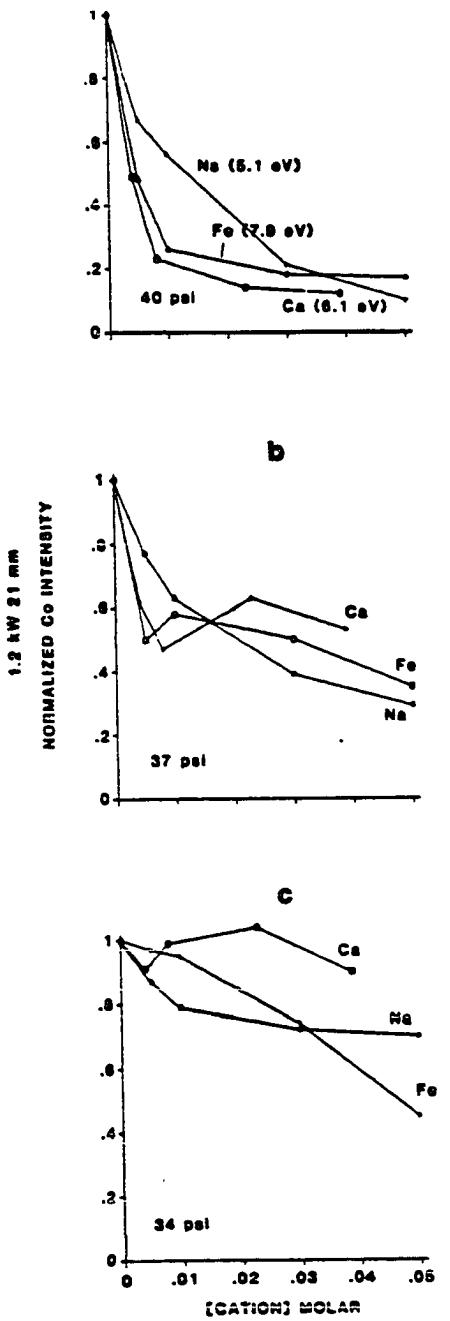

Figure 20. Effect of matrix ion on ionization suppression at 1.2 kW, 21 mm at three different aerosol pressures

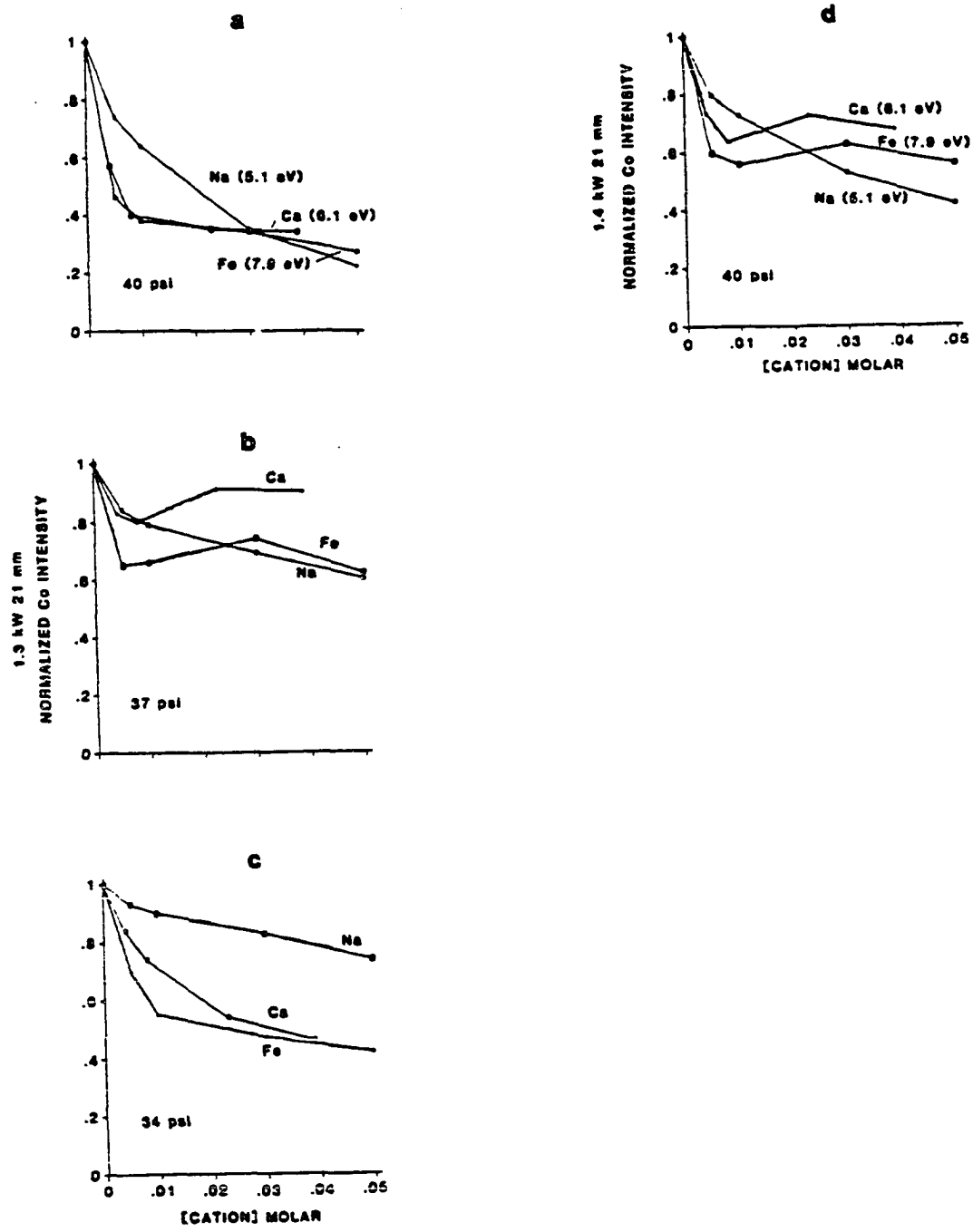

Figure 21. Effect of matrix ion on ionization suppression at 1.3 kW, 21 mm (three aerosol pressures) and at 1.4 kW, 21 mm, 40 psi

aerosol gas flow rate. These changes were visibly observable in the present case because all three matrix ions produced intense emission at a concentration of 0.05 M. The tip of the initial radiation zone was seen to move relative to the load coil depending upon which matrix ion was being nebulized. This type of interference is called a "lateral diffusion interference effect" [30], and is used to explain the signal enhancements observed for some elements in ICP-AES. It is also possible that at high salt concentrations, the ICP must take a longer time to break up the larger particles, and therefore the ionization of analyte is not completed until it reaches a point further downstream in the plasma [32].

The data from a similar experiment are shown in Figs. 19-21. This time the torch position was held constant at 21 mm while the aerosol gas flow rate (pressure) was varied at 1.0, 1.2, and 1.4 kW. Again, Fe was seen to suppress Co ionization to a greater extent than Na although some inversions were produced (Fig. 20b,c; Fig. 21d). These inversions in the order of suppression might be due to reasons described above. Also, at low power (Fig. 19) ionization suppression was again most evident, even at low nebulizer pressures.

Thus, it was not easy to prove conclusively whether the extent of suppression was a function of the mass of the interferent or its ionization energy (or neither), since physical changes in the plasma and nebulizer could complicate matters. Boumans and de Boer found no correlation between

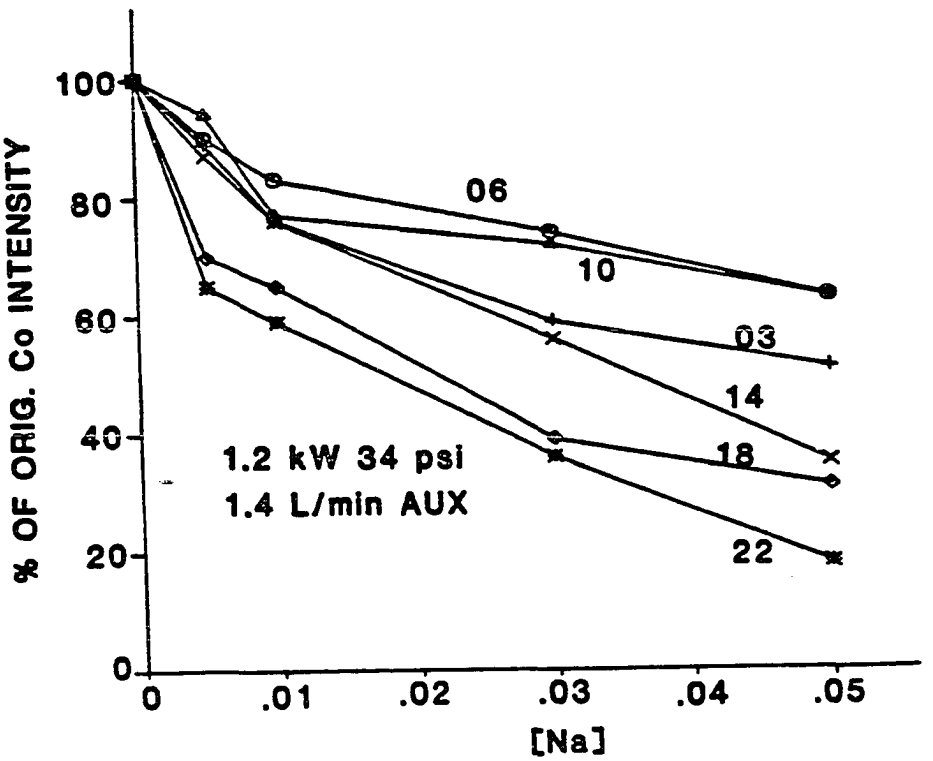

Figure 22. Effect of the ring lens setting on ionization suppression. The labels for each line are settings of the potentiometers used to control the ring lens potential

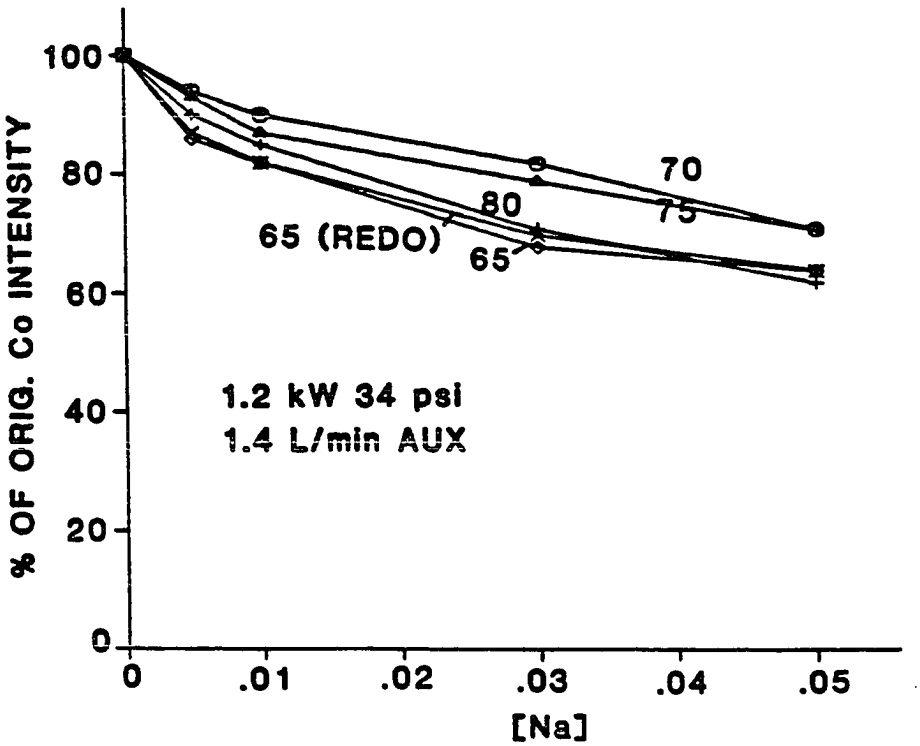

Figure 23. Effect of lens B setting on ionization suppression; REDO was a curve repeated as an accuracy check. Labels are the potentiometer settings for lens B

ionization energy of the matrix element and the extent of the matrix effect [30]. Some kind of mass relationship seemed more likely from the above data, since all three matrix elements should be 95-100% ionized in the ICP, and yet there was a significant difference in the amount of interference induced by each.

The data presented in Figs. 22 and 23 show the effect of ring lens setting (Fig. 22) and lens B setting (Fig. 23) on ionization suppression (see Fig. 6 for lens positions). The settings of the potentiometers were chosen to give a range over which the analyte count rate was fairly constant. One curve (marked REDO) was repeated, just to be sure of the accuracy of these results. Thus, the error associated with each data point in these figures is likely to be $\pm$ 5%.

The ring lens had the greater effect on the extent of suppression, which is a reasonable observation considering that it was closest to the skimmer and was thus in a region of higher local pressure than the other lenses. After all, there would probably be no matrix effects due to the extraction process if the pressure were so low that ions and electrons could not recombine. Again, the value recommended by Sciex (Table 1) was one of the worst at causing interferences. Lenses A and C were run through similar experiments and yielded suppression curves very similar to that for lens B (Fig. 23); that is, the settings on these lenses made little difference in the amount of suppression observed.

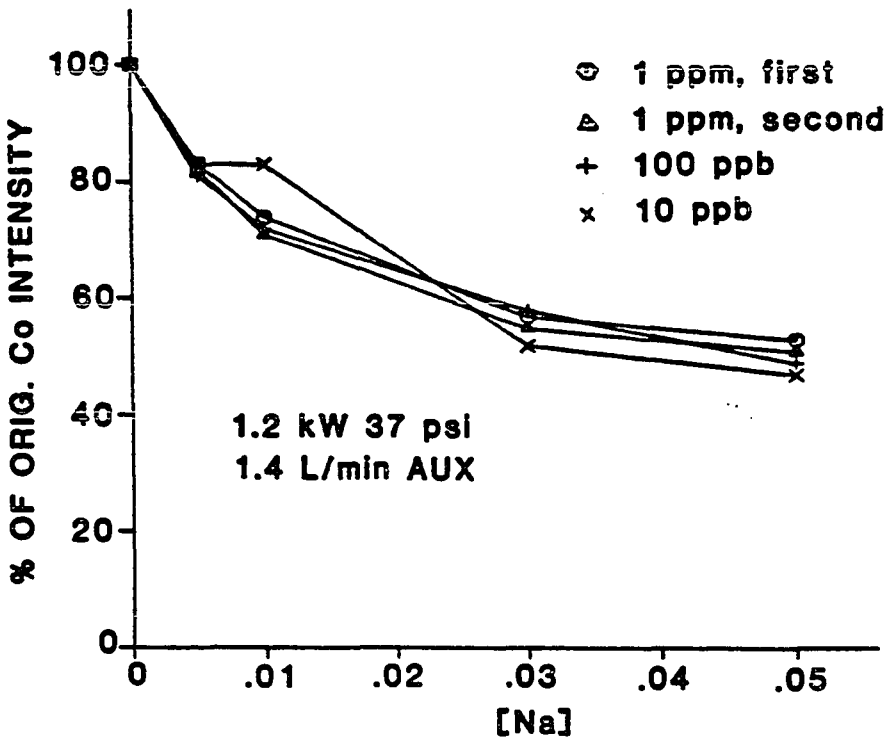

Figure 24. Effect of analyte concentration on ionization suppression; the 1 ppm experiment was repeated as shown

The experiment depicted in Fig. 24 showed that the extent of ionization suppression did not depend on the concentration of the analyte species. This experiment was repeated at three other combinations of flow rate and forward power which confirmed this result. The only effect seen in the lowering of the concentration of the analyte was a loss of precision indicated by the 10 $\mu g\ L^{-1}$ curve deviating from the others in Fig. 24. This was because the Co count rates were sometimes quite low. Reference [30] also found that interference effects depended only on matrix concentration and not on the molar ratio of matrix to analyte.

Finally, as each of the above parameters was adjusted in the direction to give minimal interference, a curve was obtained which exhibited less than 10% suppression at 0.05 M Na. However, detection limits under these conditions were only of the order of 1 mg L^{-1}. Thus, compromise conditions similar to those found by Boumans and de Boer (with good detection limits as well as minimal matrix effects) could not be attained with ICP-MS with pneumatic nebulization.

Ultrasonic nebulization

Figures 25 and 26 contain similar data as was shown in Figs. 12 and 13, except an ultrasonic nebulizer and Ames Laboratory torch were used. The extent of ionization suppression was noticeably worse than before because this nebulizer introduced about 5-10 times more material into the

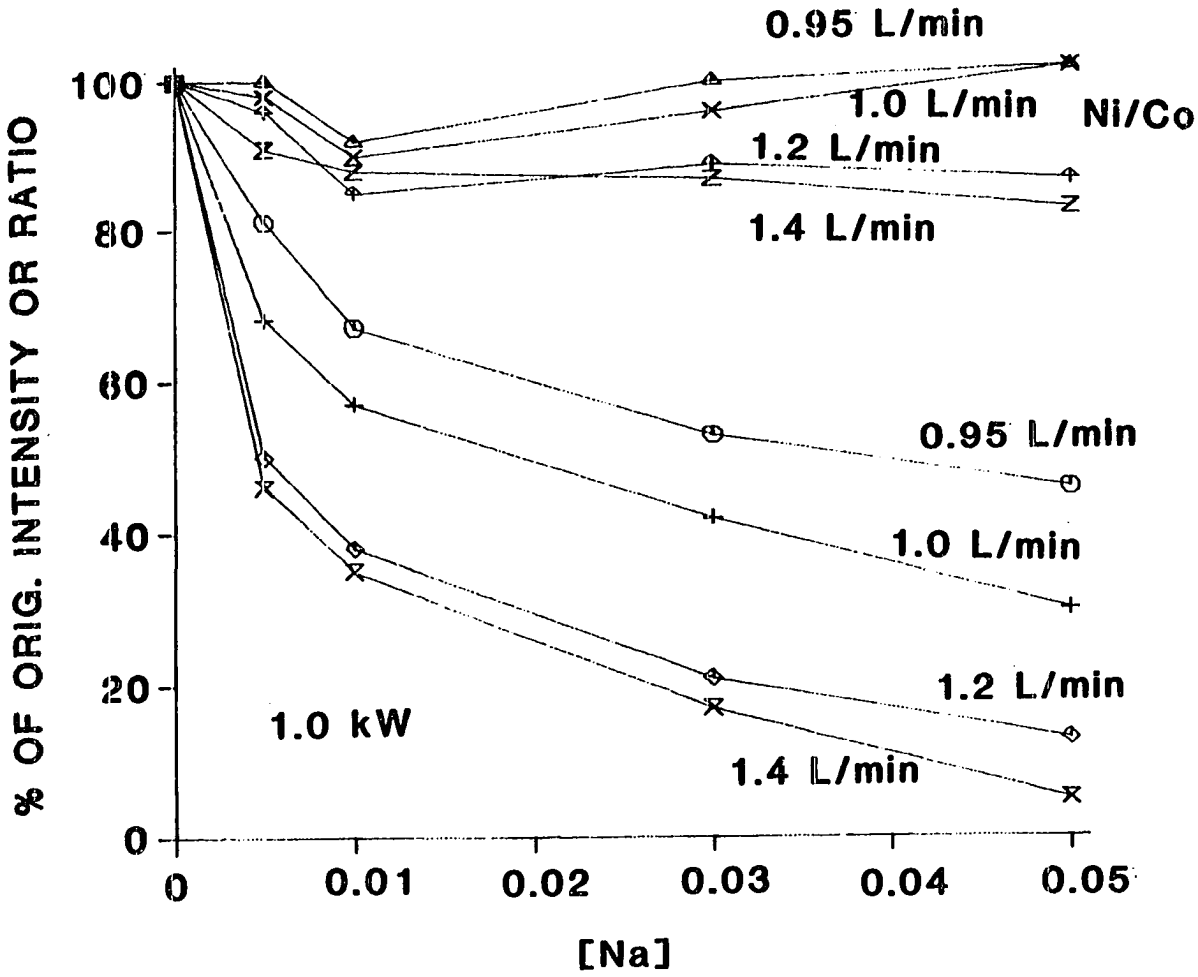

Figure 25. Effect of aerosol gas flow rate on suppression of Co by NaCl at 1.0 kW forward power using the ultrasonic nebulizer (compare Fig. 13)

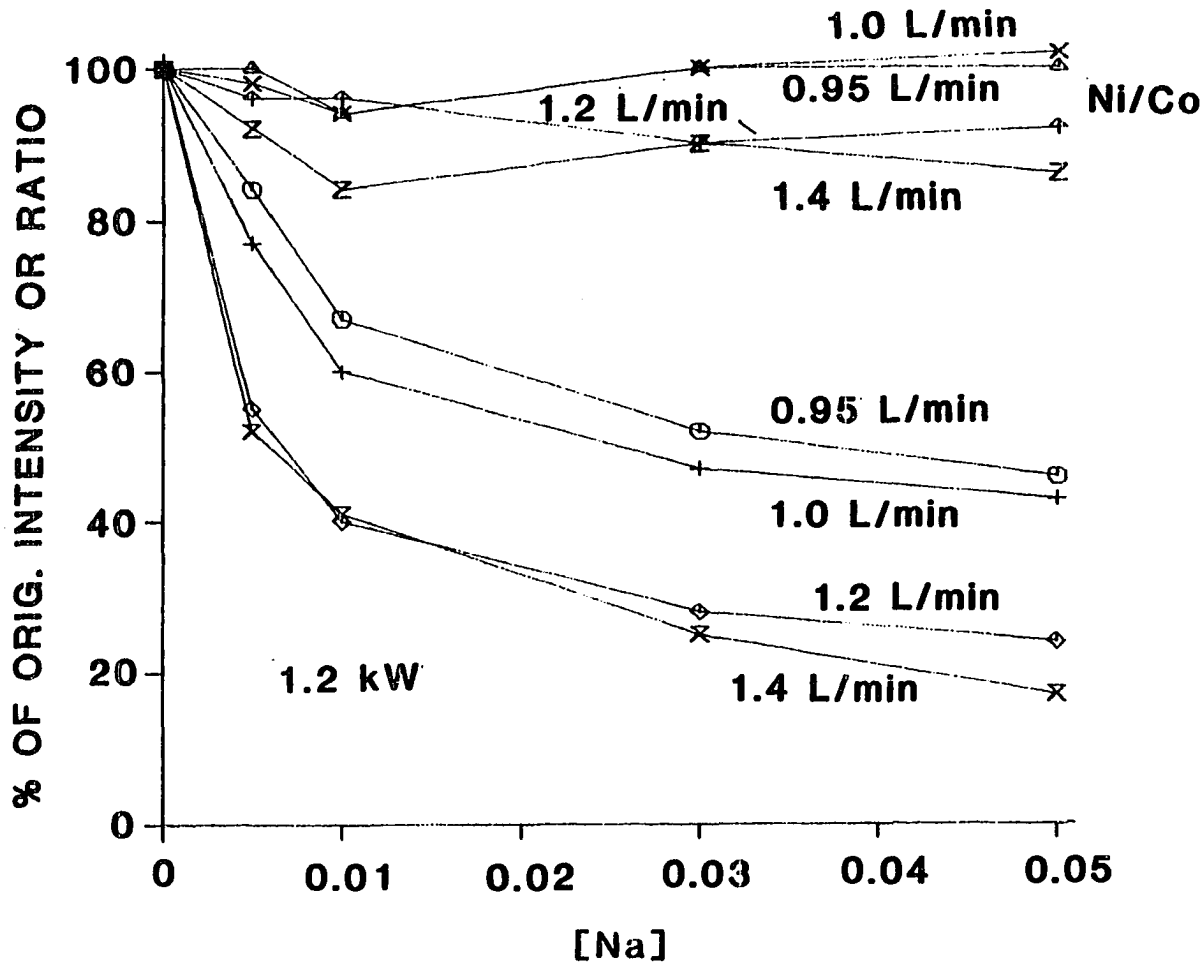

Figure 26. Effect of aerosol gas flow rate of ultrasonic nebulizer on suppression of Co at 1.2 kW forward power (compare Fig. 13)

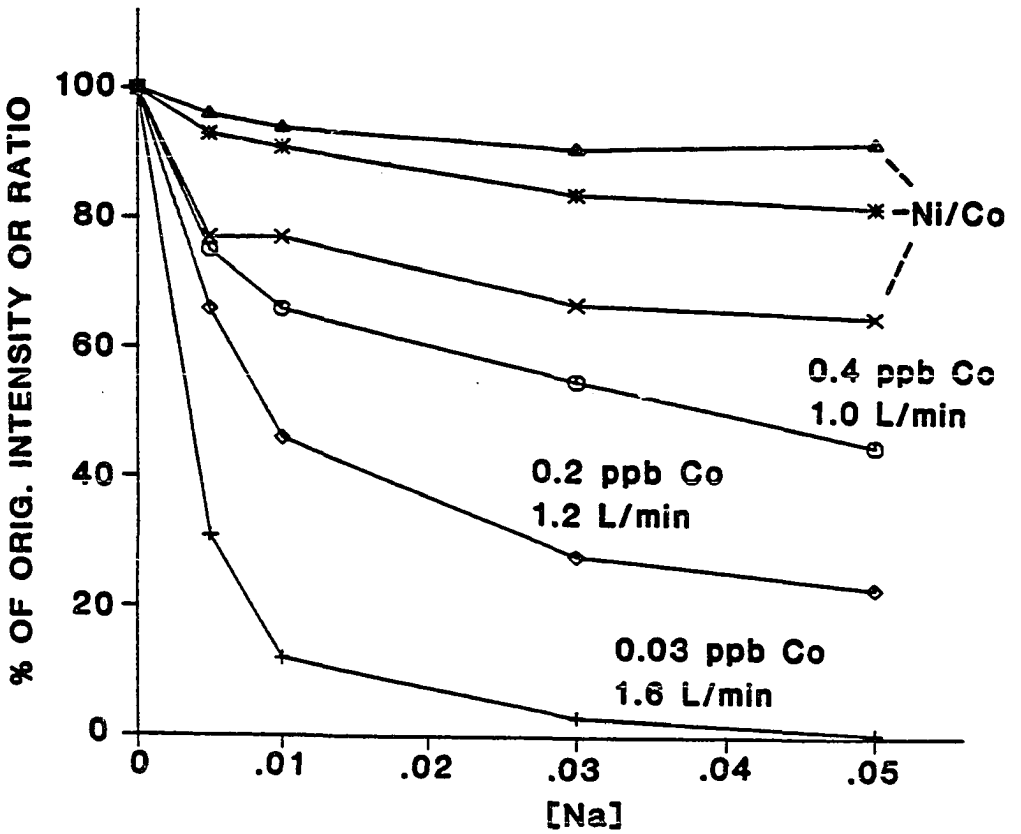

Figure 27. Illustration of the tradeoff between good detection limits obtained at high aerosol gas flow rates (ultrasonic nebulization) and the large extent of ionization suppression. Detection limits were based on the solution without Na

plasma than the pneumatic nebulizer. This takes into account the assumed efficiency of the pneumatic nebulizer (2-3%) and the measured efficiency of the ultrasonic (10-35%). However, because of the increased efficiency, detection limits are improved by, at times, a factor of ten using ultrasonic nebulization [6]. There is, therefore, a tradeoff between the increased powers of detection and the increased suppression. Fig. 27 illustrates this concept. At high aerosol gas flow rates, detection limits were excellent (0.03 $\mu g\ L^{-1}$) for Co in a deionized water matrix and in high resolution, yet ionization suppression was severe (97% at 0.05 M Na).

Simply turning down the aerosol gas flow rate was one way to reduce suppression and still maintain reasonable detection limits (50% and 0.4 $\mu g\ L^{-1}$). Another way was to find conditions which maximized the analyte signal obtained with the matrix present (Fig. 28). These data were found by maximizing the Lu signal (10 $\mu g\ L^{-1}$) from a 40 mg L^{-1} U solution. The optimization process involved turning the aerosol gas flow rate down as well as adjusting forward power, auxiliary flow rate, and the ion lens settings to obtain maximal Lu signal. The suppression curve for Co in Na shown in Fig. 28 was then recorded. Table 7 reports the figures of merit under these conditions. The whole procedure performed in this way took 5-10 min. The advantage of ultrasonic nebulization, therefore, is that aerosol flow rate, evidently the most important factor governing suppression (see above),

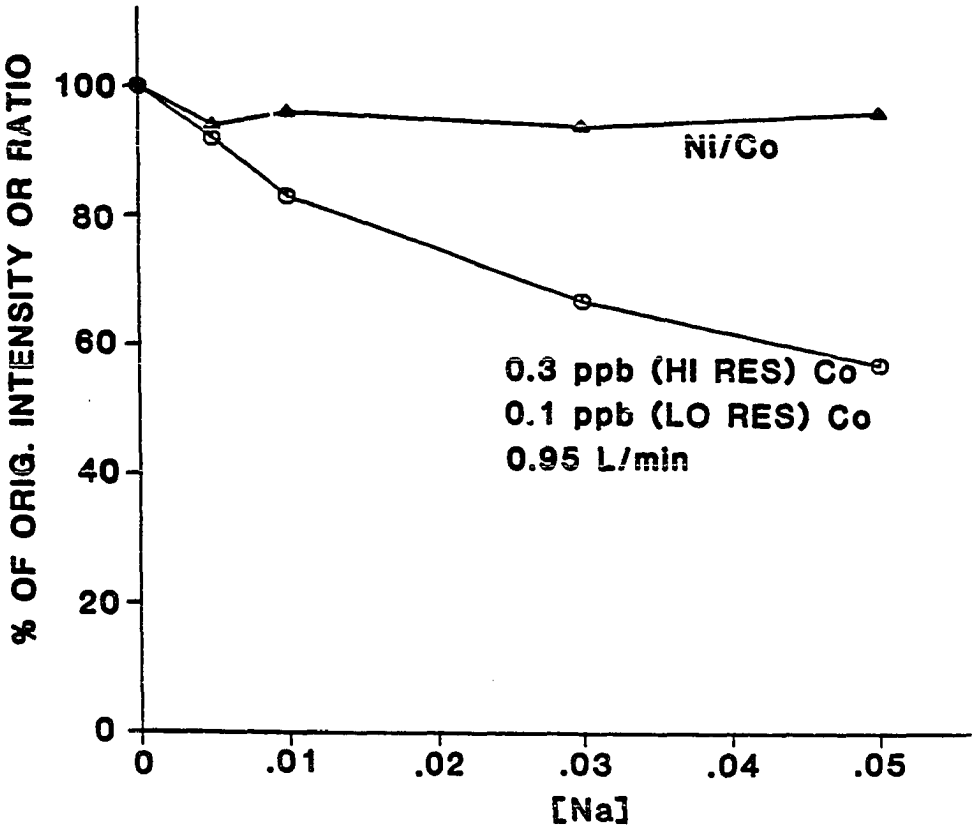

Figure 28. Example of compromise conditions reached quickly using ultrasonic nebulization by optimizing for analyte signal in a 40 mg L^{-1} uranium matrix. Ion lens, forward power, and auxiliary flow rate were changed from Fig. 27

Table 7. Figures of merit for ultrasonic nebulizer under conditions reached in Fig. 28

	Co	Co + 0.05 M NaCl
Detection Limit ($\mu g\ L^{-1}$)	0.1	0.2
Sensitivity (counts s^{-1} per mg L^{-1})	145000 58000	93000 (lo res) 33000 (hi res)
RSD ($Co+$)[a] (%)	2.0	1.2
RSD (Ni^+/Co^+)[a] (%)	0.7	1.0

[a]20 determinations of 2.5 s each.

can be varied independently without also affecting the nebulization efficiency, which is a function mainly of the RF power and frequency supplied to the transducer.

It is difficult to directly compare the two types of nebulizers because of all the variables involved, some of which might change if the instrument were shut down and the nebulizers and torches switched. However, one simple means of comparison exists: to measure detection limits for several elements in, say, a 200 mg L^{-1} U matrix, using any amount of optimization necessary with each type of nebulizer. Uranium is a good choice for this experiment since only a relatively small amount is necessary to cause a large suppression (Chapter III). Thus the possibility of clogging the sampling orifice would be minimized, provided the experiment was performed in a couple of hours. Also, the pneumatic nebulizer should be given first chance since it will deposit less U on the orifice.

The results of this "war of the nebulizers" are shown in Tables 8 and 9. Three differently sized skimmer orifices and three different torches were employed to give more generality to the results. The Sciex short torch measured 34 mm from the injector tip to the outer edge, while the long torch was 41 mm. By comparison, recall that the Ames Laboratory torch measured 38 mm (Experimental section). Detection limits and sensitivities reported in these tables were the best that could be obtained by adjusting the forward power, gas flow

Table 8. Comparison of detection limits ($\mu g\ L^{-1}$) and sensitivity (counts s^{-1} per mg L^{-1}) obtained with ultrasonic (USNEB) and pneumatic (PNEB) nebulization[a]

Conditions[b]		Li	Cu	Cd	Pb
USNEB, U, 0.51 mm	Sens.[c]	1.1 E5	53700	11800	6450
	DL	1	2	0.7	0.8
PNEB, U, 0.51 mm	Sens.	4300	2600	760	280
	DL	35	10	6	14
USNEB, DDW, 0.64 mm	Sens.	1.0 E6	4.0 E5	85000	70000
	DL	0.2	0.08	0.1	0.1
PNEB, DDW, 0.64 mm	Sens.	60000	30000	17000	25000
	DL	0.5	0.3	0.2	0.4
USNEB, U, 0.64 mm	Sens.	1.2 E5	23000	2900	3100
	DL	0.8	3	2	2
PNEB, U, 0.64 mm	Sens.	22000	11000	2200	1900
	DL	0.8	2	1	2
USNEB, U, 1.1 mm	Sens.	1300	380	90	---
	DL	20	20	40	---
PNEB, U, 1.1 mm	Sens.	400	570	100	---
	DL	7	10	30	---

[a]USNEB used with Ames Laboratory torch and PNEB with Sciex short torch.

[b]U = 200 mg L^{-1} uranium matrix; DDW = deionized water; skimmer size is also given.

[c]Blank subtracted, using the appropriate blank.

Table 9. Comparison of detection limits ($\mu g\ L^{-1}$) and sensitivity (counts s^{-1} per mg L^{-1}) in 200 mg L^{-1} uranium matrix using Ames Laboratory and Sciex torches[a]

Torch/Nebulizer	Elements	Sensitivity	Det. Lmt.
Ames/USNEB	Li	67500	0.4
	Cu	22000	5
	Cd	6350	2
	Pb	9070	2
Sciex short/	Li	203,000	0.9
USNEB	Cu	41000	3
	Cd	7800	1
	Pb	8300	1
Sciex long/	Li	160,000	2
USNEB	Cu	41000	5
	Cd	11000	1
	Pb	12000	2
Sciex short/	Li	36000	2
PNEB	Cu	30000	4
	Cd	9900	2
	Pb	6300	3

[a]See text for explanation of torches. Skimmer used had a 0.64 mm orifice.

rates, and ion lens settings while nebulizing the indicated solutions.

Some conclusions can be drawn from these data. First, the ultrasonic nebulizer nearly always exhibited greater sensitivity than the pneumatic nebulizer. The difference in sensitivity decreased as the skimmer orifice size increased (at constant sampler orifice size) and as the concentration of the matrix increased. Detection limits were also usually better using ultrasonic nebulization, but not by as much as would be expected. This was because the background and the standard deviation of the background both increased when employing the ultrasonic nebulizer, for reasons which are not clear at this time. Notice that Li showed the greatest change in sensitivity relative to the other elements when switching from a pneumatic to an ultrasonic nebulizer. This agrees with the fact that the sensitivity of the alkali metals is best at high aerosol gas flow rates [28], because the ultrasonic nebulizer was normally operated at a higher aerosol gas flow than the pneumatic nebulizer.

A second point is that the type of torch used made little difference in sensitivity or detection limits. The Ames Laboratory torch performed somewhat worse than the Sciex torches with respect to these criteria. However, the Ames torch was advantageous when running salt solutions for long periods because its wider aerosol injector tube would not clog

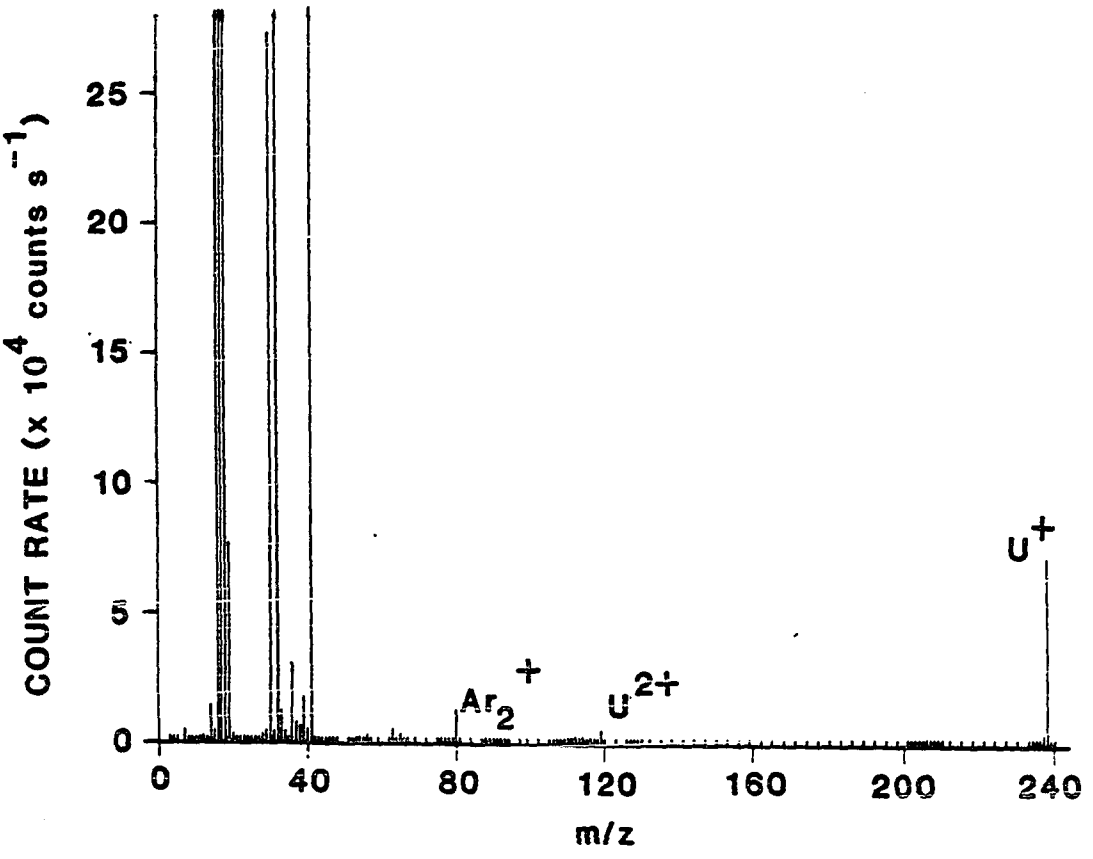

Figure 29. Mass spectrum of a 200 mg L^{-1} uranium solution using a pneumatic nebulizer. Under these conditions (1.2 kW, 0.5 L min^{-1}), the ionization of copper was suppressed by about 60% relative to deionized water. Count rates for the large peaks were not accurate since counting losses occurred

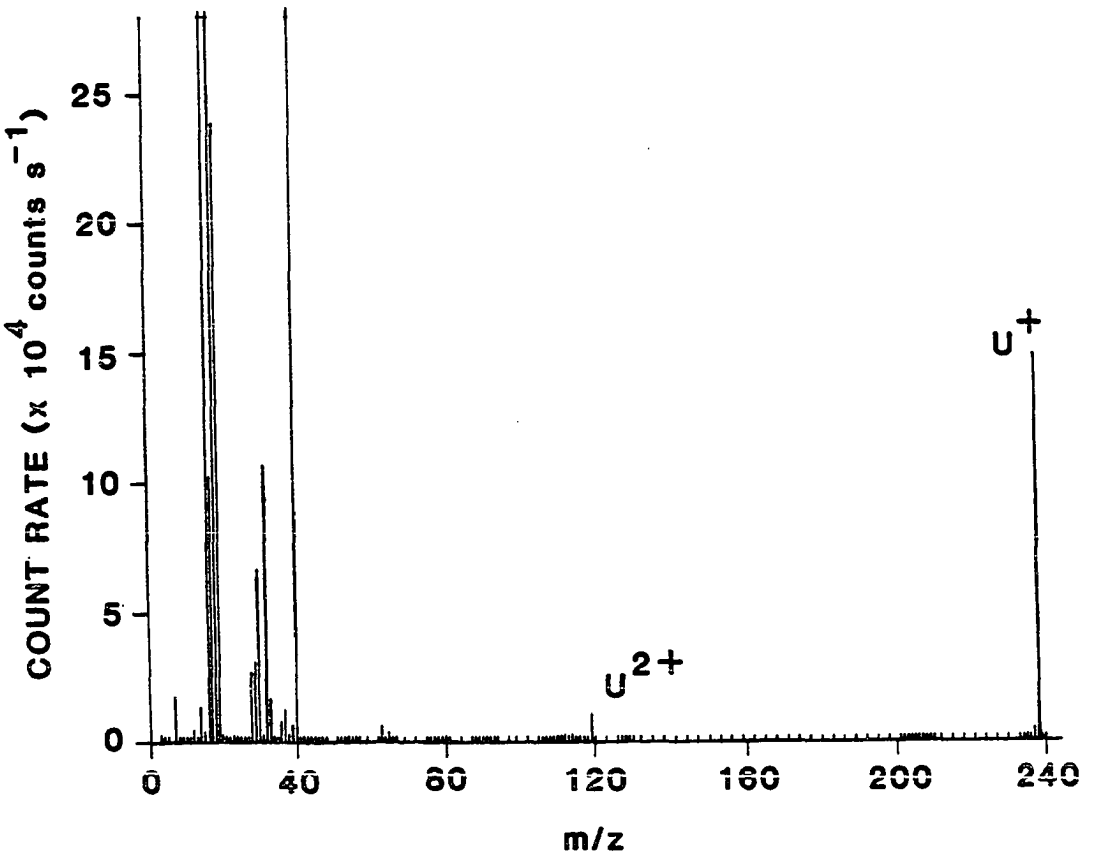

Figure 30. Mass spectrum of a 200 mg L^{-1} uranium solution using an ultrasonic nebulizer. Under these conditions (1.2 kW, 1.3 L min^{-1}), the ionization of copper was suppressed by about 94% relative to deionized water. Count rates for the large peaks were not accurate since counting losses occurred

with condensed solids as easily. There was little difference in short term precision among the three torches.

No further suppression curves were taken with the ultrasonic nebulizer corresponding to Figs. 14-24. It was assumed that responses of the ion lenses, matrix elements, and analyte concentration would be similar. The effects of outer argon flow rate and auxiliary flow rate might be somewhat different, but we have already seen that aerosol flow rate is the most important factor governing the extent of ionization suppression in ICP-MS.

Spectra were taken during the previously described experiments under conditions which gave both large and small levels of suppression with the pneumatic and ultrasonic nebulizers. As can be seen from Figs. 29 and 30, conditions which produced more extensive suppression with the ultrasonic nebulizer corresponded to spectra in which the matrix ion was increased relative to the other background ions in the spectrum. Note, for instance, that in Fig. 30 the peaks around m/z = 30 have diminished compared to Fig. 29, and that the uranium peaks have increased. Others have noted this behavior to a more extreme extent [31]. By taking preliminary mass spectra, it should thus be possible to identify matrix elements and predict which samples should experience suppression (see Chapter III for examples).

Response of various elements to a salt matrix

A solution of over 30 elements was prepared in deionized water, and also in 0.0218 M NaCl. The extent of ionization suppression was then determined using ultrasonic nebulization and the Ames Laboratory torch at three different forward powers: 1.0, 1.2, and 1.4 kW, and at four different aerosol gas flow rates at each power setting. The results of trying to classify the elements according to their general amount of suppression (an arduous task!) is shown in Table 10. In most of the 12 experiments, this order worked quite well to predict which elements would be suppressed similarly, and therefore act as good internal standards for each other. Note Co and Ni, used in Figs. 12-15, are in the same group. Lead and Hg values were unreliable since the matrix contained chloride ion. Rhenium is an element which, in our experience, always behaves erratically in the desolvation system. The behavior of the alkali metals towards suppression depends largely on the aerosol flow rate, as markedly as does their sensitivity [28]. The trends seen in Table 10 correspond roughly to trends in first ionization energy, with the most easily suppressed elements having the highest ionization energies. There are noticeable differences, however, even among the rare earths, which all have similar ionization energies. Lanthanum and Ce, for instance, always behave similarly, even when their amount of suppression varies relative to the other rare earths (see Table 6 as an example,

Table 10. Classification of elemental response to a 0.022 M NaCl matrix. First ionization energies [22] in eV are also listed. Extent of suppression is least as one moves down and to the right in the table

Group 1:	Mg	Zn	Ni	Cu	Co	As	Bi	Se	Fe
I. E.:	7.7	9.4	7.7	7.7	7.9	9.7	7.3	9.7	7.9
Group 2:	Al	Mn	Cd	Cr	Te	Ga	Ge	Pt	Ru
I. E.:	6.0	7.4	9.0	6.7	9.0	6.0	7.9	9.0	7.4
Group 3:	Au	Ir	Ca	W	Ta	V	Ti	Sn	Sb
I. E.:	9.2	9.1	6.1	8.0	7.9	6.7	6.8	7.4	8.6
Group 4:	Nb	Mo	Hf	Sr	In	Zr	Y	Yb	Tm
I. E.:	6.8	7.0	6.7	5.7	5.8	6.8	6.4	6.2	6.2
Group 5:	Er	Ba	Ho	Lu	Tb	Dy	Eu		
I. E.:	6.1	5.3	6.0	5.4	5.8	5.9	5.7		
Group 6:	Nd	Sm	Gd	Th	Pr	Tl	La	Ce	
I. E.:	5.5	5.6	6.1	6.1	5.4	6.1	5.6	5.5	

Depend on aerosol flow rate: Li(5.4), Cs(3.8), Rb(4.1), K(4.4)

where a Lu internal standard was used).

Table 11 indicates the long term precision with which ratios of several elements can be determined relative to a ^{66}Zn internal standard in deionized water. The experiment was repeated under completely different conditions (last column) in order to verify the results. The presence of ^{68}Zn in the element list allowed one to judge the best precision to be expected from this experiment, because it was not expected that the precision of an analyte/internal standard pair would be better than an isotope ratio. Elements in zinc's "group" (Table 10), namely Mg, Al, Co, and As demonstrated good long term precision while other elements did not fare as well. Thus, there was a correlation between an internal standard's effectiveness at overcoming ionization suppression and its ability to give stable long term precision in a deionized water matrix. This result was also noted in the analysis of uranium (Chapter III).

Table 12, unfortunately, shows that the situation is not so clear. As the matrix was changed from 0.0218 M Na to an equimolar amount of Fe (as $Fe(NH_4)_2(SO_4)_2.6H_2O$) the relative order of suppression changed for the elements tested. In other words, Co experienced more suppression in the Fe matrix (as was seen in Figs. 16-21), but Bi experienced a marked reduction in the extent of suppression, which would certainly displace it from the same group as Co (Table 10).

Figures 31 and 32 provide similar information in a

Table 11. Long term precision of various elements relative to ^{66}Zn internal standard: 27 determinations of 0.5 s MT (3 M/P), 100 ms DT spread out over 1 hour

Element	%RSD[a]	%RSD[b]
Li	1.6	3.8
Mg	3.3	2.1
Al	1.8	3.3
Ti	6.2	3.8
Co	2.1	2.3
As	1.3	2.3
Zr	6.1	2.3
Pb	4.5	5.5
Lu	5.4	3.7
^{68}Zn	2.0	2.1

[a]Conditions: 1.3 kW, 1.3 L min^{-1} aerosol gas flow rate, 23 mm from load coil.

[b]Conditions: 1.2 kW, 1.2 L min^{-1}, 26 mm.

Table 12. Percent of signal recovery of various elements from 0.022 M Na and Fe matrices at various aerosol gas flow rates[a]

		1.0 L min^{-1}		1.2 L min^{-1}	
Element	I.E.(eV)	Na	Fe	Na	Fe
Ba	5.3	48	60	37	49
Bi	7.3	19	45	11	27
Co	7.9	39	22	27	14
La	5.6	49	73	38	57
Rb	4.1	77	40	66	34
Tl	6.1	39	67	28	49
W	8.0	41	45	27	29
Zr	6.8	57	34	45	28
		1.4 L min^{-1}		1.6 L min^{-1}	
		Na	Fe	Na	Fe
Ba		32	33	39	37
Bi		4	9	1	6
Co		9	4	3	4
La		49	41	59	35
Rb		43	24	54	53
Tl		16	32	8	28
W		11	12	6	7
Zr		29	14	19	17

[a]Conditions: 1.2 kW, 26 mm from load coil, 0.9 L min^{-1} auxiliary flow rate, ultrasonic nebulization.

different format. Here, the normalized internal standard ratios of various elements are plotted at various molar concentrations of Na and Fe. These data were taken with a new Sciex ion lens installed. First, notice that the Fe again caused a greater change in the ratios than Na. The order of effectiveness for the four elements as an internal standard for Co was Ni>Bi>Al>Tm in both cases. This corresponded closely to trends in ionization energy (Table 10) and seemed to verify the results of Table 10. In addition, heavier elements seemed to be suppressed less than lighter ones. Thulium and Al have nearly the same ionization energy, and yet the Tm/Co ratio was substantially different from the Al/Co ratio in both matrices. Note that taking the whole suppression curve is more time consuming than taking just one point, as in Tables 10 and 12, but it avoids possible misinterpretations of the data. If only the 0.005 M matrix were examined in Fig. 32, for example, Bi would appear to be the least appropriate internal standard.

Conclusion

If we assume that the matrix effects observed in ICP-MS are a composite of interferences due to the nebulizer, ICP and the interface, then it is only logical to conclude that the ion sampling process is the main cause of the substantial ionization suppression observed in this chapter. This is because the nebulizers and ICP themselves have been shown to

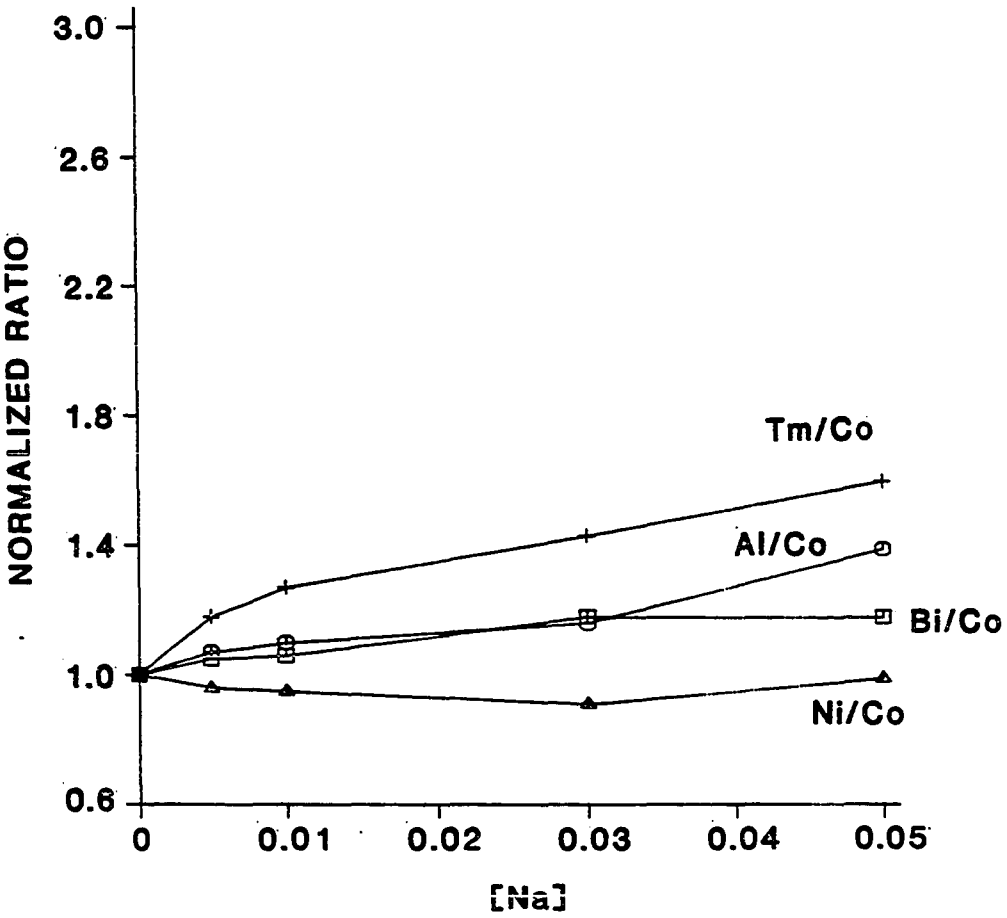

Figure 31. Effect of sodium matrix on various elemental ratios

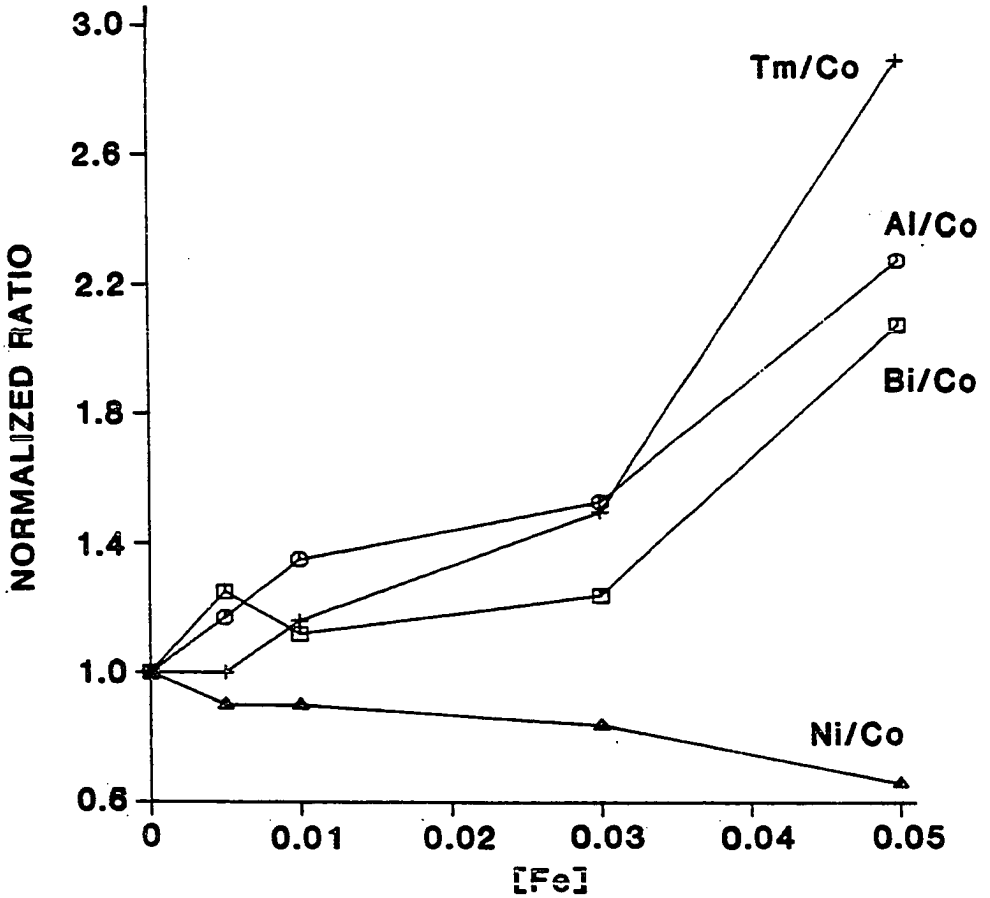

Figure 32. Effect of iron matrix on various elemental ratios

be relatively free from matrix effects by previous work in AES. The causes of matrix effects in the sampling process are now under investigation [33]. The gas expanding inside the expansion stage is much cooler than the bulk plasma and perhaps at a high enough pressure so that ion-electron recombination reactions can still occur. After any such reactions, the atoms would be at too low a temperature to experience re-ionization from collisions. The presence of large amounts of Na ions in the jet, for instance, would necessitate having a larger number of electrons nearby to maintain charge neutrality. The spatial distribution of these electrons and, therefore, the extent of analyte-electron recombination might be different in the absence of a Na matrix, because, left to themselves, the lighter electrons would disperse towards the outer regions of the jet. The "jet" dispersal might also explain why heavier matrix elements seem to cause more suppression: they tend to stay in the center of the beam, thus attracting more electrons. Another mechanism for matrix effects in the extraction process is the deposition of solids on the skimmer and inside the sampler cone. This process might trap analyte material in the matrix as it condenses, similar to nebulizer-type interferences. Thus, the extent of this removal would depend on the volatility of the analyte and matrix elements or compounds.

CHAPTER III. ANALYTICAL RESULTS

Uranium Analysis by Solvent Extraction

Introduction

In light of the previous discussion on ionization suppression, one obvious way to improve ICP-MS performance is to remove a large matrix from the trace elements of interest. The following section describes, for the first time, the coupling of solvent extraction techniques to ICP-MS. We chose the analysis of uranium as a suitable and important problem because current methods leave room for improvement in both the selectivity and efficiency of the extractant used and in the powers of detection available [34-41]. Only the procedures and results relevant to this dissertation are discussed below; the properties of the extractant used are discussed in more detail in a recent publication [13].

The above mentioned reference also describes previous techniques used for determination of trace metals in uranium, many of which employ solvent extraction with ICP-atomic emission spectrometric (ICP-AES) detection [36-41]. Both ICP-MS and ICP-AES are capable of multielemental analysis, but in the present application ICP-MS has two main advantages over its sister technique. Spectral interferences from U are not a problem in ICP-MS in that U^{+2} (m/z = 117, 117.5 and 119) is the only uranium species observed in the m/z range

corresponding to analyte elements. In contrast, excitation of U in the ICP produces thousands of emission lines [42] that obstruct analyte lines even at moderate U concentrations. A second advantage of ICP-MS is the very low detection limits (10-100 ng L^{-1}), which are often an order of magnitude better than ICP-AES [6]. With the uranium matrix removed by solvent extraction, these detection limits can be fully realized.

Apparatus and procedures

The ICP-MS instrumental parameters are listed in Table 13; again ultrasonic nebulization and the Ames Laboratory ICP torch were employed. The multichannel scanning mode was chosen (Chapter II). In this mode the mass analyzer made a 0.1 s measurement at each of three m/z positions spaced 0.1 dalton apart on the top of a chosen peak. The mass analyzer then jumped to the next chosen peak, atop which another three measurements were made at 0.1 dalton intervals. This sequence was repeated until the dwell time accumulated for each channel was 0.5 s. The three count rates for each peak were then averaged and divided by the average count rate for the internal standard to yield one "determination." Typically, six such determinations were done for each of ten elements. Therefore, the total analysis time for each sample was approximately 90 s, i.e., the mass spectrometer acquired data for a total of 9 s for each element. The standard deviations for individual sample concentrations were based on the average of the six determinations.

Table 13. Sciex ICP-MS operating parameters

ICP torch	Ames Laboratory design [18], torch extended 1.5" from aerosol injector
Outer argon flow rate	12 L min^{-1}
Auxiliary flow rate	0.8 L min^{-1}
ICP forward power	1.30 kW
Aerosol flow rate	1.2 L min^{-1}
Solution uptake rate	2.5 mL min^{-1}
Sampling position	20 mm above load coil, centered on axial channel
Sampler orifice	1.2 mm diameter
Skimmer orifice	0.90 mm diameter
Pressure, quadrupole chamber, ICP on	4 X 10^{-5} torr
Ring lens (#1 in Fig. 6)	Setting: 07 (-4.38 V at TP[a])
AC rods (#2)	Grounded
Ion shield (#3)	Grounded
Lens #4	Setting: 20 (-4.00 V at TP)
Lens #5	Setting: 65 (+6.19 V at TP)
Lens #6	Setting: 79 (-15.78 V at TP)
Entrance AC rods (#7)	-5.10 V bias (at TP)
Mass filter (#8)	Zero DC bias
Exit AC rods (#9)	-5.10 V bias (at TP)
Exit shield lens (#10)	-5.00 V (at TP)
Exit lens (#11)	-130 V (at TP)
Deflector	+3370 V (at TP)
Electron Multiplier	-2790 V (-4.18 at TP)

[a]TP = test point. Test point voltages are not necessarily identical to the voltages actually supplied to the device.

Multielement standards were prepared by combining and diluting single element reference stock solutions. The rare earths were obtained at Ames Laboratory, dried, weighed (as oxides) and dissolved in dilute nitric acid (in deionized water). The purity of these standards was verified by ICP-MS by scanning the entire mass spectrum of a 1000 mg L^{-1} solution. No impurities were found in the concentrated standards above a 10 μg L^{-1} level. Other stock solutions came from Fisher Scientific. The 1% (v/v) HNO_3 used to dilute all samples and standards was made from the reagent grade acid (Fisher Scientific), except for the experiments where the low mass blanks became substantial at the 10 μg L^{-1} level. For those experiments, sub-boiling distilled nitric acid, made in an all quartz apparatus, was required. Deionized water came from either a Milli-Q water purifier (Millipore Corporation) or from a Nanopure II system (Barnstead). The digital pipets (Rainin) used in dilution and in the addition of the internal standard were calibrated gravimetrically and found to be within the manufacturer's specifications for precision and accuracy (better than 2% at all the volumes used).

The solvent extractant used was N,N-dihexylacetamide (DHA) in toluene. Its preparation and properties are discussed in Ref. [13]. The uranyl nitrate was obtained from Fischer Scientific.

For the separation and determination of trace metals in a uranium matrix, a 119,000 mg L^{-1} (0.5 M) solution of U in 2 M

HNO_3 was made up from uranyl nitrate salt. Various trace metals were added to the uranium solution so that their final concentration was 100 or 10 $\mu g\ L^{-1}$ (0.84 or 0.084 μg per g of U). An aliquot of the spiked uranium solution was then extracted three times with an equal volume of 2 M DHA in toluene. An aliquot of the aqueous phase was taken, evaporated almost to dryness, dissolved in 1% HNO_3, spiked with the internal standard, and analyzed by ICP-MS. Lutetium was the internal standard for the rare earths while rubidium and holmium were used as internal standards for other metals.

The instrument was adjusted to give optimal performance as follows. Approximate settings of the aerosol gas flow rate and forward power were made, such as those that had worked on the previous day. A solution containing 10 $\mu g\ L^{-1}$ of both Ho and Lu in 1% HNO_3 was introduced and the ratio Ho/Lu was measured several times. This ratio was then compared to that from a 10 $\mu g\ L^{-1}$ solution made up in 50 mg L^{-1} U. If the ratios were significantly different, the forward power was slowly changed until the ratios coincided. Then the Ho/Lu ratio was monitored for about ten minutes to see if it would drift. If it did, by more than 5%, a slightly different aerosol flow rate was chosen, and the procedure was repeated.

The standards used were not run through the extractions with the samples. Instead, a single blank was carried through the procedure along with 3-4 samples. This insured that trace impurities in the 0.5 M U, which might be substantial at the

10 μg L^{-1} level, would be detected. Standards contained either 10 or 100 μg L^{-1} of the internal standard, and were matrix matched to contain the same amount of uranium as the samples. Calibration curves were prepared using 2, 5, 10, and 30 μg L^{-1} standards (or ten times higher for the high blank metals). During the analysis, the 10 μg L^{-1} standard was reintroduced after each sample to verify that the calibration curve had not shifted. If there had been a small drift, this data could be used to normalize subsequent sample concentrations.

Results and discussion

Two problems with the Sciex instrument were calibration curve drifting and severe matrix effects from $\bar{U}$, even at U concentrations as low as 100 mg L^{-1} (0.01%). Internal standardization, by itself, did not correct these faults. However, replacing the pneumatic nebulizer with the ultrasonic one facilitated selection of forward power and aerosol flow rate such that internal standardization would compensate for these effects. It was much easier to optimize performance by adjusting the aerosol flow rate with the ultrasonic nebulizer than to change the relatively fixed flow rate from the pneumatic. Furthermore, as we have seen in Chapter II, this optimization could be performed without affecting the nebulization efficiency, thereby preserving detection limits to some extent. As noted above, these conditions enabled us

to keep 10 μg L^{-1} rare earth ratios constant (within 3%) for concomitant uranium concentrations up to 50 mg L^{-1} over a two hour period. In other words, the same set of conditions alleviated both the drifting and interference problems at once, the only drawback being a three or fourfold worsening of the detection limits.

After two extractions with DHA, the uranium concentration (originally 120,000 mg L^{-1}) was found to be about 150 mg L^{-1}. The Sciex instrument, when set at the conditions noted above, had difficulty determining trace elements in this matrix; 10 μg L^{-1} was very close to the detection limit under these circumstances. However, after three extractions the uranium concentration fell below 3 mg L^{-1}. Long term drifting of the analyte signal and ratios was then the main problem encountered along with contamination of the samples by the organic phase. Spectral interferences by metal oxide ions (MO^+) were not a problem at the 10 μg L^{-1} level because the ratio MO^+/M^+ was less than 1% under the conditions employed.

Table 14 lists the relative amounts of metals in the deionized water, distilled HNO_3, and evaporated 2 M HNO_3 compared to a 2 μg L^{-1} Co signal. Values in this table are only semiquantitative in nature, since they are uncorrected for the different isotopic abundances of the elements and other sensitivity factors. The blank corrected recoveries of the trace elements added to the uranium solution are listed in Tables 15 and 16. The amount of spiked material originally

Table 14. Background signal from various elements relative to 2 $\mu g\ L^{-1}$ Co[a]

Element	m/z	Deionized H_2O	Distilled 1% HNO_3	Evaporated Distilled 2 M HNO_3
Al	27	0.1	0.3	6.5
Ba	138	0.1	0.1	9.4
Cd	180	0.3	0.3	0.1
Cr	52	0.2	0.4	0.4
Cs	133	0.05	0.09	0.1
Cu	63	0.4	0.4	0.5
Mn	55	0.07	0.1	0.3
Pb	208	1.5	5	6
Sr	88	0.1	0.1	1.5
Ti	48	0.06	0.1	0.2
Th	232	0.3	0.3	0.4
Y	89	0.05	0.1	0.1
Zn	66	0.05	0.1	2.5
Zr	90	0.06	0.2	1.7

[a]Values are not corrected for isotopic abundances or other sensitivity factors but merely reflect approximate levels of trace impurities in the reagents used, for comparison purposes.

Table 15. Recoveries of rare earth elements[a] from a 119,000 mg L^{-1} U solution

Metal Ions	m/z	Number Of Trials[b]	Average Recovery %	Relative Standard Deviation %
Ce	163	10	90	12
Dy	166	10	93	5
Er	153	10	97	4
Eu	157	10	95	16
Gd	165	10	92	11
Ho	139	10	97	5
La	139	10	92	13
Nd	146	10	90	13
Sm	152	10	95	16
Tb	159	10	95	9
Tm	169	10	99	5
Yb	174	10	100	3

[a]All the rare earths were recovered at the 0.084 μg per gram of U (10 μg L^{-1}) level.

[b]Obtained on three different days.

Table 16. Recoveries of metals from 119,000 mg L^{-1} U solution

Metal Ions	m/z	Recovery Levels $\mu g/g$ U	Number Of Trials[a]	Average Recovery %	Relative Standard Deviation %
Al	27	.84	8	112	21
Ba	138	.84	8	104	7
Cd	180	.084	13	105	16
Cs	133	.084	14	97	10
Co	59	.084	14	98	20
Cr	52	.84	11	107	10
Mn	55	.084	14	95	16
Pb	208	.84	11	112	24
Sr	88	.084	14	99	16
Ti	48	.084	14	87	13
V	51	.84	8	95	15
Y	89	.084	14	98	8
Zn	66	.84	8	99	24
Zr	90	.84	14	106	33

[a]Obtained on 3 or 4 different days.

added was varied according to the level of trace impurities present in the blank in order to avoid the imprecision of subtracting two numbers of nearly equal magnitude. The high blanks for Al, Ba, and Pb are likely due to impurities in the HNO_3 which have been concentrated in the evaporation step (see Table 14). The uranium used in the recovery studies was identical to the "unknown" in Table 17. Therefore, the metals which exhibit high blanks could also be native impurities in the uranium. Attempts to find recoveries for Fe and Cu at 100 $\mu g\ L^{-1}$ were precluded by significant background in the ICP-MS itself at these masses. Boron could not be determined with the ultrasonic nebulizer used, probably due to loss of B in the desolvation system.

The RSD (relative standard deviation) for individual sample measurements was usually less than 3%, which reflects the short term stability of the instrument. The RSD within a run of 3-4 samples (separately extracted) was between 3-10%. However, the day to day variation was larger, as is reflected by the RSD values in Tables 15 and 16. In general, those elements with lower blanks, or with one major isotope, had better RSDs in their recoveries.

Once the recoveries had been demonstrated, the method was used to determine the level of impurities in a reagent grade Fisher uranyl nitrate salt. The results in ng/g U are given in Table 17. The standard deviations are rather high because of the low levels of the elements present as well as the high

Table 17. Concentration of trace elements in a uranyl nitrate sample (four trials)

Metal Ion	Average Concentration ng/g U	SD ng/g U	Detection Limits ng/g U[a]
Al	360	190	9
Ba	940	37	0.5
Cd	31	11	2
Ce	2.8	0.6	0.3
Co	55	6	2
Cr	620	68	7
Cs	<0.3		0.3
Dy	<1.3		0.8
Er	<0.9		0.4
Eu	<0.4		0.4
Gd	<0.8		0.8
Ho	<0.1		0.1
La	<1.0		0.4
Mn	130	13	3
Nd	<2.4		0.8
Pb	400	87	0.8
Pr	<0.7		0.3
Sm	<1.3		0.8
Sr	86	9.7	0.2
Tb	<0.2		0.2
Ti	120	35	5
Tm	<0.5		0.2
V	110	8	4
Y	120	13	0.2
Yb	<0.3		0.3
Zn	560	280	8

[a]Concentrational detection limits in $\mu g\ L^{-1}$ are 0.088 x (ng/g U).

blanks (from the HNO_3) and drifting of the analyte signal. The detection limits for elements in a 2 μg L^{-1} uranium solution (calculated at three times the standard deviation of the background) are also given in Table 17. These detection limits are ten to a hundred times better than those for comparable extraction/detection experiments reported in the literature [36,38,41]. Thus, the utility of the present method is clear, especially if modest increases in precision could be made.

Isotope Ratio Measurements

Introduction

ICP-MS can quickly determine isotope ratios of trace elements in solution with moderate (1% RSD) precision. This capability has numerous potential applications, three of which are obtaining geological information from rocks and ores, using isotope dilution techniques to measure element concentrations, and tracing the pathways of various metallic elements through the body by use of stable isotope labelling.

Most geological applications require very precise isotope ratio measurements which are normally made with a magnetic sector instrument such as the one designed by Nier and improved by McKinney et al. [43]. A typical analysis [44], for example, involved determining the approximate age of a rock by use of the Rb-Sr "clock." All the geologist needed to

know was the $^{87}Sr/^{86}Sr$ ratio (in the presence of ^{87}Rb) and the concentration of Rb and Sr. Samples were crushed and dissolved in mineral acids, evaporated to dryness, and then leached with dilute HCl. The Sr was then separated from the Rb and other elements on an ion exchange column and placed as $SrCl_2$ on a Re filament in the source of the mass spectrometer. A typical result was $^{87}Sr/^{86}Sr = 0.7105 \pm 0.0007$ (0.1 % precision). The Rb and Sr concentrations were determined by X-ray fluorescence.

Although there are several "clocks" which involve elements for which ICP-MS exhibits excellent sensitivity (e.g., ^{87}Rb-^{87}Sr, ^{187}Re-^{187}Os, and ^{176}Lu-^{176}Hf [45]), ICP-MS does not, at present, make isotope ratio measurements with the precision of a magnetic sector instrument. However, less time is required to manipulate the samples and so sample throughput is higher using ICP-MS. Hence, applications might include the rapid screening of many samples in geological survey work to search for abnormal ratios that would be easily detected by ICP-MS. Lead solutions have already been analyzed with this in mind [46].

Some applications of isotope dilution are summarized in reference [6]. In isotope dilution, a solution of unknown concentration but known isotope ratio is spiked with a known amount of enriched isotope. The isotope ratio of the mixture is measured, from which the concentration of the unknown can be determined. The use of isotope dilution should provide

accurate concentration measurements in the presence of a significant background matrix. Although isotope ratios change with variations in a matrix as described below (Table 22), this should not be a problem using isotope dilution because both the original and spiked ratios are measured in the same matrix. A recent analysis of seawater by ICP-MS indicates good agreement between isotope dilution and standard addition results [47].

We are concentrating our efforts on the third application: stable isotope tracing. Workers in the fields of biomedicine, biochemistry, and nutrition have long been interested in how metallic elements, which are necessary parts of our diet, are retained, distributed, and eliminated from the body. One aspect of this research is to determine the "bioavailability" of metals in different foods, that is, whether the body absorbs a certain metal more readily if it is ingested in one foodstuff or another. Of course, the way to follow metals on their path through the body and to determine the amount absorbed is to "tag" or label the metal somehow before ingestion and then monitor the subject's blood, urine or feces for the presence of that tag. It is then of interest to verify that an extrinsically added label (simply mixed in with the food) is absorbed to the same extent as an intrinsic label (in which the food is biosynthesized with the label). If absorption is identical, it is obviously easier and faster to just add the label externally.

Traditional investigations have used radioisotopes to label elements of interest [48]. The discovery of ways to produce artificial radioisotopes in the late 1930s provided the impetus for these experiments. The methods were quite sensitive and required only inexpensive detectors (counters). However, the use of stable isotope tracers has recently come into vogue for several reasons. Most importantly, the detrimental effects of radiation on human health have been of concern, especially when the subjects are pregnant women or young children. Secondly, some elements of vital nutritional importance were not easily traced by the radioactive method, because either the isotopes used had insufficient activity, or they had too long or too short a halflife [48]. Zinc and copper are examples. A third reason was the availability of gram quantities of highly enriched materials at reasonable cost, provided by facilities such as Oak Ridge National Laboratory.

Although interest in stable isotope tracing has been high, a major obstacle in its implementation has been the lack of a suitable detector. Bioavailability studies do not require isotope ratios to be measured with exceptional precision (as opposed to geological applications) [49]. However, poor precision can lead to inaccurate estimates of the fractional absorption of a metal, especially when the absorption is low [49]. At higher absorptions it is often the biological variability that determines the accuracy of the fractional

absorption. An ideal detector, therefore, would be capable of measuring isotope ratios with better than 1% precision on small amounts or concentrations of biological material with minimal sample preparation. Because of the large numbers of samples generated by even a single bioavailability study, sample throughput is also a very important factor. Lastly, the detector should be applicable to a broad range of elements (there are at least twenty elements considered to be dietary essentials) existing in several different types of matrices.

Neutron activation analysis (NAA) is virtually the only method of stable isotope detection that does not invoke mass spectrometry. It suffers from numerous disadvantages: the measurements are slow and not especially accurate or precise; elaborate methods are required to avoid interferences, and the dangers of radiation exposure are always present. In spite of this, some nutritional studies have been made using NAA [49].

Thermal ionization mass spectrometry (TIMS) provides excellent precision and accuracy in the measurement of isotope ratios, but again suffers from very low sample throughput: perhaps a few per day. Still, this is probably the most widely used technique in nutritional studies at present [50,51].

Recently, new instrumentation has been developed for use in nutritional tracer studies. A commercial quadrupole instrument has just been introduced which uses a thermal ionization source [52], based on the work of Yergey et al.

[53]. This gives greater sample throughput, is less expensive than TIMS with magnetic instruments, and demonstrates promising precision (0.1-1.0%) in the measurement of isotope ratios. It remains to be seen if it will improve on the traditional drawbacks of TIMS: namely, the lack of multielement capability, and the tedious corrections for isotopic fractionation needed to calculate accurate isotope ratios.

Other recent work has shown that conventional organic mass spectrometers can be adapted for use in inorganic isotopic analysis. Volatile metal chelates can be formed and introduced into a mass spectrometer by either gas chromatography (GC-MS) [54,55] or by direct insertion probe, using electron impact (EI) or chemical (CI) ionization [56]. Although more rapid than TIMS (15 minutes per sample [56]), these techniques generally have not shown the required precision and accuracy needed for nutritional research, and additional sample preparation is required to form the volatile chelates. Fast atom bombardment mass spectrometry (FAB) has shown the ability to quantitate Ca isotopes very rapidly and with good precision (0.3%) and accuracy directly on small volumes of plasma [57]. However, if no sample preparation is used to separate isobaric ions, the mass spectrometer must always be operated at high resolution. This necessitates a corresponding loss of transmission. For instance, although Ref. [57] reports excellent sensitivity for Ca operating at a

resolution of 5000, the author notes that the presence of significant amounts of K would cause an interference at m/z = 40 due to ^{40}K, which would require a resolution of 28000 to separate from ^{40}Ca. Fortunately, the samples did not contain appreciable amounts of K. The analysis time requirements for FAB are not mentioned in Ref. [57] but are probably comparable to EIMS. An extension of the FAB technique to Fe [58] did require a solvent extraction to remove isobaric Ni, and precision was not as good as that reported in Ref. [57]. It remains to be seen whether FAB is a viable measurement technique for other elements and in different matrices.

Just two years after the introduction of a commercial instrument, tracer studies have already been initiated using ICP-MS detection [59-61]. This technique has several advantages over other methods. Samples are analyzed directly as dilute aqueous solutions of the metal, usually after a sample complexation/extraction step to remove isobaric interferences. The instrument need not be dedicated to the nutritional project since over 100 samples can easily be analyzed in one day (about 13 per hour). Sample preparation time then becomes the limiting factor in throughput, but this problem is related to the rate of sample procurement more than anything. Although solids are not analyzed directly, solutions are often the most convenient form of handling a sample because homogeneity is more readily assured. This is

important if isotope dilution is to be used to measure total element concentration. In fact, it is possible to simultaneously determine concentration and also monitor the label by using three isotopes: one a reference isotope, one used for isotope dilution (spiked after sample collection), and a third isotope used as the label [60]. Finally, precisions obtainable are clearly sufficient for nutritional research. For example, our current best precision of 0.5% for the $^{70}Zn/^{68}Zn$ ratio obtained from 2 mg L^{-1} total Zn is not much worse than the 0.3% precisions routinely reported for the same ratio in Zn studies using TIMS [51].

The specific purpose of this project was to compare the extrinsic and intrinsic bioavailability of Zn in babies' milk using stable isotope tracing with ICP-MS detection. This was a collaborative project with the Food and Nutrition department at Iowa State University and the University of Iowa hospital. A double labelling experiment was performed in which ^{67}Zn was injected into a cow, serving as the intrinsic label, while $ZnCl_2$, enriched in ^{70}Zn (extrinsic label) was added to the cow's milk just before it was given in the babies' milk formula. Other such nutritional studies of Zn have been performed [50,51,62], but this is the first to use ICP-MS. Also presented below is a determination of zinc isotope ratios in human blood plasma, the first time such a measurement has been demonstrated. Details of the nutritional procedures and results will be provided in a forthcoming publication [61].

Only matters relevant to this dissertation will be discussed below.

This work is also unique in that the Sciex instrument is being used with ultrasonic nebulization, as opposed to pneumatic nebulization used in another study [60]. The increased sensitivity afforded by the use of ultrasonic nebulization should:

1) improve precision at a given concentration;
2) allow for a shorter integration time to obtain the same precision;
3) determine ratios with similar precision at a lower concentration than is possible with pneumatic nebulization.

Here again, we see that as long as the problem demands that the sample matrix be removed anyway (to prevent isobaric interferences in this case), ultrasonic nebulization can improve results on the cleaned up sample.

A previous study [59] had led us to believe that ultrasonic nebulization is a viable means of introducing the sample for precise isotope ratio determinations. However, that study did not employ the Sciex instrument. The commercial instrument retains better control over the measurement parameters by using sophisticated software, and, in addition, the electronics are better shielded from RF (radio frequency) noise. It must now be shown how the measurement parameters as well as other ICP-MS parameters on

the Sciex instrument affect the precision and accuracy of ratio determinations. Also, it must be verified that the fecal matrix does not affect the accuracy of results, given the instrument's susceptibility to matrix effects (Chapter II).

Materials and reagents

Enriched ^{67}ZnO (93.11 atom %) and ^{70}ZnO (85.03 atom %) were obtained from Oak Ridge National Laboratory. HNO_3 and HCl used for preparing solutions were reagent grade, subjected to subboiling redistillation in silica. Aqueous NH_3 used for pH adjustment was reagent grade and subjected to isopiestic distillation. Deionized water with a resistivity greater than 10 MΩ-cm was used to prepare all solutions. The extractant used was diethylammonium diethyldithiocarbamate (DDDC) in CCl_4. The concentration of zinc impurity in the DDDC and CCl_4 was found to be insignificant by electrothermal vaporization-atomic absorption spectrometry (ET-AAS).

Procedures

Fecal samples were prepared by weighing the homogeneous freeze-dried sample, drying and ashing in a muffle furnace at 500°C, and then dissolving the samples in a minimal amount of 6 M HCl. The pH was adjusted to 2.5-3.0 using distilled aqueous NH_3 or 1.2 M HCl and the samples were diluted to volume using ultrapure water. AAS was used at this time to

measure Zn concentration. One 50 mL aliquot of this fecal solution of zinc (concentration 59.2 $\pm$ 0.3 μM) was taken directly for extraction as described below (sample 0-0). The remaining 250 mL of fecal solution was spiked with 2 mL of a 228 $\pm$ 1 μM solution (pH 3) of the enriched ^{67}Zn as chloride. From this spiked 250 mL, one 50 mL aliquot was taken for immediate extraction (sample 67-0). The other four 50 mL aliquots were spiked with either 1, 2, 4, or 8 mL (samples 67-1, 67-2, 67-4, and 67-8, respectively) of an enriched ^{70}Zn solution (zinc concentration 10.08 $\pm$ 0.07 μM). The uncertainties listed above represent one standard deviation from the mean.

The samples were then extracted twice with 0.04% (w/v) DDDC in CCl_4 to separate Zn (also Fe and Cu) from larger amounts of Na, K, Mg, and PO_4^{3-}. This was done to insure the accuracy of the ratios, since the only isobaric interference would be due to ^{70}Ge. Subsequent back extraction into the aqueous phase was accomplished using 1.2 M HCl. The samples were then ready for analysis by the ICP-MS. A similar procedure was followed for blanks.

For the blood analysis, a normal fasting male human subject was given 50.3 mmol (3.49 mg) of the enriched ^{70}Zn orally as the aqueous chloride and was not permitted to eat for the next four hours. Blood was drawn into purified collection tubes and centrifuged (30 min at 500 g) to separate plasma from cells and platelets. Samples of blood plasma (8

mL each) containing approximately 120 nmol of zinc were freeze-dried and ashed at 500 ^{o}C for 48 h in porcelain crucibles. Ash was dissolved in a minimal volume of 6 M HCl.

The optimization of the ICP-MS for the precise measurement of Zn isotope ratios was similar to methods described in other sections. The mass spectrometer was operated in low resolution to provide maximal sensitivity. The Zn ratios (using ^{68}Zn as a reference) were then monitored for several minutes using a 1 mg L^{-1} test solution. Changes were made mostly in the aerosol flow rate and in the ion lens settings (lens B) until maximal short term precision was obtained. Usually, this corresponded to obtaining good count rates at a modest aerosol gas flow setting. Typical conditions were 1.2 kW forward power, 1.0 L min^{-1} auxiliary flow rate, 13 L min^{-1} outer argon flow rate and 1.2 L min^{-1} aerosol gas flow rate. The ion lens settings were normally 60, 75, 50, and 12 for A, B, C, and the ring lens, respectively. After the above procedures, long term precision was monitored until the ratios stopped drifting (normally less than 1 hour). Thereafter, the absolute ratios did not change by more than 2% over a 7 hour period.

Isotope ratios were measured in the "multiple elements" software package rather than the "isotope ratio" program specifically designed for this use. This was mainly because it took approximately 4-5 times longer to execute a measurement of the same time in the latter program than in the

former. For example, when using 1 second measurement time, 3 measurements per peak, and 100 ms dwell time to quantitate the three Zn isotopes, the time for 1 determination should be nominally 9 seconds. The "multiple elements" program took about 10 seconds, while the "isotope ratio" program took over half a minute. The use of the multiple elements software (in an elemental, multichannel scan mode) precluded the use of a variable analysis time on the different Zn isotopes, which can be performed with the intended software. However, precisions obtained were excellent, even though an equal portion of the total analysis time was allotted to each of the three isotopes.

Study of precision and accuracy of isotope ratios

An analysis of the blank carried through the extraction procedure showed small amounts of S, N, C, and Cl peaks in addition to the normal background peaks [6]. Background count rate at m/z = 67, 68, and 70 was generally very low (50-100 counts s^{-1}) showing no indication of either molecular species, trace Zn, or isobaric ^{70}Ge. Sometimes, however, the background at m/z = 70 would approach 200 counts s^{-1}, possibly due to a chlorine molecular species (such as $^{35}Cl_2^+$) or $(NO^+)Ar$. Because of the small natural abundance of ^{70}Zn, best results were then obtained by subtracting the blank.

Tables 18-22 are an analysis of the various factors that affect the precision of isotope ratio measurements by ICP-MS.

The precision of these measurements is presumably a composite of the two uncertainties present in the count rate of each isotope: one due to the total number of ions counted (counting statistics) and the other due to small fluctuations in the rate at which each ion arrives at the detector. The former uncertainty is inherent in pulse counting techniques, and assuming random errors in counting, this error amounts to $N^{1/2}/N$, where N is the total number of counts made during the measurement. The latter fluctuations arise because of differences in the rate at which the Zn isotopes traverse the nebulizer, ICP and interface - a very dynamic ion source, to be sure. Thus, if the second factor predominates, precision cannot be improved beyond a certain level, determined by the ICP-MS parameters. If errors due to counting statistics predominate, then any level of precision can be obtained simply by changing the Zn count rate or increasing the integration time of each measurement.

From Table 18, it can be seen that increasing the total integration time (MT) of each determination can better the precision, up to a point. For example, the precision does not improve at all going from a 2 to 5 s MT, using a 100 ms dwell time (DT). The data in Table 18 were determined using 2 mg L^{-1} Zn, which gave a ^{68}Zn count rate of 200,000 counts s^{-1}. Therefore, the total counts obtained for these MTs would be 400,000 and 1,000,000 counts, respectively. Using Table 19 as a guide, we see that precision should thereby increase from

Table 18. Effect of dwell time and total measurement time (MT) on Zn isotope precision (% RSD of ten consecutive measurements of the indicated MT is in parentheses)[a]

Dwell time:	50 ms		100 ms		200 ms	
MT[b] (s)	$^{67}Zn/^{68}Zn$	$^{70}Zn/^{68}Zn$	$^{67}Zn/^{68}Zn$	$^{70}Zn/^{68}Zn$	$^{67}Zn/^{68}Zn$	$^{70}Zn/^{68}Zn$
0.2	0.2147 (1.1)	0.0335 (1.2)	0.2114 (2.1)	0.0343 (2.3)	0.2148 (2.9)	0.0336 (3.5)
0.4	0.2152 (1.5)	0.0337 (1.4)	0.2114 (1.3)	0.0340 (1.6)	0.2157 (2.0)	0.0336 (2.9)
0.8	0.2147 (0.8)	0.0333 (1.1)	0.2123 (0.7)	0.0343 (1.3)	0.2153 (1.4)	0.0334 (1.8)
1.0	0.2151 (0.5)	0.0335 (1.3)	0.2130 (0.6)	0.0341 (1.0)	0.2163 (1.7)	0.0336 (1.3)
2.0	0.2147 (0.3)	0.0333 (0.7)	0.2132 (0.4)	0.0339 (0.3)	0.2161 (1.6)	0.0334 (1.3)
5.0	------ ------	------- -------	0.2140 (0.4)	0.0338 (0.4)	0.2154 (0.7)	0.0333 (0.6)

[a]Conditions: 1.2 kW forward power, 1.0 L min^{-1} aerosol flow rate (ultrasonic nebulization), 1.0 L min^{-1} auxiliary flow rate; 2 mg L^{-1} total Zn (200,000 counts s^{-1} at ^{68}Zn); background < 50 counts s^{-1} at all three masses.

[b]At each of three measurements per peak.

Table 19. Precisions expected as a function of ^{68}Zn total counts, if errors are due only to counting statistics and assuming natural abundance

Counts ^{68}Zn	% RSD-$^{67}Zn/^{68}Zn$	% RSD-$^{70}Zn/^{68}Zn$
10,000	2.1	5.5
50,000	1.0	2.5
100,000	0.7	1.7
200,000	0.5	1.2
500,000	0.3	0.8
1,000,000	0.2	0.6

about 0.4 % to 0.2 % for the $^{67}Zn/^{68}Zn$ ratio, or somewhat better if one considers the averaging of the three measurements per peak. The fact that it does not improve probably indicates that the ICP-MS parameters dictate the precision at this level, rather than counting statistics. Actually, the precision of the $^{70}Zn/^{68}Zn$ ratio does better than what counting statistics would allow (at 100 ms DT).

Table 18 also shows the difference that the DT makes on precisions. If the DT is too short, the quadrupole must switch from peak to peak very rapidly, which may cause a loss of accuracy. Fifty ms are about as low as we normally find useful for this parameter, however 100 ms does just as well in terms of precision and accuracy (some of the data at low MT are not accurate because the ICP-MS was warming up at this point) but it speeds up analysis time slightly by avoiding the overhead time associated with so many "hops." A longer DT (200 ms) does not perform as well, probably because it does not efficiently average out the low frequency noise. However, as the number of cycles (MT/DT) per measurement becomes similar, precision levels approach those of shorter dwell times. Using 5.0 s MT and 200 ms DT (25 cycles), for example, precision is similar to that obtained at 2.0 s MT, 100 ms DT (20 cycles), albeit at the expense of increased analysis time. The sequential scanning mode was also tried under identical conditions, using a 1.0 s measurement time. This effectively means a 1000 ms dwell time, and results were not very precise: 3-4% short term variation. Therefore, the multichannel mode

Table 20. Effect of Zn concentration (count rate) on isotope precision[a]

[Zn] (mg L^{-1})	^{68}Zn Count Rate (c/s)	$^{67}Zn/^{68}Zn$ (% RSD)	$^{70}Zn/^{68}Zn$ (% RSD)
0.1	10090	0.2175 (2.3)	0.0325 (3.0)
0.5	54990	0.2204 (1.2)	0.0316 (2.3)
1.0	107700	0.2204 (1.2)	0.0321 (2.1)
2.0	224300	0.2176 (0.9)	0.0319 (0.7)
5.0	564700	0.2183 (0.9)	0.0319 (1.4)
10.0	1030000	0.2179 (0.9)	0.0317 (1.0)

[a]Conditions: 1.25 kW, 1.4 L min^{-1} aerosol flow rate; ten determinations of 1 second each (100 ms dwell time).

is always recommended for quantitative work.

Table 20 seems to indicate that increasing total counts by increasing the concentration (count rate) of Zn does not improve the precision as well as increasing the measurement time. Yet these data were taken using a higher aerosol flow rate than in Table 18 (1.4 vs 1.0 L min^{-1}). Different ICP-MS conditions could change the ultimate level of precision attainable. This is verified in Table 21, where it is seen that for sets of conditions yielding similar count rates, the lower aerosol flow rate usually gives better precision. This was similar to what was found in the previous section (uranium analysis), where decreased flow rates reduced the drifting of the calibration curves.

What factors influence the accuracy of ratios determined with ICP-MS? The true natural values of $^{67}Zn/^{68}Zn$ and $^{70}Zn/^{68}Zn$ are 0.2213 and 0.0334, respectively. Determined values for the former ratio were usually low by about 1-2 %, regardless of ICP-MS parameters (Table 21) but the latter ratio depended greatly on experimental conditions. Because of the lower number of counts in the ^{70}Zn channel, a small rise in the background due to increased noise levels, molecular species, or Zn memory could substantially affect the ratio. Finally, changes in the background matrix can influence the accuracy. Table 22 shows the results of adding NaCl at various levels to a 5 mg L^{-1} zinc solution. The instrument had been warmed up and was giving very reproducible ratios prior to this experiment. Analysis of a blank solution of

Table 21. Effect of aerosol flow rate and forward power on Zn isotope ratios: () = % RSD, [] = ^{68}Zn counts s^{-1} a

ICP power:	1.0 kW		1.2 kW		1.4 kW	
Flow rate L min^{-1}	$^{67}Zn/^{66}Zn$	$^{70}Zn/^{68}Zn$	$^{67}Zn/^{68}Zn$	$^{70}Zn/^{68}Zn$	$^{67}Zn/^{68}Zn$	$^{70}Zn/^{68}Zn$
1.8	------	------	------	------	0.2176 (1.6) [160,000]	0.0273 (4.5)
1.6	------	------	0.2051 (1.1) [150,000]	0.0282 (2.6)	0.2164 (0.4) [260,000]	0.0330 (0.8)
1.4	0.2210 (4.4) [30,000]	0.0236 (4.2)	0.2025 (0.8) [155,000]	0.0354 (0.7)	0.2230 (2.7) [40,000]	0.0352 (3.4)

1.2	0.2004	0.0381	0.2173	0.0329	------	------
	(1.1)	(1.5)	(0.3)	(0.8)		
	[105,000]		[230,000]			
1.0	0.2124	0.0346	0.2226	0.0313	------	------
	(0.7)	(1.5)	(1.7)	(1.4)		
	[140,000]		[110,000]			
0.9	0.2227	0.0317	0.2204	0.0327	------	------
	(1.6)	(1.3)	(0.8)	(2.9)		
	[70,000]		[45,000]			

[a]RSD is for ten consecutive measurements of 1.0 s each, 100 ms dwell time, 3 measurements/peak.

Table 22. Effect of sodium matrix on Zn isotope ratios (5 mg L^{-1} total Zn)[a]

[Na] (molar)	^{68}Zn Counts s^{-1}	$^{67}Zn/^{68}Zn$ (% RSD)	$^{70}Zn/^{68}Zn$ (% RSD)
0	565,000	0.2183 (0.9)	0.0319 (1.4)
1×10^{-4}	530,000	0.2184 (1.4)	0.0319 (1.0)
5×10^{-4}	446,000	0.2195 (1.2)	0.0315 (0.8)
1×10^{-3}	372,200	0.2198 (0.5)	0.0316 (1.3)
5×10^{-3}	145,000	0.2232 (0.7)	0.0307 (0.7)
1×10^{-2}	76,450	0.2264 (0.6)	0.0310 (1.4)

[a]Conditions: same as Table 20.

NaCl verified the absence of Zn in the reagents used. Note that both absolute ratios changed systematically even at moderate NaCl concentrations where the absolute suppression of the zinc signal was not excessive. At 0.01 M Na, the change in both ratios amounted to about 4%. The precisions, which are also listed, showed that these changes represented real, detectable differences in the isotope ratios. One possible explanation for the observed difference in the $^{67}Zn/^{68}Zn$ ratio would be the loss of linearity of the electron multiplier at high count rates. However, as Table 20 shows, the multiplier was linear to at least 10^6 counts s^{-1}. It is also doubtful that interfering chlorine molecular species were being formed at the increased NaCl concentrations, since none were observed from the 1.2 M HCL matrix. A more likely explanation was that the ICP and/or nebulizer underwent real changes as the salt concentration increased, which affected the absolute isotope ratios. For this reason, the accuracy of the ratios in the fecal matrix had to be verified.

Verification of accuracy in fecal matrix

For planned clinical studies, the linear range required for $^{70}Zn/^{68}Zn$ measurements is from about 50 to 400 atom % excess of ^{70}Zn. For comparison of the bioavailability of zinc from two separate dietary sources in the same meal, using ^{70}Zn and ^{67}Zn simultaneously as tracers, for example, both relative precision and accuracy should be 1% or better over this range.

The linearity, precision and accuracy of response were tested using the samples spiked with ^{70}Zn (67-1 to 67-8). The addition of ^{67}Zn before extraction served as an internal check on the stability of the instrumentation as well as to verify the AAS determination of the zinc concentration. The zinc isotope ratio results by ICP-MS are shown in Table 23. The precision of the $^{70}Zn/^{68}Zn$ determinations was near 1% (mean 1.1%). The precision of the $^{67}Zn/^{68}Zn$ determinations was 1% RSD or less (mean 0.5%). The $^{70}Zn/^{68}Zn$ and $^{67}Zn/^{68}Zn$ ratios of the unspiked fecal sample (0-0) were within the experimental uncertainty of the ratios of a natural abundance zinc standard in 1.2 M HCl.

The $^{70}Zn/^{68}Zn$ and $^{67}Zn/^{68}Zn$ ratios of the fecal solutions are shown in Table 24 normalized to the ratios for the natural abundance zinc standard. The expected values have been calculated from AAS determinations of the molar zinc concentrations of the original fecal solution and the enriched solutions used to make the spikes, taking into account the relative amounts of ^{67}Zn, ^{68}Zn, and ^{70}Zn that were added when spiking. The linear regression line through the $^{70}Zn/^{68}Zn$ values of Table 24 was $y = 0.9984x + 0.0023$. The correlation coefficient was $r = 0.99988$. The slope and intercept did not differ significantly from the ideals of 1.0 and 0, respectively. For the ^{70}Zn-spiked solutions (67-1 to 67-8), the observed $^{70}Zn/^{68}Zn$ values were 100.0 $\pm$ 1.0 (mean $\pm$ SD)% of the expected values. The observed $^{67}Zn/^{68}Zn$ values of the ^{70}Zn-spiked solutions decreased compared with the

Table 23. Observed zinc isotope ratios of fecal solutions[a]

	$^{70}Zn/^{68}Zn$		$^{67}Zn/^{68}Zn$	
Sample	Ratio	% RSD	Ratio	% RSD
STD	0.03155	0.98	0.2262	0.43
0-0	0.03159	1.4	0.2275	0.60
67-0	0.03159	1.1	0.4148	0.42
67-1	0.04610	0.85	0.4141	0.20
67-2	0.06036	1.3	0.4119	0.84
67-4	0.09151	1.3	0.4113	0.28
67-8	0.1479	1.0	0.4109	1.00

[a]ICP-MS conditions: 1.0 L min^{-1} aerosol gas flow rate, 1.25 kW, 0.8 L min^{-1} auxiliary flow rate, 2 s measurement time, 100 ms dwell time, 10-12 determinations per sample.

Table 24. Label recovery[a]

	$^{70}Zn/^{68}Zn$		$^{67}Zn/^{68}Zn$	
Sample	Observed	Expected	Observed	Expected
0-0	1.001	1.000	1.006	1.000
67-0	0.991	0.997	1.834	1.841
67-1	1.461	1.464	1.831	1.840
67-2	1.913	1.930	1.821	1.839
67-4	2.900	2.860	1.819	1.837
67-8	4.688	4.710	1.817	1.833

[a]Ratios normalized to ratios from natural abundance standard in 1.2 M HCl. Conditions same as Table 23.

^{67}Zn-spiked solution that was not spiked with enriched ^{70}Zn (solution 67-0). This was because of the increasing amounts of ^{68}Zn relative to ^{67}Zn that were added when spiking with multiple volumes of ^{70}Zn. For the ^{67}Zn-spiked solutions (67-0 through 67-8), the observed $^{67}Zn/^{68}Zn$ values were 99.3 $\pm$ 0.3% of the expected values. Considering that the expected values were based on zinc concentrations determined by AAS, the precision and accuracy of which were not better than 0.4 to 0.5% relative, it is evident that the observed and expected values agree within the overall experimental error.

In vivo enrichment of blood plasma zinc

The $^{70}Zn/^{68}Zn$ ratios (normalized to natural abundance zinc standards) of zinc extracts of samples of ashed blood plasma are shown in Table 25. Simultaneous determinations of $^{67}Zn/^{68}Zn$ ratios at natural abundance (not shown) served to confirm instrument stability. The times listed are those at which blood was drawn from the volunteer. Plasma zinc enrichment peaked (366 atom % excess) approximately one hour after ingestion, and decreased gradually thereafter, remaining at substantial levels even seven days later. Interpretable results could have been achieved with half as much ^{70}Zn, bringing the enriched stable isotope cost per subject under $90 at current prices. The precision of these plasma ratios was not as good as for the fecal samples because of the lower zinc concentrations in the plasma solutions. However, precision was acceptable for the intended purpose.

Table 25. In vivo enrichment of blood plasma zinc with ^{70}Zn

Time (h)	Norm. Ratio[a]	% RSD
-48	1.014	1.4
-24	0.986	1.5
0.5	1.709	1.5
1	4.656	1.2
2	3.160	1.2
4	2.529	1.5
24	1.931	2.4
168	1.494	2.7

[a]Ratios for $^{70}Zn/^{68}Zn$ were normalized to a natural abundance standard in 1.2 M HCl. Conditions same as Table 23; 5-8 determinations per sample.

Iron isotope ratios

In a different tracer study, iron isotope ratios were measured in rat hair digests. This was a feasibility study designed to determine the natural variance in the $^{54}Fe/^{57}Fe$ ratio among several different samples of rat hair, so that an appropriate level of enriched ^{54}Fe might be fed to the rat. The problem encountered was that the digests were too strongly acidic and had to be diluted 1:20 in order to avoid corroding the sampler. After this dilution, samples were only 0.3 mg L^{-1} or less in total Fe. Standards of natural abundance prepared in an identical way as the digests were compared to standards of similar concentration prepared in 1% HNO_3 and little difference was found in the 54/57 ratio. This increased confidence in the accuracy of the ratios (the detailed composition of the matrix was not available). The 54/57 ratio was then determined with 2-3 % precision even though count rates for ^{57}Fe sometimes fell below 500 counts s^{-1}. The one sample known to contain an enriched ratio showed this clearly, its ratio lying about four standard deviations from the mean of the natural samples. In fact, the client reported that when doing this same experiment by neutron activation analysis (thermal ionization mass spectrometry was not available) the analysis took many weeks and the "hot" sample registered only about one standard deviation away from the mean of the different digests!

Other Analyses

This section is a collection of odds and ends relating to the analytical performance of the ICP-MS. It is not designed for publication; however, the author does not wish the information gained from experience to be wasted.

Leaching procedures

All volumetric flasks and plastic storage bottles were leached with 5% HCl (v/v) for several days before use. After leaching, these containers were rinsed thoroughly and stored with deionized water in them. It was found that the concentrations of standards stored in the plastic bottles were quite stable over long periods of time. A 1 mg L^{-1} solution was stable for at least one month; a 10 μg L^{-1} solution for about a week. An experiment showed that a 1 μg L^{-1} solution of 10 elements stored in leached plastic container experienced an average drop of 10% of its original concentration after the first day. The type of plastic used did not seem to matter. The effect of glass or unleached plastic on such low concentrations was not evaluated. The conclusion: for careful work, at low concentrations, the standards must be made up daily (such as in our uranium analysis experiment).

The elemental equation and spectral interferences

The Sciex software has the capability of correcting the count rate of an analyte peak for known spectral interferences, which might be isotopes of another element occurring at the same mass, or perhaps an interfering molecular species, such as a metal oxide ion. Gray has reported rather extensively on the possibilities of these spectral interferences in ICP-MS [3].

In order to test the usefulness of this program, we conducted the following experiments. First, we determined Zn in the presence of Ni. If ^{64}Zn is chosen as the analyte peak, ^{64}Ni will be an interference (see Appendix A). Theoretically, the computer will measure the count rate at m/z = 60 (^{60}Ni) and, using assumed natural abundances, will use an "elemental equation" to calculate how much of the peak at m/z = 64 is due to Ni and how much is Zn. It will then subtract the Ni contribution, plus any other interferences, before it reports a Zn concentration.

For this experiment, conditions were set for low ionization suppression (1.1 L min^{-1} aerosol gas flow, 1.5 kw power, using ultrasonic nebulization) and an internal standard (Co) was added to all samples and standards. Thus, varying amounts of Ni should have had little effect on the Zn/Co ratio. Three calibration curves were made simultaneously using ^{64}Zn, ^{66}Zn and ^{68}Zn and 0.5 to 10 mg L^{-1} Zn standards in 1 % HNO_3. The latter two isotopes are free of interference

Table 26. Quantitative analysis results (mg L^{-1})of 5.0 mg L^{-1} solutions of Zn in varying Ni matrices. Calibration curves were based on ^{64}Zn (corrected for ^{64}Ni), ^{66}Zn, and ^{68}Zn

[Ni] mg L^{-1}	% of 64 peak due to ^{64}Ni[a]	^{64}Zn	% error	^{66}Zn	^{68}Zn
0	0	4.97	0	4.95	4.93
10	5	4.91	<1	4.99	4.95
50	19	4.73	5	5.06	5.00
100	33	4.42	12	5.08	4.97

[a]This assumes uniform sensitivity and zero background. Actual background was negligible, but in reality these percentages should be higher since Ni is more easily ionized than Zn in the ICP.

Table 27. Quantitative analysis of 100 μg L^{-1} Lu solutions in varying concentrations of Tb: comparison with and without use of an empirically determined elemental equation (EE) to correct for TbO interference

[Tb] mg L^{-1}	[Lu] (μg L^{-1}) no EE used	[Lu] (μg L^{-1}) EE used	[Lu] (μg L^{-1}) EE used 1 hr later
0	102.3	103.4	98.3
0.5	109.3	----	111.8
5	168	246	244
10	---	598[a]	---

[a]The mass spectrometer was put into a throttle mode for this measurement because it read over 2 X 10^6 counts s^{-1} while measuring ^{159}Tb.

from any Ni isotopes. Calibration curves were all linear (r = 0.9991 or better). Next, the standards were reintroduced to verify that the curves had not drifted. Then "unknowns" consisting of 5 mg L^{-1} Zn in 0, 10, 50 and 100 mg L^{-1} Ni were analyzed. The results are shown in Table 26. The unknowns were reported as 5 mg L^{-1} regardless of the Ni concentration using the ^{66}Zn and ^{68}Zn calibration curves. On the other hand, the result using the ^{64}Zn curve was 12% low at 100 mg L^{-1} Ni, which must be attributed to inaccuracies in the use of the elemental equation for Zn.

A second experiment was slightly different. This time the $^{159}Tb^{16}O/^{175}Lu$ system was examined to see if spectral interferences due to oxide formation could be corrected for by an empirically determined elemental equation. A solution of Tb only was introduced and the TbO/Tb ratio was measured; this was 0.0079 $\pm$ 0.0003 for 1 mg L^{-1} Tb. One parameter set was formed with this ratio inserted into the elemental equation for Lu:

$$1.000\ ^{175}Lu - (TbO/Tb)(^{159}Tb)$$

Another parameter set was left uncorrected; that is, the mass spectrometer monitored only m/z = 175. Two calibration curves were then prepared separately, using the two different parameter sets. The standards used were 20, 100, 250 and 500 $\mu g\ L^{-1}$ Lu with 100 $\mu g\ L^{-1}$ Ho internal standard. The "unknowns" were 100 $\mu g\ L^{-1}$ Lu and Ho prepared in 0, 0.5, 5, and 10 mg L^{-1} Tb. Results are shown in Table 27. The first

column is reported concentration without the use of an elemental equation, the second column used a correction and the third column data were also corrected for TbO, but were obtained an hour after column two. Note the terrible results obtained if just 5 mg L^{-1} Tb were present (i.e., Tb/Lu = 50) - worse, in fact, than if no correction had been made! Also, note that the 100 μg L^{-1} standard read 100 $\pm$ 3 μg L^{-1} over 1 hour; i.e., there was little drift in the calibration curve under these optimized conditions (as in Chapter II).

In both the first and second experiments, the errors introduced by use of the elemental equation were much greater than one would expect from a statistical analysis of the data, using the known precisions of each count rate. When faced with a spectral interference, therefore, it is recommended to simply choose another isotope, if this is possible. It must be noted that an interference-free isotope was available for each element of interest in all the samples the author has analyzed thus far. In the rare cases where interferences cannot be corrected for by using another isotope, it might be wiser, but, alas, more time consuming, to reduce the data manually.

Clay mineral samples for agronomy

There were three interesting things learned when clay mineral samples were analyzed for trace elements as part of an agronomy project. First, the samples were supplied as

suspensions of colloidal particles less than 2 μm in size, rather than as true solutions. The ultrasonic nebulizer performed normally on these, except that some inconsistency was noticed when the particle size in the standards was varied from 0.5 to 2 microns (unfortunately, these data were not recorded).

Second, internal standardization was not used in parts of this analysis, but there was surprisingly little drift in the calibration curves (using just intensities) at low aerosol flow rates.

Finally, one of the agronomy clients was vitally interested in K concentration, or more precisely, the ratio of K to the other trace elements in order to determine structural formulas of the clay minerals. This was a real challenge because flame emission instruments did not have the required sensitivity for the transition elements (low $\mu g\ L^{-1}$). Perhaps ICP-AES would have been better suited for this task, although its sensitivity for K is also limited. The main isotope of K is ^{39}K which, of course, is adjacent to the largest peak in the background spectrum: ^{40}Ar. However, by turning up the aerosol flow rate to about 1.3 L min^{-1} the ^{40}Ar peak shrank to the point where it was completely separated from the ^{39}K peak in high resolution. Fortunately, the alkali metals show excellent sensitivity at high flow rates [28], and there were no matrix effects to worry about in the samples. The count rates were less precise, but the client was willing to sacrifice precision in order to quantitate potassium.

Arsenic in hair

A sample of dissolved hair was received from Veterinary Medicine which had been analyzed for arsenic by both neutron activation and by hydride generation-AAS. The As concentration differed by an order of magnitude and the client wanted a third "opinion." However, he only had about 100 μL of solution left! Luckily, ICP-MS exhibits excellent sensitivity for this element and there was no Cl^- in the matrix ($ArCl^+$ sometimes interferes at m/z = 75). The sample was diluted to 5.0 mL and FIA (flow injection analysis) was performed using a cobalt internal standard. Standards were matrix matched to contain 20 mg L^{-1} Ca. At the time of analysis, concentration of As was only 15 μg L^{-1}. Results agreed closely with the AAS determination.

Iron in groundwater

This was the first of several samples obtained from the undergraduate quantitative analysis laboratories at Iowa State. The purpose of analyzing these samples, containing major, minor and trace amounts of the elements under study, was to verify the accuracy of ICP-MS results. These results were compared to known values determined by other instrumental methods, upon which students are graded. Similar accuracy studies have been conducted by Date and Gray [12] for trace elements in NBS standards. As will be seen, each seemingly simple analysis has some traps and pitfalls associated with

it. It is essential to attempt these analyses in order to obtain a "feel" for how the instrument performs.

A number of questions suggested themselves before this first analysis began. Which isotope of Fe would the calibration be based upon? Both ^{54}Fe and ^{56}Fe have spectral interferences: ArN^+ and ArO^+, respectively. Iron-57 and ^{58}Fe are not abundant enough to give useful detection limits. Does internal standardization give better accuracy, as it does precision? Will Ca present in the groundwater interfere due to CaO^+ and $CaOH^+$ formation? Also, if Cr is present it will interfere at m/z = 54. These are the types of considerations an experienced ICP-mass spectroscopist must face.

The first step in all of these analyses is to dilute the samples so that all analyte intensities will fall within the linear range of the multiplier. Using ultrasonic nebulization, the upper concentration limit possible appears to be about 5 mg L^{-1}. Next, a qualitative analysis of the groundwater was obtained. The software is already supplied for this and it takes less than five minutes to identify all the elements present in the solution which give count rates above about 300 counts s^{-1}. [Ultratrace components will sometimes be missed or erroneously reported as present with this program.] Calcium must be located manually because the major isotope ^{40}Ca is masked by the ^{40}Ar peak. An inspection of the count rate at m/z = 44 showed a significant amount of Ca and therefore a ^{57}Fe calibration had to be ruled out immediately because of the $CaOH^+$ interference.

Table 28 shows the results using no internal standard for the analysis at both m/z = 54 and 56. Using a blank appeared to make a difference only in the case of ^{56}Fe. A "yes" in the "blank" column means that the intensity of ArO^+, for instance, was subtracted from ^{56}Fe before the calibration curve was drawn. Each sample was also blank subtracted (this is similar to what an elemental equation would do (see above), only it was performed manually). A "no" in this column means that samples and standards are run just as if no interference were present, i.e., without any blanks. The assumption was that the ArO^+ (or ArN^+) was present at a constant amount in both samples and standards and thus would "cancel out." This, of course, is not true unless [Fe] >> [ArO]. The results with no internal standard were all low; the true value was 7.3 mg L^{-1}.

Next, an internal standard was used in the analysis. Co was not found in the qualitative analysis and seemed to be an excellent choice for this. Table 28 also shows the new results, which were all high this time. Using ^{56}Fe without a matrix match of Ca gave 7.80 and 7.68 mg L^{-1}. Since it was hard to evaluate the amount of CaO at m/z = 56 (due to ArO^+), the amount of Ca in the samples was determined and this amount (6 mg L^{-1}) was added to the standards. The matrix matched result was 7.55 mg L^{-1} - only an error of 2.5%.

To conclude, when determining Fe it is best to use ^{56}Fe for maximal sensitivity. If any amount of Ca is present, matrix matching is necessary. The ArO^+ interference presents

Table 28. Results of quantitative analysis of Fe in groundwater by various methods (true value = 7.36 mg L^{-1})

Calibration Mass	Blank Subtracted?	Internal Standard?	Matrix Matched?	Result mg L^{-1}
56	YES	NO	NO	6.9
56	NO	NO	NO	6.4
54	YES	NO	NO	6.4
54	NO	NO	NO	6.6
54	NO	YES	NO	8.0
56	NO	YES	NO	7.8
56	NO	YES	YES	7.55

Table 29. Quantitative analysis of 500 μg L^{-1} Mn standards at various concentrations of Fe (standards used for Mn calibration curves were matrix matched to 75 mg L^{-1} Fe)[a]

[Fe] (mg L^{-1})	[Mn] (mg L^{-1})-day 1	[Mn] (mg L^{-1})-day 2
50	508 $\pm$ 2	483 $\pm$ 3
75	509 $\pm$ 4	509 $\pm$ 1
100	513 $\pm$ 1	510 $\pm$ 4
75[b]	443 $\pm$ 4	515 $\pm$ 5

[a]Standard deviation reported is for three determinations done successively in about two minutes.

[b]One hour later.

no problem at high Fe concentrations and can be blank subtracted for best results. Internal standardization gives good results, but might not be necessary unless the instrument response drifts (which is usually the case).

Manganese in steel

During this analysis, it was quickly discovered that 15% acid solutions cannot be run by ICP-MS because they erode the orifice! Dilutions to 1-2% total acid are safely run.

The problem expected in this case was that ^{55}Mn would have to be measured next to a very intense ^{56}Fe peak from the steel. Thus the mass spectrometer was operated in high resolution and standards were matrix matched to the samples by adding 75 mg L^{-1} iron. Table 29 shows the reported concentrations of a 500 μg L^{-1} Mn standard (with Co internal standard) made up in 50, 75 and 100 mg L^{-1} Fe. The amount of Fe did not appear to make a difference. The accuracy of the result was better than 0.5%.

The same samples were analyzed again three days later to monitor day to day changes in accuracy. The average result increased from 0.62 to 0.68 % Mn (w/w). However, all solutions had been stored in glass, which casts some doubt on the second result. Table 29 shows that the calibration curve for the second analysis was stable for over 1.5 hours.

Arsenic in flour

This sample had to be dissolved in concentrated NaOH, but after dilution the Na concentration was only 10 mg L^{-1}. Everything appeared to go smoothly until the result, 3.8% As, was compared to the correct answer - 67.8%! This was not surprising when it was found out that the As compound had originally been diluted with flour. The organic material present in the samples and not in the standards caused great inaccuracy in the results. This was found to be true in the uranium analysis project (Chapter III). When toluene was known to contaminate the aqueous phase, rare earth concentrations were exceedingly abnormal.

Calcium and magnesium in limestone

The analysis of Ca as a major component (49.4%) posed no problems. The ^{44}Ca isotope was used in the calibration. The amount of Mg was found to be negligible and was neglected in the calculation of total Ca + Mg.

Copper in brass

Copper was obviously the major component and so no matrix effects were anticipated or found once the sample had been diluted. One point was learned, however. When the analysis was first performed, standards of 0.5, 1 and 3 ppm Cu were used. The samples, though, fell in the range of 2.5 - 4 ppm. Apparently, the computer did not extrapolate the high end of

the calibration curve very accurately because the result (86.4%) was far from the true value (89.9%). Upon diluting the samples and repeating the analysis, a value of 89.2% was obtained.

Copper in CuS ore

Again, no matrix effects were observed, since Cu was a major component. This time, a casual initial analysis forced the computer to extrapolate the lower end of the calibration curve and a 10% error occurred. When the analysis was repeated with a broader calibration range which bracketed the samples, the error was only 4%.

Iron in iron ore

Since Fe was the major constituent, little interference was expected, even from Ca. A dual calibration curve was prepared, one using ^{56}Fe and the other ^{57}Fe. Both curves produced an answer in the range of 34-35% iron, whereas the true value was nearly 41%!. The analysis was repeated on another day, obtaining 37.1 % ($\pm$ 0.5 %). The cause of this inaccuracy is still unknown. The precision of the result (on three samples) suggested that it was not a problem with the dissolution of the iron ore. A quick qualitative analysis of the samples did not reveal any unexpected matrix ions.

Trace elements in brass

Copper and trace elements were determined simultaneously on a single solution of dissolved brass. The results, indicated in Table 30, show that ICP-MS has a useful dynamic range: it could accurately determine the copper at 82% at the same time as a minor component such as Ni (0.3%). The results for tin (Sn) were quite precise, but not accurate (too low). This suggested that the old standard used had hydrolyzed, as Sn is known to do. Europium was a trace component in this sample. Both samples showed 0.012% Eu, but specific rare earth concentrations were not provided for this brass, only that total RE (rare earth) was 0.1%. A substantial amount of Sb was found in the sample by ICP-MS, but not reported in the known assay. Possibly, this caused an error in their analysis of Cu, since the sum of the weight percentages would exceed 100% if the 1% Sb were included.

Summary

Table 31 summarizes the sample analyses described in this section. Accuracies of 2-3% were usually obtained with careful work. Drifting of the calibration curves is usually the main obstacle to obtaining better accuracy. Also, it was possible that unknown spectral interferences existed in some samples, such as the iron ore.

Table 30. Simultaneous quantitative analysis of major, minor and trace elements in Hach brass

Element	% found (w/w)[a]	% known (w/w)
Cu	83.1, 81.2	84.08
Ni	0.26, 0.27	0.30
Pb	4.76, 4.95	4.84
Sb	1.01, 0.97	----
Sn	2.72, 2.89	9.23
Zn	0.97, 1.06	1.13
Eu	0.012, 0.012	(b)

[a]Only 2 samples were run.

[b]All that was known was that the rare earth sum = 0.1%.

Table 31. Summary of quantitative analyses

Sample	Found	Known (method)	Notes
Fe in grd. H_2O	7.55 mg L^{-1}	7.36 mg L^{-1} (colorimetric)	Use int. std.; match Ca; use ^{56}Fe in spite of ArO^+
Mn in steel	0.617 %	0.619 % (colorimetric)	Allow for cal curve drifting by checking standards every so often; use hi res
Ca in limestone	49.7 %	49.44 % (EDTA titr.)	Use ^{44}Ca
Cu in brass	89.2%	89.87 % (electrodepos.)	Dilute samples to <2 mg L^{-1} for maximum accuracy
Cu in CuS ore	22.5 %	23.4 % (iodometric)	Make sure computer won't have to extrapolate cal. curves
Fe in ore	37.1 %	40.88 % (MnO_4^- titr.)	Unresolved problem here
Cu in Hach brass	82.2 %	84.08 % (electrodepos.)	Use correct dilution
As in flour	3.8 %	67.81 % (coulometric)	Organic contamination problem

CHAPTER IV. ICP-MS AS A MULTIELEMENT DETECTOR FOR LIQUID CHROMATOGRAPHY

Introduction

One of the final frontiers in trace elemental analysis is that of element "speciation": the identification and quantitation of the individual chemical forms of a metal, rather than the sample's total metal content. These forms might be different oxidation states, different complexes, or perhaps organometallic compounds. Only recently has it been realized that the toxological and biochemical importance of the metals and metalloids depends greatly upon their chemical form in the environment [63,64]. Hence, although rudimentary speciation studies began in the early 1970s [65,66], it was not until this decade that the full attention of analytical chemists has been given to this matter.

The problems associated with any chemical analysis, and especially difficult in speciation studies, are threefold: sample preparation, separation of the analyte species, and detection. What makes this field so challenging is that, prior to about 1980, very little expertise had been developed in any one of these areas, as it applied to speciation! It is easy to see the problem in the sample preparation step: a "real" sample (e.g., biological tissue) must be put into solution without changing the oxidation state or chemical form

of the analyte element(s). Next, a method of separation must be found which is broad and selective enough to allow all the species of interest to be individually quantitated. Finally a method of detection must be devised which would have the sensitivity necessary to quantitate trace elemental species in the environment and would not be subject to interferences from the complex sample types that could be anticipated.

As usual in applications as broad as this one, it is rare to find research groups with the capability to tackle the problem in its entirety. The sample preparation step requires a chemist very familiar with wet reactions and inorganic chemistry. The separation step is best performed by a chromatographer or similar type of chemist, and the detection aspect is likely to tax even an expert spectroscopist. Thus, almost all publications to date on this subject, including this report, have been feasibility studies designed to show that a particular separation/detection scheme "would work" if applied to a real sample. Those reports which actually describe speciation of practical samples have picked very specific and somewhat simple systems upon which to demonstrate their technique. Some of their experiments work quite handily [67-69]. What is clearly called for, however, are instrumental techniques that can solve general speciation problems without the need to develop specific methods for each type of sample. Obviously, this is a very young field at present.

Some progress has recently been made in the area of sample preparation for speciation [70], but, at this point we shall ignore this area and briefly comment on the modes of separation and detection that have been used in speciation studies.

Methods of separation for speciation include gas chromatography (GC) [67], including a purge and trap variation of this [69], liquid chromatography (LC) with ion exchange [71], paired ion reversed phase [72-75], and gel permeation [66,76,77], anodic stripping voltammetry [78], solvent extraction [79], and even thin layer chromatography (TLC) [80]. Solvent extraction is cumbersome, and is difficult to place on-line, as is TLC. Electrochemical methods of separation/detection are subject to too many interferences, although, again, very specific systems have shown good results [81]. By far, most applications have used some sort of chromatography to separate the analyte species. The use of GC requires that compounds of interest be volatile and thermally stable at minimum temperatures of about 150°C. LC, therefore, has seen the most extensive use in speciation studies. Many forms of LC exist, and this gives the chemist maximum flexibility in choosing a system which will separate the species of interest. One, in particular, reversed phase LC (RPLC) seems to be the recent method of choice. It can be used to separate both ionic and nonionic components. It shows greater resolution capabilities than ion exchange [82],

meaning it is applicable to a broader range of species. Also, the RP packings are considerably cheaper than those for ion exchange [83].

Reversed phase columns have been used extensively in the past to separate charged organic compounds [84]. Now, expertise has been developed in using them as metal ion and organometallic separators. Part of this experience comes from recent attempts to use HPLC as part of an inexpensive "multielement" detection system by means of post column derivatization [85]. RP-HPLC requires a nonpolar stationary phase and a polar mobile phase. To speciate metals, an "ion pairing" reagent is added to the mobile phase at moderate concentrations. The organic anion (cation) from this reagent forms a neutral ion pair with the analyte cation (anion) which is then retained by the stationary phase. As the charge of the analyte ion increases, so does the size of the ion pair, and it is retained longer on the column. Reference [84] describes the basic theory of RP-ion pairing chromatography and how various other parameters affect the separation.

Conventional detectors for LC such as refractive index, ultraviolet, or conductance detectors, are not adequate by themselves for speciation studies because they respond universally to various metal species. Thus element specific or multielement detectors are needed. Of the element specific detectors, colorimetry [86,87], flame atomic absorption (FAA) [67-69], and graphite furnace atomic absorption

spectrophotometry (GFAA) [88] have found the most use. FAA has not exhibited sufficiently low detection limits as a chromatographic detector except where preconcentration is possible [67,69]. GFAA exhibits useful detection limits, but suffers from an inability to monitor the LC effluent in a continuous fashion (fractions must be taken, which is cumbersome even if the process is done automatically).

Multielement detection of LC effluents offers additional advantages over other techniques. Sample introduction methods are simple and readily coupled to an LC column. Also, besides being inherently selective and sensitive techniques, they offer the possibility of performing simultaneous speciation of two or more elements on the same injection. Until now, emphasis has been placed on a multielement detector's ability to avoid chromatographic interference (coeluting peaks of different metals). Given enough time, however, wet chemists will surely be able to devise ways to dissolve samples while ascertaining that species from a small group of different elements have remained intact. When we reach this point, multielement techniques will save time in speciation studies. A few simple multielement speciation analyses have already been described [71,76,89].

The four multielement detectors that have been tried in combination with LC are atomic fluorescence spectrometry (AF), microwave induced plasma (MIP), direct current plasma atomic emission spectrometry (DCP-AES), and inductively coupled

plasma atomic emission spectrometry (ICP-AES). Reports describing AF detection have been limited and not very impressive [90,91]. The same is true of MIP detectors [92]. Many references concerning DCP-AES [74,75,77,93] and ICP-AES [71,72,76,89,94] exist. Until recently, DCP-AES showed better detection limits [74,77]. However, Lawrence et al. have improved their direct injection nebulizer (DIN) for the ICP [73]. Their current detection limits are among the best seen in the literature for FIA [95] and HPLC [96]. Reference [97] contains a thorough review of all the atomic spectroscopic methods applied to LC detection.

We now describe, for the first time, the use of ICP-MS as a multielement detector for liquid chromatography. This present work is described in a recent publication [98]. The advantages ICP-MS offers as an LC detector are its very low detection limits, multielement capability, and the ability to measure isotope ratios on eluting peaks. No other technique mentioned above can boast this latter advantage. It should be of use in biological speciation - tracer studies (a field which is probably nonexistent at this point) as well as in measuring the concentrations of each species by isotope dilution, which saves the time of running several chromatograms to obtain a calibration curve and further avoids matrix effects. LC offers advantages to ICP-MS users as well: the ability to preconcentrate analytes on-line or remove a troublesome matrix. A paper describing the off-line

preconcentration of sea water using ICP-MS detection has just been published [47].

As far as we know, this is also the first reported use of an ultrasonic nebulizer with an ICP for LC detection. This is surprising, since an ultrasonic nebulizer has proven to give better detection limits than conventional pneumatic nebulizers on continuous or transient samples [95], and good detection limits are essential in speciation experiments. Also, any increase in matrix ionization suppression (Chapter II) would likely be alleviated by the separation of the analyte from the matrix. Perhaps one concern of potential users of ultrasonic nebulization was that volatile species such as organometallic compounds would condense in the desolvation chamber. But many current speciation studies, for instance the separation of Cr(III) from Cr(VI), certainly would not experience this problem. The exit temperature of aerosol in our system is only 100-110^{0}C, which is considerably below the temperature of a GC injection port. It is also below the recommended temperature of about 150^{o}C for maximum analyte signal from nonvolatile compounds [17]. Note that if a species <u>decomposes</u> in the desolvation tube, rather than volatilizes, and if the products are nonvolatile, then there is no problem because separation has already occurred on the LC column. A glance at the melting points and boiling points of organometallic compounds [99] shows many entries that would not liquefy or condense at the boiling point of water. If one were

particularly interested in volatile species or liquids, GC-ICP-MS could be performed. This technique has already been demonstrated for the separation and quantitation of volatile metal chelates [100].

This feasibility study will attempt to prove the following points about LC-ICP-MS:

1) Use of ultrasonic nebulization is warranted. Organometallic compounds of interest can be detected with desolvation.
2) Absolute detection limits are as good as or better than for any current multielement technique, including DIN-ICP-AES and DCP-AES methods.
3) These detection limits are little compromised by the matrix typically used in ion pair chromatography (methanol, buffers etc.)
4) Detection limits are not much worsened by doing multielemental analysis on a single injection. This must be proved since ICP-MS is a rapid sequential technique and the duration of the signal near the top of an LC peak is typically 10 - 20 seconds. Note that we sometimes prefer a certain amount of band broadening, in order to allow time to measure all the elements of interest with adequate precision and accuracy.
5) The precision of isotope ratios on eluting peaks is adequate for biological tracer applications or for isotope dilution analysis. Here, the number of

elements we can determine on the same injection will necessarily decrease in order to obtain good precision.

Apparatus

A schematic diagram of our LC-ICP-MS system is shown in Fig. 33. Typical ICP operating conditions were 1.2 kW forward power, sampling position 26 mm from the load coil, 13 L min^{-1} outer argon flow, 0.8 L min^{-1} auxiliary flow and 1.2 L min^{-1} aerosol gas flow rate. The mass spectrometer was operated in the multichannel, elemental scanning mode in low resolution (Chapter II). Total measurement times at each of three measurements per peak were necessarily short due to the transient nature of the signals. The most abundant isotope of each element was monitored unless otherwise indicated.

An Ames Laboratory torch and ultrasonic nebulizer (35% efficient - see Chapter II) were substituted for the standard Sciex equipment, as in previous experiments. The distance between nebulizer and ICP torch (through the desolvation apparatus) was approximately two meters. The column to nebulizer connection was made with a 25 cm length of 0.25 mm i.d. stainless steel tubing. This corresponds to about 13 μL of dead volume in this region. One end of the tubing was connected to the column using an Alltech Universal Column Adapter. The tubing then passed through a one holed rubber stopper epoxied to a glass socket joint. The nebulizer spray

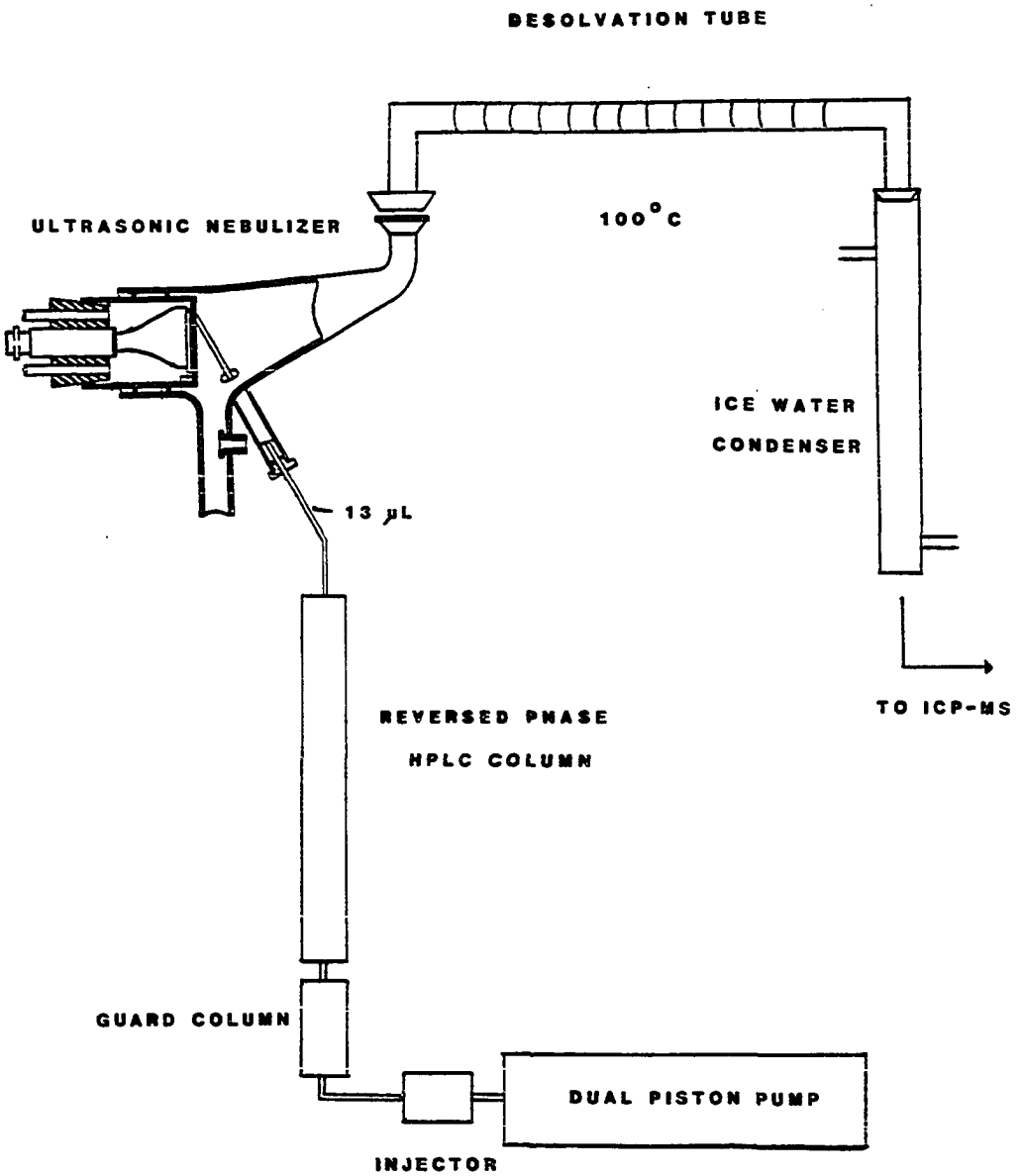

Figure 33. Schematic diagram of LC-ICP-MS apparatus

chamber contained the ball part of the joint. The tubing was carefully bent so that liquid emerging from the column would stream onto the transducer and not roll back down the tubing, which was not difficult. This ball and socket arrangement facilitated the quick replacement of the LC tubing with our normal tubing from a peristaltic pump whenever we desired to do routine experiments.

A Varian Model 2010 dual piston HPLC pump, Rheodyne 7125 injector and SSI purge valve (for rapid flushing) comprised the LC system. The column used in all studies was an Alltech Associates Econosphere C_{18} type of the usual dimensions: 25 cm long, 4.6 mm i.d. and with 5 μm particle size. A cartridge system was purchased so that no nuts or ferrules were needed in the entire apparatus (including the sample loops). A C_{18} guard column and a filter element were placed between the injector and analytical column. Samples were loaded with a syringe onto loops of various sizes.

The mobile phases were prepared as follows. Ion pairing reagents PIC-B5 (sodium pentanesulfonate) and PIC-A (tetrabutylammonium phosphate) were obtained from Waters Associates. These were prepared according to the manufacturer's directions by adding to a 1 liter volumetric flask and filling to the mark with HPLC grade methanol (Fisher) and deionized water (Millipore). Reagents then had been buffered to the necessary pH: 3.0 and 7.1 for the PIC-B5 and PIC-A, respectively. The sodium hexanesulfonate used in

FIA studies was obtained in solid form from Regis Chemical Co. The mobile phases were filtered with a 0.45 μm pore nylon filter and degassed under a light vacuum (aspirator) for 20 minutes. It could then be used by the Varian HPLC pump. After a day's run, columns were flushed with 50/50 methanol/water overnight at a flow rate of 0.5 mL min^{-1}.

The ethylenediaminetetraacetic acid (EDTA) was reagent grade and prepared as a 0.01 M solution from the disodium salt. Sodium arsenate and arsenite were obtained from Fisher, methanearsonic acid from Sigma, dimethylarsinic acid from the EPA, and sodium selenate and selenite from Alfa. Standards containing 100 mg L^{-1} (as element) were prepared of each individual species, using an analytical balance. These standards were then combined and diluted in deionized water for these experiments.

Cadmium and Pb enriched isotopic materials were obtained from Oak Ridge National Laboratories, weighed to the nearest 0.1 mg and dissolved in dilute HNO_3. Aliquots of these concentrated standards were mixed with natural abundance solutions in known amounts.

Results and Discussion

FIA results

Flow injection analysis (FIA) was performed prior to HPLC separations to see the ideal response of the instrument to a

transient signal. In all cases, detection limits were calculated as the amount of the element necessary to give a peak height (blank subtracted) equal to three times the standard deviation of the background count rate at each mass. It should be noted that the detection limits reported (for LC also) were later found to be identical even when injecting analyte amounts close to (i.e., about 10x) the detection limit.

Table 32 illustrates the change in the absolute and relative detection limits as the injection size is varied. As expected, the concentrational detection limits become worse as smaller volumes of analyte were injected, while absolute detection limits became better. Relative detection limits were consistent with data presented in Chapter II where it was found that monoisotopic Co yielded a detection limit of 0.1 μg L^{-1} under continuous flow conditions.

Another experiment was performed in which the solution uptake rate was varied keeping the injection volume and concentration constant at 100 μL and 20 μg L^{-1}, respectively. No significant difference in detection limits (i.e., more than a factor of two) was observed as the flow rate was varied between 0.5 and 1.5 mL min^{-1}. However, as the ultrasonic transducer aged it became apparent that the amount of mist produced at the low flow rates had decreased, and so only flow rates above 1.0 mL min^{-1} continued to be used. Many IP-RPLC separations can be implemented at these flow rates.

Table 32. FIA absolute (ng) and relative ($\mu g\ L^{-1}$) detection limits (3σ) as a function of injection size[a]

Sample Size	Pb		Cu		Cd	
(μL)	Abs	Rel	Abs	Rel	Abs	Rel
1000	0.49	0.49	0.30	0.30	0.35	0.35
250	0.20	0.78	0.11	0.43	0.13	0.51
100	0.13	1.3	0.07	0.70	0.08	0.80

[a]1% aqueous HNO_3 solutions, 20 $\mu g\ L^{-1}$ in each element, 1 mL min^{-1} solution uptake.

Table 33 shows FIA absolute and relative detection limits for many elements under identical ICP-MS conditions. The experiment was meant to simulate typical RPLC conditions: the matrix was 15% methanol in water with 0.005 M sodium hexanesulfonate added. Plumbing was identical to the HPLC experiments, except the column was bypassed with an equivalent length of 0.51 mm internal diameter stainless steel tubing. Four elements, each 40 ng, were determined on each injection. Since the FIA peak heights varied by 10-20% at this injection volume, three injections were made for each set of elements and the largest peak was used to calculate the detection limit. A similar FIA study using 100 μL injections showed 1-4% reproducibility in the peak heights and similar detection limits. This imprecision seen in the measurement of smaller volumes was not a cause of concern, since the LC column would broaden analyte peaks considerably and improve the precision compared to the FIA experiment.

FIA detection limits for the rare earths and Y are listed separately in Table 34. This shows that if the background can be kept low, detection limits are excellent. We have already seen the problem with high background in the analysis of uranium (Chapter III). Table 35 is a comparison of the blanks for each element in deionized water, 5% methanol and then with methanol and 0.005 M sodium hexanesulfonate. The data indicate only trace impurities in the methanol but substantial background for Mg, Al, Mn, Ni, and some other metals in the

Table 33. FIA absolute (ng) and relative ($\mu g\ L^{-1}$) detection limits (3σ) under conditions similar to HPLC[a]

Element	Abs	Rel	Element	Abs	Rel
Ag	0.01	1	Mg	1.5	150
Al	0.2	20	Mn	0.01	1
As	0.04	4	Mo	0.2	20
Au	0.1	10	Nb	0.004	0.4
Ba	0.07	7	Ni	0.2	20
Bi	0.03	3	Pb	0.1	10
^{44}Ca	2	200	Pt	0.07	7
Cd	0.04	4	Rb	0.01	1
Co	0.008	0.8	Re	0.02	2
Cr	2	200	Ru	0.01	1
Cs	0.009	0.9	Sb	0.09	9
Cu	0.02	2	Sn	0.6	60
Fe	2	200	Sr	0.01	1
Ga	0.04	4	Ta	0.02	2
Ge	0.04	4	Te	0.05	5
Hg	1.5	150	Ti	0.3	30
In	0.007	0.7	V	0.02	2
Ir	0.02	2	W	0.06	6
K	0.9	90	Zn	0.2	20
Li	0.2	20	Zr	0.01	1

[a]Conditions: same plumbing as for HPLC experiments, only without column. Injection: 10 μL, 4 mg L^{-1}; 4 elements determined each injection. Matrix: 15% methanol in water, 0.005 M sodium hexanesulfonate. ICP-MS parameters identical for all elements.

Table 34. FIA absolute (pg) and relative ($\mu g\ L^{-1}$) detection limits (3σ) for some rare earth elements[a]

Element	Blank (c/s)	Abs	Rel
Ce	50	6	0.6
Dy	50	20	2
Er	50	20	2
Eu	50	9	0.9
Nd	50	10	1
Sm	50	20	2
Tm	50	6	0.6
Yb	50	20	2
Y	100	8	0.8

[a]10 μL, 2 mg L^{-1} (20 ng) injections; 15% methanol in water, 0.005 M sodium hexanesulfonate.

Table 35. Background count rates (counts s^{-1}) for various elements in water, 5% methanol, and 15% methanol + 0.005 M sodium hexanesulfonate

Element	Water	5% MeOH	15% MeOH + Ion Pr.
Al	125	300	1470
As	75	350	500
Ba	200	50	700
Cd	60	40	90
Co	60	20	175
Cr	800	35000	100000
Cu	300	100	450
Mg	400	700	39000
Mn	60	50	900
Ni	150	70	2000
Pb	70	50	300
^{78}Se	200	200	300
Sr	40	20	300
V	60	80	400

ion pairing reagents. Some of these interferences might be due to molecular ions formed from the alkyl sulfonates. Zinc, for example, showed a large background, which was probably due to SO_2^+. The background at 52 amu (Cr) was undoubtedly ArC^+ and Mg and Al were probably masked by molecular carbon species (C_2^+ etc.) formed from the methanol. In general, detection limits for the low mass elements became poorer as the methanol concentration in the mobile phase increased, although little change in the higher mass blanks or detection limits were observed. A detailed investigation into the identity of these spectral interferences was not performed.

HPLC results

The effluent from the LC column produced an excellent mist in the ultrasonic nebulizer even at column flow rates as low as 0.75 mL min^{-1} (with a fresh transducer for the nebulizer). The maximum amount of methanol that could be tolerated by the plasma was about 20%. A light coating of carbon was visible on the sampling cone after a day's operation, but the HPLC experiments did not seem to harm the ICP-MS in any way over the course of one month.

Some initial experiments were conducted to investigate the retention processes on a RP column. First, the detection limits obtained by FIA were to be compared to those where the analyte was passed through the column but not retained. This is similar to the experiments in Ref. [101] where a dummy

column using glass spheres as a column "packing" was used in a feasibility study. However, after injecting large doses of Co and not seeing any response, we finally decided to put the Co into the mobile phase. Still, after pumping 1 mg L^{-1} Co in 5 % methanol through the unused column for over 1/2 hour, no Co signal was seen from the ICP-MS! The Co could be completely washed off the column with EDTA. Later, it was learned that it is impossible to completely "end-cap" a reversed phase column, i.e., chemically modify all the reactive silanol groups on the silica support. This explained the disappearance of the Co on the new column.

Ion pairing reagent was then added to the mobile phase. Surprisingly, after injection the Co eluted at about 10 minutes. Apparently, the presence of the ion pairing reagent kept the metals from adsorbing onto the silica. However, when EDTA was injected following the metals, a small amount of metals were still rinsed off the column, indicating some remaining absorption problems since the metals were not in the EDTA blank.

Another problem experienced was that cations with a +3 or greater charge were retained on the column, even in 15% methanol 25 minutes after injection. Flushing with EDTA confirmed the presence of these ions on the column. Judging from the literature, Cr^{3+} seems to be the only tripositive species claimed to be separated using a RP column [74]. Were the +3 ions more strongly adsorbed by the silica or were the

ion pairs formed simply too hydrophobic to elute within a reasonable amount of time? Some sources claim that the ion pairing reagent is "permanently bonded" to the stationary phase after its first use, so that the column becomes essentially an ion exchanger [82]. Highly charged ions still could not be eluted after the addition of 0.1% morpholine to the mobile phase (no ion pairing reagent), which was supposed to deactivate (block) the silanol sites. By that time, it might have been the "ion exchange" sites that "sucked up" the ions rather than the silica. Hopefully, solutions to these types of problems will be suggested by chromatographers as experience grows in this field. One possibility might be the use of a short chain alkyl sulfonate which would have less affinity for the C_{18} stationary phase. Or, conversely, one could use a C_5 phase with the PIC-B5 reagent. These possibilities have probably not been tried because they are not ideal for the traditional types of samples run on RP columns. It is possible that irreversible adsorption processes such as those described are a reason for unexpectedly poor detection limits seen in the literature [72].

We proceeded to test over 30 elements with the PIC-B5 reagent to see qualitatively how many of them would produce peaks. Table 36 summarizes this information, including the approximate retention times, baseline peak widths, and detection limits obtained. Some peaks were very broad, but

Table 36. HPLC qualitative results: injection of 20 μL, 10 mg L^{-1} of metal standards onto C_{18} column. Mobile phase: 5% methanol in water, 0.005 M PIC-B5, pH = 3.0; flow rate: 1.5 mL min^{-1}

Element	t_r (min.)	Det. Lmt.(ng)[a]	Approximate Peak Width (min)
Cr	2	1	2.5
As	2	0.1	1.5
Mo	2	6	1.5
Pt	2	0.3	1.5
Ir	2	0.5	1.5
Li	3.5	0.08	0.5
Ru	2*, 4, 11	0.04	1.5, 1.5, 2.5
V	4, 13	---	2.5, 2.5
K	4.5	7	2.5
Rb	5.5	0.1	>3
Ag	8	7	>3
Cs	8.5	0.3	>3
U	12.5	0.1	1.5
Pb	13	0.7	1.5
Cu	13	4	1.5
Fe	13.5	6	2.5
Co	13.5	0.06	1.5
Ni	13.5	0.4	2.5
Mn	14	0.4	1.5
Cd	14	0.3	1.5
Zn	14	0.9	1.5
Sr	14	0.1	1.5
Mg	14	2	2.5
^{44}Ca	14	4	2.5
Ba	14.5	0.1	2.5
Tl	18?	---	>3

Ti, Al, Y, Zr, Au, Ga, In, Sn did not elute over 25 min.

[a]Detection limits based on largest peak present, indicated with an asterisk.

this was not a dead volume problem because other peaks were quite narrow: 1.5 minutes at the baseline, which is three times the width of the FIA peaks. In other words, the contribution of the nebulizer to the total band broadening was about half of the amount due to the presence of the column. Most of this dead volume existed between the nebulizer and ICP, and relatively little between the the column and nebulizer. These results agreed with the findings in Ref. [102]: that in LC-ICP interfacing it is better to minimize the length of time in solution at the expense of increased time in aerosol transport. If the best relative FIA detection limits in Tables 33-34 are compared to those obtained under continuous flow conditions (about 0.1 μg L^{-1} [6]), it is concluded that detection limits are degraded by about a factor of ten due to dispersion in our sample delivery system. Comparing the best HPLC detection limits in Table 36 to the FIA results reveals an additional factor of ten being lost due to band broadening within the column. This latter effect is to be expected and is a major reason why high sensitivity and good detection limits are so necessary in an LC detector. It must also be kept in mind that we have not verified that the standards used contained only a single species. There might also have been additional adsorption onto the column, as explained above. For these reasons, the reported detection limits here and in the following tables are conservative values. However, the detection limits using ICP-MS are quite competitive in comparison to current techniques [74,77,96].

Qualitatively, elements in Table 36 which one would expect to exist as anions in solution (As, Mo, Pt etc.) gave peaks which eluted with the void volume [74], while singly charged cations eluted at 4-8 min. and doubly charged cations at 10-15 min. To reiterate, chromatographic resolution is not a problem when using a multielement (or element specific) detector. If one were using a refractive index or UV detector, all of the metals in the bottom half of Table 36 would have appeared as a single peak, perhaps with shoulders. However, the ICP-MS can monitor the m/z of each metal separately. The only concern is to be able to separate <u>each species of each element</u> with adequate resolution.

Additional experiments were performed using varying concentrations of methanol in the mobile phase and various LC flow rates. It was found that increasing the flow rate from 1.5 to 2.1 mL min^{-1} and increasing the methanol concentration from 5 to 10% reduced the retention times in Table 36 substantially - doubly charged ions now eluted at about 8 min. This is similar to behavior reported by others [72].

The use of the PIC-A reagent, which should pair with anions only, was explored next. Table 37 shows the retention times and detection limits. The alkali and alkaline earth metals (except Ba) eluted close to the void volume because they are cations. However, other highly charged cations, listed at the bottom of the table, still were adsorbed by the column. The other metals which eluted can plausibly exist as

Table 37. HPLC qualitative results using PIC-A: inject 10 μL, 10 mg L^{-1} using 10% methanol in water mobile phase; pH = 7.1; flow rate = 2.0 mL min^{-1}

Element	t_r (min)	Det. Lmt.[a] (ng)
Li	1.2	0.2
Rb	1.2	0.009
K	1.5	4
Sr	2.1	0.2
Mg	1.6	1.5
Cs	2.0	0.1
Ru	1.8	---
Ir	2.5, 2.7, 8.5*	1
In	2.6	3
Pt	3.0*, 6.9	2
Au	2.5	---
Mn	3.6*, 4.1	1.5
Ni	3.0, 5.8	---
Fe	1.5, 6.0, 13.6	---
Co	6.0	1
Mo	6.6	0.3
Cr	5.5	---
As	3.2	1

Cd, Tl, Ba, Pb, V, Cu, Zn, Zr, Y, Ca, Ga, Al, Ti, U, and Sn did not produce any noticeable peaks.

[a]Detection limits based on largest peak, indicated by an asterisk. A blank indicates either a very small peak or a large background.

anions in the standards. No attempt was made to identify any of these species.

Detection limits were generally poorer with the PIC-A reagent. This could have had several causes: the content of methanol in the mobile phase was higher, peaks were generally broader, and more species were present as anions than cations.

Next, these same metals were injected as EDTA complexes. The stock solutions were mixed with an excess of EDTA in solution before injection. EDTA is a strong complexing agent that reacts almost universally with metals to form 1:1 coordination compounds:

$$M^{n+} + HY^{3-} = MY^{(n-4)-} + H^{+}$$

where Y^{4-} represents the particular form of the weak acid EDTA which complexes. The charge of these complexes will usually be negative unless the metal exists in a high oxidation state. As can be seen from the above equilibrium, the stability of the complex formed depends on the pH. At the pH at which the PIC-A reagent was used, most metal-EDTA complexes should have been quite stable, unless their formation constants were very small. Appendix B contains a list of these formation constants. Upon injection of the metals in Table 37 as EDTA complexes (using only 0.0025 M PIC-A this time), it was found that Ba, Fe, V, Ag, Ca, Ti, Sn, Au, and U still did not produce any peaks. These are generally the elements with the

lowest formation constants for EDTA complexes (if the V and Ti existed as V(II) and Ti (IV)), except for Fe and U [103,104]. The absence of an Fe peak can be explained by the lack of sensitivity for this element due to the $^{40}Ar^{16}O$ background peak. Uranium (VI) probably formed a doubly charged cationic complex and was adsorbed onto the column. The elements Cd, Tl, Pb, Cu, Zn, Zr, Y, Ga, and Al, which did not show peaks in Table 37, now gave distinct peaks as anionic EDTA complexes.

Complexation with EDTA insured that a wide variety of elements could be used in demonstrating the multielement capabilities of ICP-MS. Table 38 shows the results of determining 15 elements on a single injection of 100 ng of each element. A blank chromatogram was run with just EDTA on a previous injection in order to subtract out any EDTA impurities. The "chromatograms" were followed by using the Sciex software normally used for quantitative analysis, except that a string of "detailed reports" had to be generated consecutively (using 40-50 repeats/integration) and the chromatograms reconstructed manually. There may have been more efficient ways to use the present software, but, at any rate, it would not be hard to obtain new programming which could take multielement chromatograms automatically.

The data in Table 38 were obtained by "peak hopping" from one element to another, spending a total of 0.9 s on each element. The total time for a complete scan of all 15 elements was therefore about 16-17 s. Every 17 s, a report

Table 38. RP-HPLC-ICP-MS multielement detection limits (3σ)[a]

Element	t_r(min)[c]	Blank (c/s)	Detection Limits[b] $\mu g\ L^{-1}$	ng
Li	1.5	30	200	2
Rb	2.2	100	3	0.03
Ir	3.3, 12.6	60	90	0.9
In	3.3	100	0.8	0.008
Co	3.0, 3.6, 8.5, 10.6	400	90	0.9
Y	4.2	200	1	0.01
As	6.2	1500	20	0.2
Ni	7.7, 9.7	2200	20	0.2
Ga	9.7	100	5	0.05
Cu	9.7	25000	600	6
Pb	10.0	60	30	0.3
Zn	10.0, 11.2	4000	2000	20
Cd	10.2	100	200	2
Mo	10.0	600	40	0.4
Al	no pk	1500	---	---

[a]Conditions: all elements determined as EDTA complexes on same injection of 10 μL, 10 mg L^{-1} (100 ng) solution. RP-C_{18} column; mobile phase: 5/95 methanol/water, 0.005 M PIC-A, pH = 7.1. Mobile phase and EDTA blanks subtracted from prior injection.

[b]The largest peak height has been used, where more than one peak is present.

[c]Each element integrated for 0.9 s; one scan (each point of chromatogram) takes 17 s.

would be printed which represented the integrated count rate of each element over that period. Each report, therefore, represented a point of an element's chromatogram. The 17 s time resolution was enough to form good outlines of eluting peaks, as shown by the multielement chromatogram in Fig 34.

In spite of the greater number of peaks monitored in Table 38, the detection limits obtained for some elements were actually better than those in Table 37, in which only four elements were determined each injection. This may have been because of the lower methanol concentration used in Table 38. Perhaps the EDTA prevented column adsorption effects and "collected" various species into a single species - the metal-EDTA complex. Iridium, for example, was otained from a ten year old solution of $(NH_4)_2IrCl_6$ in HCl. The Ir(IV) stored in such a manner probably contained some Ir(III) [105]. The likely species present in such a mixture include $IrCl_6^{3-}$, $Ir(H_2O)Cl_5^{2-}$, $Ir(H_2O)_2Cl_4^{-}$, $IrCl_6^{2-}$, $Ir(H_2O)Cl_5^{-}$, etc. [105]. These species would show up as separate or broadened peaks on a chromatogram, depending on whether they had different or the same ionic charges. However, when combined with EDTA, only two species might remain, an anionic and neutral complex. This scenario might explain why three Ir peaks (one a shoulder) were seen in Table 37, but only two in Table 38, and consequently why the detection limit (based on total Ir injected) might improve.

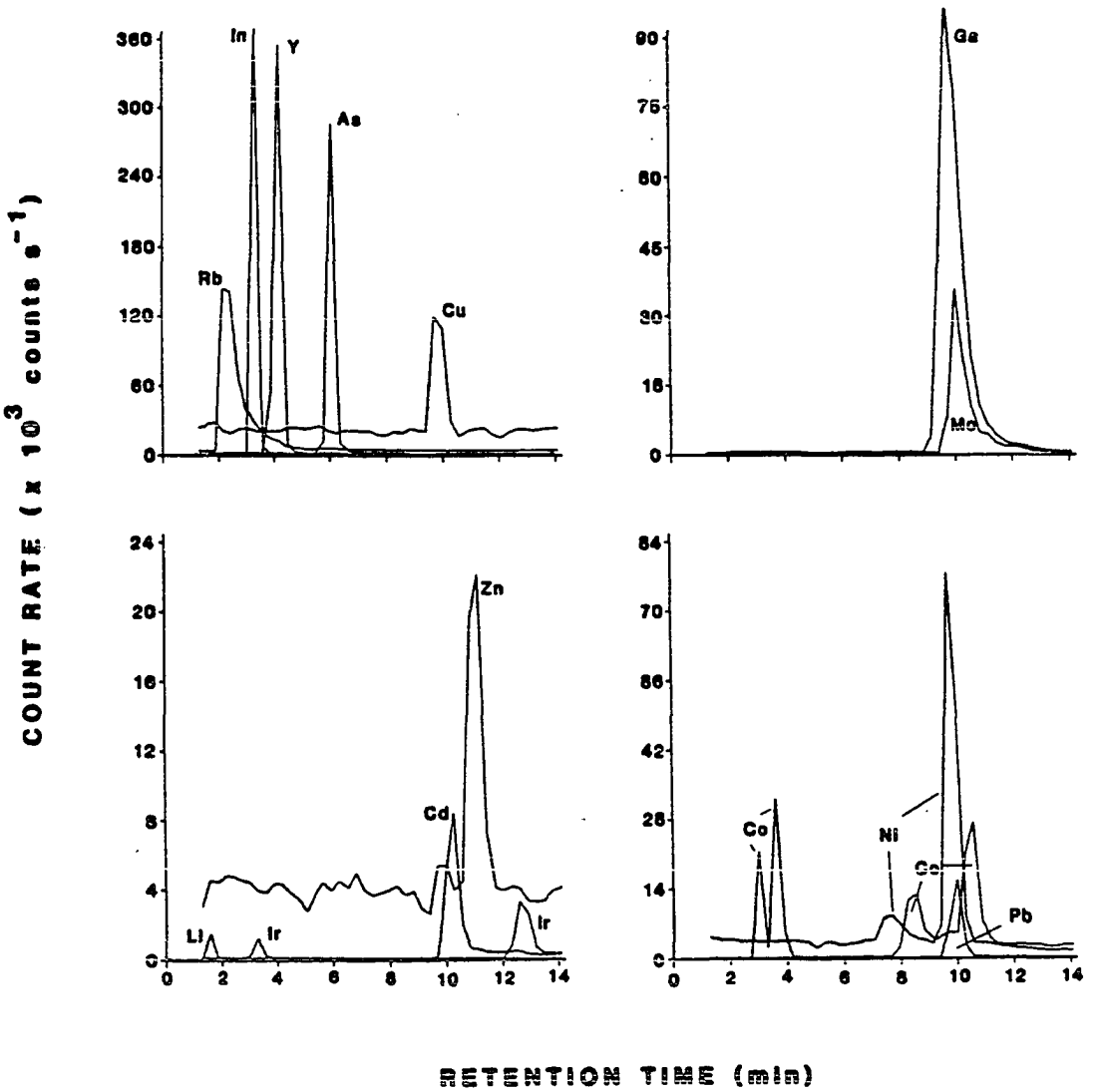

Figure 34. Reconstructed chromatogram of 14 elements from a single 10 μL injection. See Table 35 for conditions. Individual species were not identified

Examination of Table 38 reveals that, as usual, detection limits were limited by the background count rates at the m/z value at which each element was measured. Nevertheless, ICP-MS shows excellent sensitivity for several elements of environmental interest: As, Se, Pb, Cd, and others. Methods will need improvement in order to speciate Cr and Hg, two important elements.

Figure 35 is a simultaneous two element chromatogram of a standard mixture of As and Se species (each 5 ng as element): AsO_2^-, $CH_3AsO_3^{2-}$, $(CH_3)_2AsO_2^-$, $HAsO_4^{2-}$, SeO_3^{2-}, and SeO_4^{2-}. It was taken with the ICP-MS optimized for As signal. Detection limits were 0.2, 0.08, 0.2, 0.1, 0.1, and 0.1 ng for each species, respectively. Peaks were identified by separate injections of each species. It was not possible to separate arsenite (AsO_2^{2-}) from the monomethylarsonic acid even at 1% methanol and 0.6 mL min^{-1}. Calibration curves based on 5, 20, 40, and 100 ng (average of two injections, blank subtracted) were all linear with correlation coefficients ranging from 0.9991 (dimethylarsinic acid) to 0.9999 (selenate). Evidently, organometallic compounds can be quantitated at low levels using ultrasonic nebulization with aerosol desolvation.

The ability to measure accurate and precise isotope ratios on eluting HPLC peaks was next investigated. Chapter III documented the effects of concentration, operating parameters, measurement parameters, and matrix on the precision and accuracy of zinc isotope ratios determined by ICP-MS using

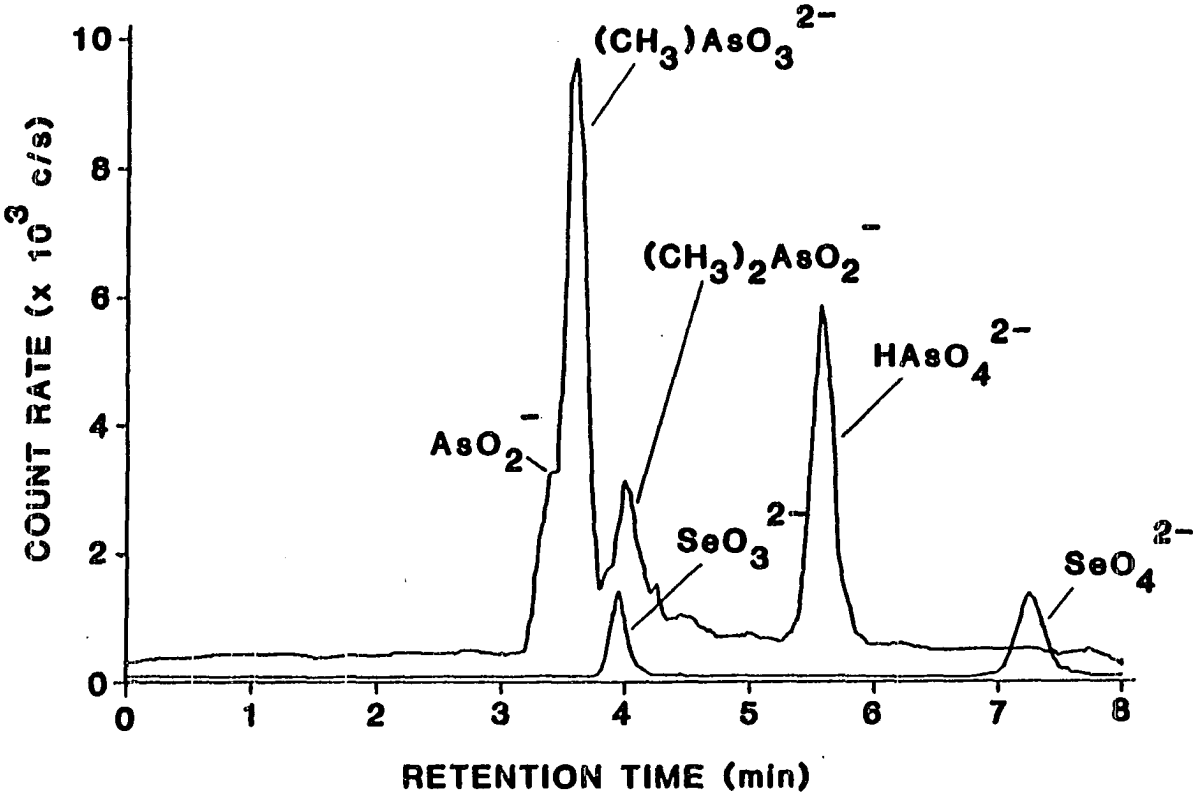

Figure 35. Detection of As and Se species by ICP-MS. ^{78}Se was monitored. Amount injected: 10 μL of 0.5 mg L^{-1} (5 ng as element). Mobile phase: 5% methanol, 0.005 M PIC-A; flow rate = 1.0 mL min^{-1}

ultrasonic nebulization with continuous sample introduction. Recall that a precision of 0.5% RSD was obtained on a routine basis, when the isotope ratio measured was not larger than 1:10. Accuracy of 1% was possible when the isotope ratios were normalized to a natural abundance standard. Extending the measurement period could compensate for decreased analyte concentration.

In contrast, one does not have the luxury afforded by long integration times when determining isotope ratios on transient signals. Therefore, the amount of sample injected appears to be the predominant factor affecting precision in this present case. Table 39 shows the effect of sample size, concentration, and measurement time (MT) on the precisions obtained from a single injection. The isotope ratios $^{114}Cd/^{116}Cd$ and $^{208}Pb/^{206}Pb$ were determined on the same injection. After a few trials, it became clear how to handle the data in order to get the best results. Isotope ratios determined on the front side of an eluting peak were neither precise nor accurate. Therefore, either the peak maximum or the point immediately following was used to calculate the first ratio. Several points along the backside of a peak could then be used before the count rate fell too low for adequate precision.

Surprisingly, the faster measurement times used in Table 39 did not seem to improve the level of precision obtained. In fact, at low count rates the precision worsened using 0.1

Table 39. Effect of measurement time[a] and sample size on precision of isotope ratios from LC[b]. Figures in parentheses are RSD for single injection; brackets denote blank subtracted count rate of largest Cd, Pb isotopes.

Sample Size	Element	0.5 s	0.1 s
10 μL,	Cd	3.64 (3.8)	3.64 (2.0)
100 mg L^{-1}	Pb	2.03 (2.0)	2.05 (2.6)
		[13000,30000]	[13500,30000]
10 μL,	Cd	3.72 (3.1)	-----
10 mg L^{-1}	Pb	1.93 (3.5)	-----
		[1800,1100]	
10 μL,	Cd	3.91 (10)	-----
1 mg L^{-1}	Pb	not detectable	-----
		[100,0]	
100 μL,	Cd	3.86 (2.6)	3.67 (5.0)
10 mg L^{-1}	Pb	1.92 (2.4)	2.07 (2.1)
		[12000,25000]	[11000,23000]
100 μL,	Cd	3.80 (5.0)	3.76 (15)
1 mg L^{-1}	Pb	2.02 (3.7)	2.15 (12)
		[1600,1150]	[1500,1100]

[a]Dwell times were 100 ms and 20 ms for the 0.5 s and 0.1 s measurement times, respectively.

[b]Conditions were different than for other tables (detection limits were obviously worse here).

and 0.05 s (not shown) measurement times. One advantage of the shorter times was that more data points were collected, making the choice of suitable ratios seem less arbitrary. For example, using 0.5 s MT, the time resolution (i.e., length of time between each point of chromatogram) was 7 s, making only 3-4 points available to determine an average ratio. Using 0.1 s MT, the time resolution was 2 s, and about 10 data points were collected for each injection.

The width of the LC peaks did not make a significant difference in precision, either. The Pb peaks were almost a full minute broader than the Cd peaks at the baseline, but there was little difference in the level of precision obtained from Cd and Pb ratios. Injection of the same amount of analyte in a larger volume did not affect the precision. For example, compare the 100 μL, 1 mg L^{-1} and 10 μL 10 mg L^{-1} data. Note the similar peak heights produced in both cases; the peak widths were approximately equal as well. Of course, one advantage of using larger sample sizes was that lower concentrations could be determined. For instance, a 1 mg L^{-1} solution gave worse than 10% precision for Cd when a 10 μL sample was used; Pb could barely be detected at all. However, a 100 μL injection improved this precision to 5% for the Cd ratio.

On the other hand, count rate had a great affect on the precision obtained. As the count rate dropped from 10000 to about 1000 counts s^{-1}, precision dropped from 1-3% to 3-6% per

injection. As mentioned above, the precision level became worse than 10% when the amount of analyte fell below ten times the detection limit.

Table 40 illustrates that ICP-MS could accurately follow changes in the enrichment level of Cd and Pb isotopes eluting from the LC column. Also, the precision obtained by averaging the mean ratios from multiple injections was always better than that from a single injection. This is one way, after all, of effectively increasing the integration time on the peak. Further increases in precision could undoubtedly be realized by monitoring only a single element (two isotopes) and by increasing the analyte concentration and/or sample size. Relative precisions of 1.5%, with comparable accuracy, could therefore be routinely expected in these LC experiments provided analyte concentration was at least 10 mg L^{-1} and the background was below 100 counts s^{-1}. These figures of merit are certainly suitable to warrant initial investigations of tracing various species of the more abundant elements through the body (compared to tracing total zinc, for example, as in Chapter III). As for isotope dilution, a precision of 3-6% would be acceptable to determine analyte concentrations in the 1 mg L^{-1} range using just two injections: one to determine the initial ratios, and one to determine the "spiked" ratios.

There are a few remaining observations. Reproducibility of retention times was always good to within a few seconds. Peak height reproducibility of the LC peaks was not as

Table 40. Cd and Pb isotope ratio measurements on eluting LC peaks[a]

Sample	Isotopes	# injections	Ratio (RSD)[b]	Expected
Natural	$^{114}Cd/^{116}Cd$	3	3.61(1.3)	3.81
	$^{208}Pb/^{206}Pb$	4	2.06(2.2)	2.05
Partly Enriched	$^{114}Cd/^{116}Cd$	4	0.359(1.7)	0.359[c]
	$^{208}Pb/^{206}Pb$	4	0.418(1.0)	0.415[d]
Fully Enriched	$^{114}Cd/^{116}Cd$	3	0.0145(2.0)	0.0146[e]
	$^{208}Pb/^{206}Pb$	-	^{208}Pb not detected	

[a]Conditions: 10 μL of 10 mg L^{-1} (100 ng) Cd, Pb injected; both ratios determined on the same injection. Mobile phase 5% methanol in water, 0.005 M PIC-B5. t_r(Cd) = 7:40 $\pm$ 6 s. t_r(Pb) = 8:05 $\pm$ 6 s.

[b]RSD from each individual injection was 1-5% based on 3 or 4 measurements along the profile of the peak following peak maximum. Measurement time was 0.4 s, dwell time 100 ms.

[c]Determined by normalizing to a standard at natural abundance under continuous flow conditions (no column).

[d]Determined by gravimetric and volumetric preparation of the sample using Oak Ridge certified enrichments.

[e]Oak Ridge certified value.

commendable - 10% or so, but this might well be due to drift of the ICP-MS over relatively long time frames (see uranium analysis in Chapter III). Thus, for quantitation it is recommended that either isotope dilution or internal standardization be used.

Very little is mentioned in the literature about the applications of IP-RPLC to "real" samples. Fig. 36a is a chromatogram of the same species in Fig. 35, taken on a different day and injecting 40 ng of each species in a deionized water matrix. Sodium and calcium were monitored at the same time as As and Se. The increase in Na count rate at about 3 min. was due to the Na injected with the the arsenate and selenate species. Apparently, this singly charged cation was not adsorbed by the column and eluted close to the void volume. Figure 36b illustrates the result of injecting the same amount of analyte in a 100 mg L^{-1} Na matrix (as chloride), to simulate a "real" sample. A small amount of suppression was observed both during and slightly after the Na eluted. When the sample was reinjected, a very similar chromatogram was obtained. Presumably, the suppression of signal was due mainly to ionization suppression in this case. However, when the analyte species were injected with 100 mg L^{-1} Ca (as chloride - Fig. 36c), only a fraction of the Ca^{2+} eluted. The rest was probably adsorbed by the column. Perhaps as a consequence of this, the chromatograms taken on this and subsequent injections (Fig. 36d) showed reduced and

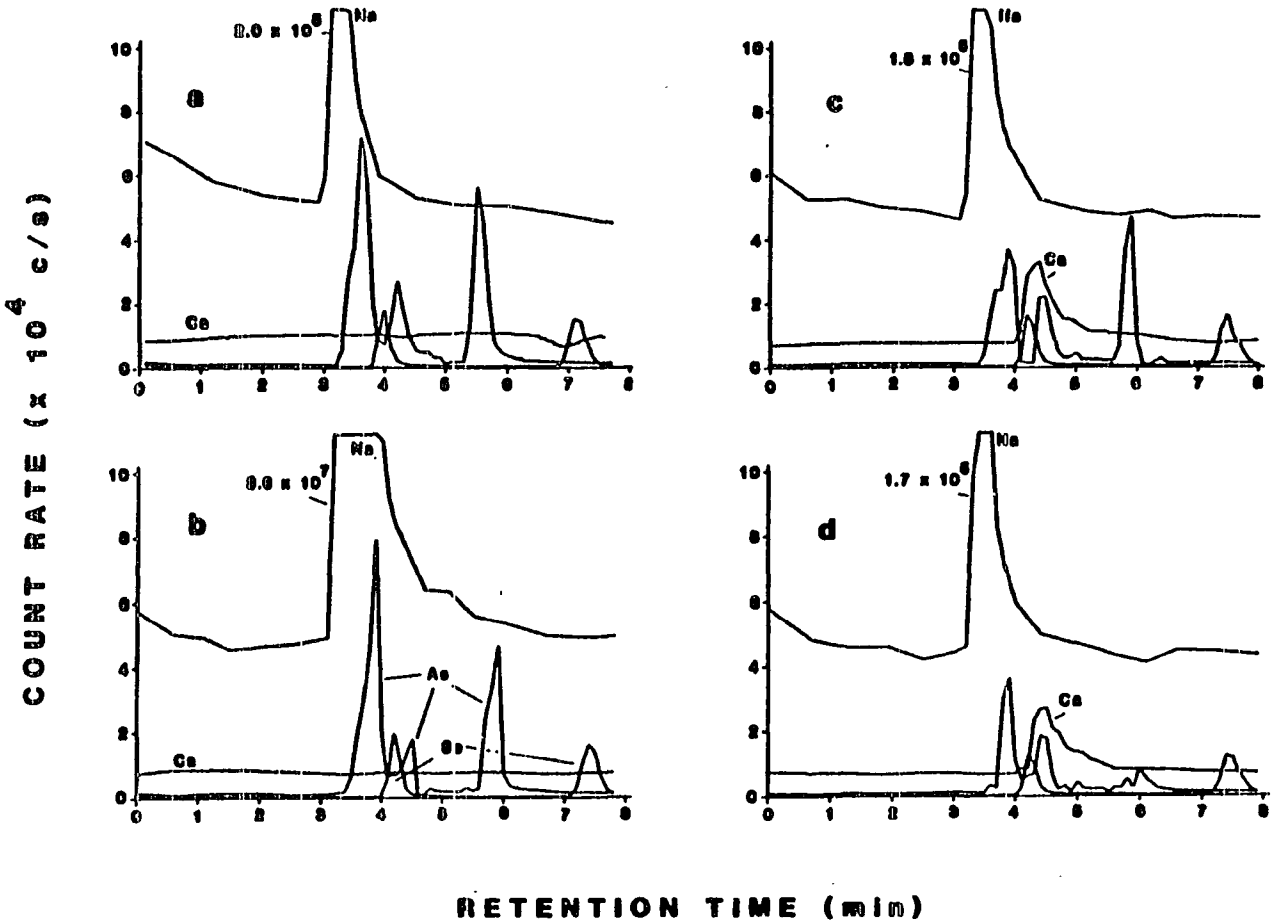

a) Chromatogram of 40 ng of each species in Fig. 35, injected in deionized water; Na and ^{44}Ca are also monitored b) Same; matrix is 100 mg L^{-1} Na^{+} c) Same; matrix is 100 mg L^{-1} Ca^{2+} d) Repeat injection (c)

Figure 36. Injection of As, Se species in simulated "real" matrices

differently proportioned peak heights. Further work will investigate the adverse affects of various matrices on the chromatography, as well as the ability of LC to prevent ionization suppression in ICP-MS by separation of matrix elements.

CHAPTER V. SUMMARY AND OBJECTIVES FOR FUTURE RESEARCH

By studying the performance of ICP-MS in a wide variety of applications, we have reached a better understanding of the limitations of the technique, as well as its positive aspects. It is now quite clear, as the result of data presented in Chapter II, that a greater extent of ionization suppression exists in ICP-MS than in ICP-AES over a wide range of operating conditions, at least with the Sciex instrument. Furthermore, the level of suppression varies with the analyte element, and different matrix elements cause a different relative degree of suppression among various concomitant analyte elements. Internal standardization has been shown to alleviate this problem to some extent, but is limited in its applicability (e.g., not even the rare earth elements behave similarily as an entire class; Ce and La are not good internal standards for Ho or Tm). Obviously, this spells trouble for those chemists who want to do routine multielement determinations in an industrial environment. Judging from the initial application papers, Sciex users are using isotope dilution and standard addition methods to obtain more accurate results. Although isotope dilution does appear to give accurate results, it is a costly and time consuming way to do multielement analysis. Standard addition methods are not time-effective either, since each sample must be analyzed four or five times, after each addition of a multielement "spike."

It will be interesting to see if users of other commercial instruments report similar matrix interference problems. Preliminary indications from Alan Gray's laboratory, whose ICP-MS is similar to the commercial VG instrument, are that suppression is not nearly as bad with his instrument [106]. This suggests that future work must systematically explore the effects of sampler and skimmer orifice size and shape, expansion stage pressure, and the degree of residual "pinch" on the extent of matrix effects. These experiments must carefully separate the individual effects since, for example, the extent of the "pinch" discharge is related to the sampling orifice size and the pressure behind it. Even if suppression is not reduced as the result of these experiments, a more uniform response of the analyte elements to different matrices would result in a more effective use of internal standardization.

ICP-MS, however, is still a highly worthwhile technique because of its tremendous powers of detection. Even in the presence of a matrix element which suppresses the analyte count rate by 99%, the detection limits are still about 1 $\mu g\ L^{-1}$ using ultrasonic nebulization. In those applications where the matrix can be removed by solvent extraction or by LC separations, the ICP-MS will almost always exhibit superior detection limits compared to other multielement techniques. Isotope ratio determinations usually require that the analytes be separated from the matrix (to prevent isobaric

interferences), and so ICP-MS does not handicap the user in this respect, compared to other techniques.

In all the application studies presented herein, it is to be noted that compromise measurement and operating parameters had to be chosen carefully in order to optimize the performance of the instrument for the job at hand. Almost always, lower aerosol gas flow rates must be chosen than those which would give optimal count rate for the analyte ions. It has been shown that lowering the aerosol gas flow rate decreases the extent of ionization suppression, increases the long term stability of calibration curves, and enables isotope ratios to be measured with better precision. Other ICP-MS parameters do not play nearly as important a role in defining the instrument's performance. Another aspect in which the application studies were similar was that the presence of either trace impurities or molecular species in the blank spectrum considerably reduced the detection limits obtained by ICP-MS. The problem of reagent purity is becoming more common in instrumental analysis as a whole, as chemists attempt to quantitate elements below the 1 μg L^{-1} level. Indeed, the point is rapidly being reached where contamination of the sample in the preparation steps precludes determining native impurities in the sample at any lower concentration. The second cause of high blanks in ICP-MS - molecular species - should be addressed in future research. Methods of dissociating these species (ArO, ArN, Ar_2, etc.) in the vacuum

chamber are already being investigated in our laboratory. Further research into these and other aspects of ICP-MS should make the technique even more useful and reliable in the future.

LITERATURE CITED

1. Houk, R. S.; Fassel, V. A.; Flesch, G. D.; Svec, H. J.; Taylor, C. E. Anal. Chem. 1980, 52, 2283.

2. Gray, A. L. Spectrochim. Acta, Part B 1985, 40B, 1525.

3. Gray, A. L. Spectrochim. Acta, Part B 1985, 40B, 1.

4. Gray, A. L.; Date, A. R. Spectrochim. Acta, Part B 1983, 38B, 29.

5. Olivares, J. A.; Houk, R. S. Anal. Chem. 1985, 57, 2674.

6. Douglas, D. J.; Houk, R. S. Prog. Anal. Atomic Spectrosc. 1985, 8, 1.

7. Houk, R. S.; Thompson, J. J. American Mineralogist 1982, 67, 238.

8. Houk, R. S.; Thompson, J. J. Biomed. Mass Spectrom. 1983, 10, 107.

9. Douglas, D. J.; Quan, E. S. K.; Smith, R. G. Spectrochim. Acta, Part B 1983, 38B, 39.

10. Date, A. R. presented at the 1984 Winter Conference on Plasma Spectrochemistry, San Diego, 1984.

11. Date, A. R.; Gray, A. L. Proceedings 1984 Winter Conference on Plasma Spectrochemistry, Spectrochim. Acta 1984.

12. Date, A. R.; Gray, A. L. Spectrochim. Acta, Part B 1985, 40B, 115.

13. Palmieri, M. D.; Fritz, J. S.; Thompson, J. J.; Houk, R. S. accepted for Anal. Chim. Acta 1986.

14. Fassel, V. A. Science 1978, 202, 183.

15. Larson, G. F.; Fassel, V. A.; Kniseley, R. N.; Scott, R. H. Anal. Chem. 1975, 47, 238.

16. Olson, K. W.; Haas, W. J., Jr.; Fassel, V. A. Anal. Chem. 1977, 49, 632.

17. Bear, B. R.; Fassel, V. A. Spectrochim. Acta, Part B 1986, in press.

18. Scott, R. H.; Fassel, V. A.; Kniseley, R. N.; Nixon, D. E. Anal. Chem. 1974, 46, 75.

19. Kalnicky, D. J.; Kniseley, R. N.; Fassel, V. A. Spectrochim. Acta, Part B 1975, 30B, 511.

20. Houk, R. S.; Montaser, A.; Fassel, V. A. Appl. Spectros. 1983, 37, 425.

21. Douglas, D. J.; French, J. B. Spectrochim. Acta, Part B 1986, 41B, 197.

22. Huheey, J. E. "Inorganic Chemistry: Principles of Structure and Reactivity"; Second Ed., Harper & Row Publishers: New York, 1978, p. 140.

23. Vaughan, M. A.; Horlick, G. Appl. Spectros. 1986, 40, 434.

24. Tan, S. H.; Horlick, G. Appl. Spectros. 1986, 40, 445.

25. Dawson, P. H., ed. "Quadrupole Mass Spectrometry and Its Applications"; Elsevier: New York, 1976.

26. Timothy, J. G.; Bybee, R. L. Rev. Sci. Instrum. 1978, 49, 1192.

27. Gray, A. L. personal communication, on visit to Ames from University of Surrey, 1985.

28. Horlick, G.; Tan, S. H.; Vaughan, M. A.; Rose, C. A. Spectrochim. Acta, Part B 1985, 40B, 1555.

29. Boumans, P. W. J. M.; de Boer, F. J. Spectrochim. Acta, Part B 1975, 30B, 309.

30. Boumans, P. W. J. M.; de Boer, F. J. Spectrochim. Acta, Part B 1976, 31B, 355.

31. Olivares, J. A.; Houk, R. S. Anal. Chem. 1986, 58, 20.

32. Blades, M. W.; Horlick, G. Spectrochim. Acta, Part B 1981, 36B, 881.

33. Crain, J. S.; Houk, R. S. unpublished theory.

34. Scribner, B. F.; Mullen, H. R. J. Res. Nat. Bur. of Std. 1946, 37, 379.

35. Pepper, C. E. "A Review of Spectrochemical Emission Methods and Associated Problems for the Determination of Impurities in Nuclear Grade Uranium"; Atomic Energy Commission NLCO-999, 1967.

36. Maney, J. P.; Luciano, V.; Ward, A. F. Jarrell-Ash Plasma Newsl. 1979, 2, 11.

37. Bear, B. R.; Edelson, M. C.; Gopalan, B.; Fassel, V. A. Anal. Chem. Spectrosc. Symp. Ser. 1984, 19 (Anal. Spectrosc.) 187.

38. Floyd, M. A.; Morrow, R. W.; Farrar, R. B. Spectrochim. Acta, Part B 1983, 38B, 303.

39. Coleman, C. J. Anal. Chem. Spectrosc. Symp. Ser. 1984, 19 (Anal. Spectrosc.), 195.

40. Short, B. W.; Spring, H. S.; Grant, R. L. "Determination of Trace Impurities in Uranium Hexafluoride by Inductively Coupled Argon Plasma Spectrometer"; Goodyear Atomic Corporation: Piketon, Ohio, CAT-T-3184, 1983.

41. Seshagiri, J. K.; Babu, Y.; Jayanth Kumar, M. L.; Dalvi, A. G. I.; Sastry, M. D.; Joahi, B. D. Talanta 1984, 31, 773.

42. Winge, R. K.; Fassel, V. A.; Peterson, V. J.; Floyd, M. A. "Inductively Coupled Plasma Atomic Emission Spectometry: An Atlas of Spectral Information"; Elsevier: New York, 1985.

43. McKinney, C.; McCrea, J.; Epstein, S.; Allen, H.; Urey, H. Rev. Sci. Instrum. 1950, 21, 724.

44. Robinson, B. W. Ed. "Stable Isotopes in the Earth Sciences"; Wright & Carmon Ltd.: Wellington, 1978.

45. Faure, G. "Principles of Isotope Geology"; John Wiley & Sons: New York, 1977.

46. Date, A. R.; Gray, A. L. Int. J. Mass Spectrom. Ion Phys. 1983, 48, 357.

47. McLaren, J. W.; Mykytiuk, A. P.; Willie, S. N.; Berman, S. S. Anal. Chem. 1985, 57, 2907.

48. Clarke, H. T., et al. (contributors) "A Symposium on the Use of Isotopes in Biology and Medicine"; University of Wisconsin Press: Madison, 1948.

49. Janghorbani, M.; Ting, B. T. G.; Young, V. R. Clin. Chim. Acta 1980, 108, 9.

50. Turnlund, J. R.; Michel, M. C.; Keyes, W. R.; King, J. C.; Margen, S. Am. J. Clin. Nutr. 1982, 35, 1033.

51. Wada, L.; Turnlund, J. R.; King, J. C. J. Nutr. 1985, 115, 1345.

52. Schmidt, M.; Northup, M. A. Am. Lab. 1986, 18, 125.

53. Yergey, A. L.; Vieira, N. E.; Hansen, J. W. Anal. Chem. 1980, 52, 1811.

54. Veillon, C. in "Stable Isotopes in Nutrition"; Turnlund, J. R.; Johnson, P. E., eds. American Chemical Society: Washington, D. C., 1984; Chapter 7.

55. Hachey, D. L.; Blais, J. C.; Klein, P. D. Anal. Chem. 1980, 52, 1131.

56. Shaw, N. S.; Millen, D. D.; Gilbert, M.; Roe, D. A.; Van Campen, D. R. in "Stable Isotopes in Nutrition"; Turnlund, J. R.; Johnson, P. E., eds. American Chemical Society: Washington, D. C., 1984, Chapter 8.

57. Smith, D. L. Anal. Chem. 1983, 55, 2391.

58. Eagles, J.; Fairweather-Tait, S. J.; Self, R. Anal. Chem. 1985, 57, 469.

59. Olivares, J. A.; Houk, R. S.; Serfass, R. E.; Lindstrom, G. L. submitted to J. Nutr., 1986.

60. Janghorbani, M.; Ting, B. T. G. submitted to Spectrochim. Acta, Part B, 1986.

61. Serfass, R. E.; Thompson, J. J.; Houk, R. S. accepted for Anal. Chim. Acta, 1986.

62. Evans, G. W.; Johnson, P. E. Am. J. Clin. Nutr. 1977, 30, 873.

63. Hammond, B. P.; Beliles, R. P. in "Toxicology - The Basic Science of Poisons"; Second Ed.; Doull, J.; Klaasen, C. D.; Amdur, M. O. Eds.; MacMillan Publishing Co.: New York, 1980; p.468.

64. Sigel, H., ed. "Metal Ions in Biological Systems. Carcinogenicity and Metal Ions"; Vol. 10; Marcel Dekker: New York, 1980.

65. Manahan, S. E.; Jones, D. R. Anal. Lett. 1973, 6, 745.

66. Yoza, N.; Ohashi, S. Anal. Lett. 1973, 6, 595.

67. Chakraborti, D.; De Jonghe, W. R. A.; Van Mol, W. E.; Van Cleuvenbergen, R. J. A.; Adams, F. C. Anal. Chem. 1984, 56, 2692.

68. Ebdon, L.; Hill, S. J.; Jones, P. Analyst 1985, 110, 515.

69. Rapsomanikis, S.; Donard, O. F. X.; Weber, J. H. Anal. Chem. 1986, 58, 35.

70. Cutter, G. A. Anal. Chem. 1985, 57, 2951.

71. McCarthy, J. A.; Caruso, J. A.; Fricke, F. L. J. Chromatogr. Sci. 1983, 21, 389.

72. Bushee, D.; Krull, I. S.; Savage, R. N.; Smith, S. B. J. Liq. Chromatogr. 1982, 5, 463.

73. Lawrence, K. E.; Rice, G. W.; Fassel, V. A. Anal. Chem. 1984, 56, 289.

74. Krull, I. S.; Panaro, K. W.; Gershman, L. L. J. Chromatogr. Sci. 1983, 21, 460.

75. Uden, P. C.; Quimby, B. D.; Barnes, R. M. Anal. Chim. Acta 1978, 101, 99.

76. Hausler, D.W.; Taylor, L. T. Anal. Chem. 1981, 53, 1223.

77. Gardiner, P. E.; Bratter, P.; Negretti, V. E.; Schulze, G. Spectrochim. Acta, Part B 1983, 38B, 427.

78. Birnie, S. E.; Hodges, D. J. Environ. Tech. Lett. 1981, 2, 433.

79. Mok, W. M.; Shah, N. K.; Wai, C. M. Anal. Chem. 1986 58, 110.

80. Robinson, J. W.; Boothe, E. D. Spectros. Lett. 1984, 17, 673.

81. Pratt, K. W.; Koch, W. F. Anal. Chem. 1986, 58, 124.

82. MacDonald, J. C. in "Chemical Analysis"; Vol. 78; MacDonald, J. C., ed.; John Wiley & Sons: New York, 1985; Chap. 6.

83. Alltech Associates Inc., Applied Science Laboratory; Catalog No. 70, 1985.

84. Johnson, E. L.; Stevenson, R. "Basic Liquid Chromatography"; Varian Associates, Inc.: Palo Alto, 1978, p. 143.

85. King, J. Ph.D. Dissertation; Iowa State University, 1985.

86. Noden, F. G. in "Lead in the Marine Environment"; Branica, M.; Konrad, Z., eds.; Pergamon Press: Oxford, 1980; p. 83.

87. Linares, P.; Luque de Castro, M. D.; Valcarcel, M. Anal. Chem. 1986, 58, 120.

88. Brinckman, F. E.; Blair, W. R.; Jewett, K. L.; Iverson, W. P. J. Chromatogr. Sci. 1977, 15, 493.

89. Irgolic, K. J.; Stockton, R. A.; Chakraborti, D. Spectrochim. Acta, Part B 1983, 38B, 437.

90. Van Loon, J. C.; Lichwa, J.; Radziuk, B. J. Chromatogr. 1977, 136, 301.

91. Siemer, D. D.; Koteel, P.; Haworth, D. T.; Taraszewski, W. J.; Lawson, S. R. Anal. Chem. 1979, 51, 575.

92. Mulligan, K. J.; Zerezhgi, M.; Caruso, J. A. Spectrochim. Acta, Part B 1983, 38B, 369.

93. Panaro, K. W.; Krull, I. S. Anal. Lett. 1984, 17, 157.

94. Nisamaneepong, W.; Haas, D. L.; Caruso, J. A. Spectrochim. Acta, Part B 1985, 40B, 3.

95. LaFreniere, K. E.; Rice, G. W.; Fassel, V. A. Spectrochim. Acta, Part B 1985, 40B, 1495.

96. LaFreniere, K. E.; Fassel, V. A.; Eckels, D. E. submitted to Anal. Chem., 1986

97. LaFreniere, K. E. Ph.D. Dissertation; Iowa State University, 1986.

98. Thompson, J. J.; Houk, R. S. accepted for Anal. Chem. 1986.

99. "Handbook of Chemistry and Physics"; 58th ed.; CRC Press: Cleveland, 1977.

100. Chong, N. S. M.S. Thesis; Iowa State University, 1986.

101. Fraley, D. M.; Yates, D.; Manahan. S. E. Anal. Chem. 1979, 51, 2225.

102. Whaley, B. S.; Snable, K. R.; Browner, R. F. Anal. Chem. 1982,54, 162.

103. Ringbom,A. "Complexation in Analytical Chemistry"; Interscience Publishers: New York, 1963; p. 335.

104. Kotrly, S.; Sucha, L. "Handbook of Chemical Equilibria"; John Wiley & Sons: New York, 1985; p. 176.

105. Cotton, F. A.; Wilkinson, G. "Advanced Inorganic Chemistry - A Comprehensive Text"; 4th ed., John Wiley & Sons: New York, 1980; pp. 945-50.

106. Gray, A. L. submitted to Spectrochim. Acta, Part B, 1986.

APPENDIX A.

RELATIVE ABUNDANCES OF NATURALLY OCCURRING ISOTOPES

Z↓	A→	1	2	3	4	5	6	7	8	9	10	11	12	13	14	15	16	17	18	19	20
1	H	99.9	.01																		
2	He				100																
3	Li						7.4	92.6													
4	Be									100											
5	B										18.3	81.7									
6	C												98.9	1.1							
7	N														99.6	0.4					
8	O																99.8	0.04	0.20		
9	F																			100	
10	Ne																				90.9
Z↓	A→	21	22	23	24	25	26	27	28	29	30	31	32	33	34	35	36	37	38	39	40
10	(Ne)	0.3	8.8																		
11	Na			100																	
12	Mg				78.6	10.1	11.3														
13	Al							100													
14	Si								92.2	4.7	3.1										
15	P											100									
16	S												95.0	0.8	4.2		0.02				
17	Cl															75.5		24.5			
18	Ar																0.34		0.06		99.6
19	K																			93.1	0.01
20	Ca																				97.0
Z↓	A→	41	42	43	44	45	46	47	48	49	50	51	52	53	54	55	56	57	58	59	60
19	K	6.9																			
20	Ca		0.6	0.1	2.1		.003		0.2												
21	Sc					100															
22	Ti						8.0	7.3	74.0	5.5	5.2										
23	V										0.3	99.7									
24	Cr										4.3		83.8	9.6	2.3						
25	Mn															100					
26	Fe														5.8		91.7	2.2	0.3		
27	Co																			100	
28	Ni																		67.8		26.2
Z↓	A→	61	62	63	64	65	66	67	68	69	70	71	72	73	74	75	76	77	78	79	80
28	(Ni)	1.2	3.6		1.2																
29	Cu			69.1		30.9															
30	Zn				48.9		27.8	4.1	18.6		0.6										
31	Ga									60.5		39.5									
32	Ge										20.5		27.4	7.7	38.7		7.7				
33	As															100					
34	Se														0.9		9.0	7.6	23.5		49.8
35	Br																			50.6	
36	Kr																		0.4		2.3
Z↓	A→	81	82	83	84	85	86	87	88	89	90	91	92	93	94	95	96	97	98	99	100
34	(Se)		9.2																		
35	(Br)	49.4																			
36	(Kr)		11.5	11.5	56.9		17.4														
37	Rb					72.2		27.6													
38	Sr				0.8		9.9	7.0	82.5												
39	Y									100											
40	Zr										51.5	11.2	17.1		17.4		2.8				
41	Nb													100							
42	Mo												15.9		9.1	15.7	16.5	9.5	23.7		9.6
43	Tc	DOES NOT OCCUR NATURALLY																			
44	Ru																5.6		1.9	12.7	12.6

원소	A→	101	102	103	104	105	106	107	108	109	110	111	112	113	114	115	116	117	118	119	120
44	(Ru)	17.1	31.6		18.5																
45	Rh			100																	
46	Pd		1.0		11.0	22.3	27.3		26.7		11.8										
47	Ag							51.4		48.6											
48	Cd						1.2		0.9		12.4	12.7	24.1	12.3	28.8		7.6				
49	In													4.3		95.7					
50	Sn												0.9		0.6	0.3	14.2	7.6	24.0	8.6	33.0
51	Sb																				
52	Te																				0.1

원소	A→	121	122	123	124	125	126	127	128	129	130	131	132	133	134	135	136	137	138	139	140
50	(Sn)		4.8		6.0																
51	(Sb)	57.3		42.7																	
52	(Te)		2.4	0.9	4.6	7.0	18.7		31.8		34.5										
53	I							100													
54	Xe				0.1		0.1		1.9	26.4	4.1	21.2	26.9		10.4		8.9				
55	Cs													100							
56	Ba										0.1		0.1		2.4	6.6	7.8	11.3	71.7		
57	La																		0.1	99.9	
58	Ce																0.2		0.2		88.5

원소	A→	141	142	143	144	145	146	147	148	149	150	151	152	153	154	155	156	157	158	159	160
58	(Ce)		11.1																		
59	Pr	100																			
60	Nd		27.1	12.1	23.8	8.3	17.3		5.8		5.6										
61	Pm	DOES NOT OCCUR NATURALLY																			
62	Sm				3.2			15.1	11.3	13.8	7.5		26.6		22.5						
63	Eu											47.9		52.1							
64	Gd												0.2		2.1	14.7	20.5	15.7	24.9		21.9
65	Tb																			100	
66	Dy																0.1		0.1		2.3

원소	A→	161	162	163	164	165	166	167	168	169	170	171	172	173	174	175	176	177	178	179	180
66	(Dy)	18.9	25.5	24.9	28.2																
67	Ho					100															
68	Er		0.1		1.6		33.4	22.9	27.1		14.9										
69	Tm									100											
70	Yb								0.2		3.0	14.3	21.8	16.1	31.9		12.7				
71	Lu															97.4	2.6				
72	Hf														0.2		5.2	18.5	27.1	13.8	35.2
73	Ta																				0.01
74	W																				0.2

원소	A→	181	182	183	184	185	186	187	188	189	190	191	192	193	194	195	196	197	198	199	200
73	(Ta)	99.9																			
74	(W)		26.4	14.4	30.6		28.4														
75	Re					37.1		62.9													
76	Os				0.02		1.58	1.6	13.3	16.1	26.4		41.0								
77	Ir											38.5		61.5							
78	Pt										.01		0.8		32.9	33.8	25.2		7.19		
79	Au																	100			
80	Hg																0.2		10.0	16.8	23.1

원소	A→	201	202	203	204	205	206	207	208	209	210	211	212	213	214	215	216	217	218	219	220
80	(Hg)	13.2	29.8		6.8																
81	Tl			29.5		70.5															
82	Pb				1.4		25.2	21.7	51.7												
83	Bi									100											

84 (Po), 85 (At), 86 (Rn), 87 (Fr), 88 (Ra), 89 (Ac), DO NOT OCCUR NATURALLY

원소	A→	221	222	223	224	225	226	227	228	229	230	231	232	233	234	235	236	237	238	239	240
90	Th												100								
91	Pa										100										
92	U														0.06	0.7			99.3		

APPENDIX B.

FORMATION CONSTANTS FOR METAL-EDTA COMPLEXES

Metal Ion	$\log K_{my}$	Metal Ion	$\log K_{my}$
K^{+}	0.8	Cd^{2+}	16.46
Na^{+}	1.66	Hg^{2+}	21.7
Li^{+}	2.79	Al^{3+}	16.3
Mg^{2+}	9.12	Ga^{3+}	20.3
Ca^{2+}	11.00	In^{3+}	25.0
Sr^{2+}	8.80	Tl^{3+}	6.54
Ba^{2+}	7.78	Tl^{3+}	35.3
Ra^{3+}	7.1	Sn^{2+}	18.3
Ti^{3+}	21.3	Pb^{2+}	18.0
TiO^{2+}	17.5	Bi^{3+}	27.8
Zr^{4+}	29.5	Sc^{3+}	23.1
Hf^{4+}	29.5	Y^{3+}	18.09
Th^{4+}	23.2	La^{3+}	15.50
V^{2+}	12.7	Ce^{3+}	15.70
V^{3+}	26.0	Pr^{3+}	16.05
VO^{2+}	18.8	Nd^{3+}	16.28
VO_2^{2+}	15.55	Sm^{3+}	16.88
Cr^{2+}	13.6	Eu^{3+}	17.10
Cr^{3+}	23.4	Gd^{3+}	16.94

Metal Ion	log K_{my}	Metal Ion	log K_{my}
Mn^{2+}	13.87	Tb^{3+}	17.27
Mn^{3+}	25.3	Dy^{3+}	17.42
Fe^{2+}	14.32	Ho^{3+}	17.38
Fe^{3+}	25.1	Er^{3+}	17.40
Co^{2+}	16.31	Tm^{3+}	17.48
Co^{3+}	41.4	Yb^{3+}	17.78
Ni^{2+}	18.62	Lu^{3+}	17.81
Cu^{2+}	18.80	Pd^{2+}	18.5
Zn^{2+}	16.50	Ag^{+}	7.32
Mo^{5+}	6.4	U^{4+}	25.8
		UO_2^{2+}	19.7

From Refs. [103] and [104].

ACKNOWLEDGEMENTS

Many people have had a role in bringing this work to completion. I begin by thanking Robert Houk, who, of course, has been very "instrumental" in supervising my research. I was the first graduate student to enter his group, which is always a special relationship, and I must say it was a pleasure to work for him, in spite of him being a Steeler fan. Jose Olivares supplied many ideas and helped equip our two laboratories at the start. Together we were responsible for the building of one, and the maintenance of two ICP-MS instruments, all of which proceeded smoothly due to his expertise. Of course, I am indebted to my collaborators, Margo Palmieri and Robert Serfass, without whom the studies on uranium analysis and stable isotope tracing could not have been done. Robert Jackson and the rest of the Sciex Customer Service department were most reliable and prompt in their answering my many questions regarding the instrument.

Ours was, and is, a highly instrument-oriented group. My work surely would not have progressed very rapidly were it not for the expert help of Eldon Ness, John Sauke, George Steininger, and Thomas Johnson in the machine shops, who built various parts of our vacuum systems, besides my bothering them with numerous odd jobs, which they patiently accomplished. I must thank George Holland, John Homer, Raymond Prior and the rest of the instrumentation services group for their prompt

service of our RF power supplies and other equipment. Harold Hall and Charles Patterson provided several ICP torches and other pieces of glassware. I also wish to express gratitude to Gerald Flesch, who always lended a hand to solve various technical problems.

There are several others who have been quite helpful in my research and in the preparation of this dissertation. Edward DeKalb furnished many of the standards we have used, and Rodney Walters supplied our deionized water. Bryant and Kimberly LaFreniere showed me several short cuts in writing this dissertation, as well as supplied some equipment and chemicals for the liquid chromatography experiments. Jiang Shiuh-Jen aided me in some tedious data reduction, which was most appreciated. Daniel Wiederin and Timothy Brown took some of the initial data found in Chapter II, while working as summer employees. I also must acknowledge our secretary, Betty Beymer, for her help in the innumerable little things: typing reports, answering the telephone, bringing "treats", etc.

Searching further back, I now realize the quality of the education I received at the College of St. Thomas and I am indebted to all my teachers there, especially Dr. James Ryan, who steered me on the course to graduate school.

Lastly, I thank my parents, family, and my aunt who have been very supportive, both financially and emotionally through my many years of education away from home. I owe much of this achievement to them.